High Pressure Oxy-fired (HiPrOx) Direct Contact Steam Generation (DCSG) for Steam Assisted Gravity Drainage (SAGD) Application

Paul Emanuel Cairns

Thesis submitted to the
Faculty of Graduate and Postdoctoral Studies
In partial fulfillment of the requirements
For the M.A.Sc. degree in Chemical Engineering

Department of Chemical and Biological Engineering
Faculty of Engineering
University of Ottawa

Statement of Contribution of Collaborators

Chapters 2-5 of this thesis take the form of research papers which includes work from collaborators, as detailed below. I am the sole author of all other chapters. Bruce R. Clements, my supervisor at Natural Resources Canada, CanmetENERGY, Dr. Arturo Macchi of the Department of Chemical and Biological Engineering at the University of Ottawa, and Dr. Edward J. Anthony from the School of Applied Sciences at Cranfield University in the United Kingdom, supervised my work during the M.A.Sc. program and provided editorial corrections.

For Chapter 2, I co-authored the work with Bruce Clements who wrote 80% of the introduction. I authored Sections 2.3, 2.4 and 2.5. I performed the process simulations, analyzed the results, wrote the discussion, and wrote the conclusions (Section 2.6).

For Chapter 3, I authored the paper. The introduction, literature review, experimental methods, analysis, discussions, and conclusions were entirely my work. Francine Verdon assisted with the experiments.

For Chapter 4, I co-authored the paper with Bruce Clements. Bruce Clements wrote about 50% of the introduction, while Dr. Robin Hughes wrote the paragraph regarding Pintle injectors and I wrote the rest of the introduction. The pilot-scale testing was directed by Dr. Robin Hughes. I performed the analysis of the pilot-scale data and process simulations, and authored the results and discussion sections. With the exception of the equipment description (Dr. Robin Hughes) and fuel description (Bruce Clements), I authored the methodology section as well.

For Chapter 5, I authored the paper. Dr. Robin Hughes directed the pilot-scale testing. I performed the analysis of the pilot-scale data, the process simulations, and the sensitivity studies. I authored the results and discussion sections as well as the conclusions.

Signature: _____ Date:_____

Abstract

Production in Canada's oil sands has been increasing, with a projected rate of 4.5 million barrels per day by 2025. Two production techniques are currently used, mining and *in-situ*, with the latter projected to constitute ~57% of all production by that time. Although *in-situ* extraction methods such as Steam Assisted Gravity Drainage (SAGD) are less invasive than mining, they result in more greenhouse gas (GHG) emissions per barrel and require large amounts of water that must be treated and recycled with a make-up water requirement of about 10%. CanmetENERGY is developing a steam generation technology called the High Pressure Oxy-fired Direct Contact Steam Generator (HiPrOx/DCSG, or DCSG for short) that will reduce these water requirements and sequester GHGs. This study evaluates the technical feasibility of this technology using process simulations, bench-scale testing, and pilot-scale testing.

At first, a method in which to integrate the DCSG into the SAGD process was presented and process modeling of expected system performance was undertaken. The process simulations indicated that DCSG decreased the energy intensity of SAGD by up to 7.6% compared to the base SAGD case without carbon capture and storage (CCS), and up to 12.0% compared to the base SAGD case with CCS.

Bench-scale testing was then performed using a pressurized thermogravimetric analyzer (PTGA) in order to investigate the effects of increased pressure and high moisture environments on a Canadian lignite coal char's reactivity. It was found that under reaction kinetic-controlled conditions at atmospheric pressure, the increased addition of steam led to a reduction in burning time. The findings may have resulted from the lower heat capacity and higher thermal conductivity of steam compared to CO_2. At increased pressures, CO_2 inhibited burnout due to its higher heat capacity, lower thermal conductivity, and its effect on C(O) concentrations on the particle surface. When steam was added, the inhibiting effects of CO_2 were counteracted, resulting in burnout rates similar to pressurized O_2/N_2 environments. These preliminary results suggested that the technology was feasible at a bench-scale level. Conflicting literature between bench-scale

and pilot-scale studies indicated that pilot-scale testing would be advantageous as a next step.

At the pilot-scale, testing was performed using n-butanol, graphite slurry, and n-butanol/graphite slurry mixtures covering lower and upper ends in fuel reactivity. It was found that stable combustion was attainable, with high conversion efficiencies in all cases. With the n-butanol, it was possible to achieve low excess oxygen requirements, which minimizes corrosion issues and reduce energy requirements associated with oxygen generation. With graphite slurry, it was found that it was possible to sustain combustion in these high moisture environments and that high conversion was achieved as indicated by the undetectable levels of carbonaceous materials observed in downstream equipment.

Overall, these studies indicate that DCSG is technically feasible from the perspectives of energy and combustion efficiencies as well as from a steam generation point of view. Future work includes the investigation of possible corrosion associated with the product gas, the effect of CO_2 on bitumen production, the nature of the mineral melt formed by the deposition of the dissolved and suspended solids from the water in the combustor, and possible scaling issues in the steam generator and piping associated with mineral deposits from the dissolved and suspended solids in the produced water is recommended.

Sommaire

La production de pétrole dans les sables bitumineux du Canada augmente continuellement et le taux est prédit d'atteindre 4.5 million de barils par jour en 2025. Présentement, il y a deux techniques de productions utilisées: l'exploitation minière et l'exploitation *in-situ*. L'exploitation *in-situ* est projeté de constituer ~57% de la production par ce temps. Bien que les méthodes d'exploitation *in-situ*, tel que Steam Assisted Gravity Drainage (SAGD) ne soit aussi invasive que l'exploitation minière, cette forme de production entraîne plus d'émissions de gaz à effet de serre (GES) par baril et nécessite une énorme quantité d'eau. De plus, l'eau doit être traitée et recyclée avec 10% d'eau d'appoint. CanmetENERGY est en train de développer une technologie de génération de vapeur appelée High Pressure Oxy-fired Direct Contact Steam Generator (HiPrOx/DCSG, ou DCSG) qui a pour but d'enfermer les GES, éliminer la majorité des traitements d'eau et réduire le montant d'eau d'appoint. Cette recherche évaluera la possibilité de réalisation de cette technologie à l'aide de simulations et d'essais à l'échelle laboratoire et pilote.

Premièrement, une méthode pour intégrer le DCSG dans le procédé SAGD est présenté et la modélisation et simulation du procede est performé pour évaluer sa performance. La résultats indiquent que DCSG peut réduire l'intensité énergique par 7.6% comparé avec un processus SAGD sans le capture et stockage du carbone (CSC) et jusqu'à 12.0% comparé avec un processus SAGD avec le CSC.

Des essais à l'échelle laboratoire ont été effectués en utilisant un analyseur thermogravimétrique pressurisé afin d'investiguer les effets d'augmentation de pression et d'un environnement à niveau d'humidité élevé sur la réactivité de char de charbon lignite canadien. A pression atmosphérique, sous contrôle de la cinétique de la réaction, l'addition de la vapeur d'eau a réduit la durée de la combustion. Ce résultat est probablement due à la capacité calorifique inférieure et la conductivité thermique supérieure de la vapeur comparé au CO_2. Dans un environnement O_2/CO_2, l'impact de la pression sur la capacité calorifique, la conductivité thermique et sur la concentration de

C(O) à la surface des particules inhibe le taux de réaction. Par contre, lorsque la vapeur d'eau est ajoutée, les effets inhibant du CO_2 sont contrés et les taux de réactions sont similaires à ceux dans des environnements d' O_2/N_2 pressurisés. Ces résultats préliminaires démontrent le potentiel de cette technologie à l'échelle laboratoire, mais des tests dans un environnement réactif et hydrodynamique plus réel à l'échelle pilotes sont nécessaires comme prochaine étape.

À l'échelle pilote, des expérimentes de combustion avec n-butanol, de graphite, et des mélanges de n-butanol et graphite ont été performés. Une combustion stable avec des conversions élevées ont été obtenues pour tous les cas. Avec le n-butanol, il a été possible de minimiser l'oxygène en excès et donc réduire le potentiel de corrosion et l'énergie associée avec la production d'oxygène.

Globalement, ces études ont indiqué que DCSG est techniquement faisable. Travaux futures vont investigués la corrosion associée avec les produits gazeux, l'effet du CO_2 sur la production du bitume, la nature des minéraux fondues dans la chambre de combustion et la nature des dépositions minéraux dans le générateur de vapeur et la tuyauterie.

Acknowledgements

First and foremost, I would like to thank my supervisor at CanmetENERGY, Bruce R. Clements, and my thesis co-supervisors Dr. Arturo Macchi and Dr. Edward J. Anthony for providing guidance, and their help in producing this thesis.

I would also like to thank my friends and colleagues at Natural Resources, CanmetENERGY for their passion, dedication, and guidance. Thanks to Ted Herage, Richard Pomalis, and Ligang Zheng for their guidance and leadership. Thank you to Dr. Robin Hughes and David McCalden as they were integral in operating the pilot-scale reactor and PTGA. Special thanks are due to Francine Verdon for her help in running the PTGA and to Jeffery Slater and Ryan Burchat for their help in running the pilot-scale reactor. Thanks also to Robert Symonds, Ajae Hall, Robert Dureau, and Terry Giddings who were always there to help when I was in a jam; as well as the characterization lab, and many more at the CanmetENERGY Bell's Corner's complex.

Industry colleagues that I would like to acknowledge include: Todd Pugsley and Gary Bunio of Suncor, and Paul Sudlow of Cavalier Energy Inc. for their direction and help navigating the literature.

I am indebted to my family and friends for their care and encouragement. Thanks to my father and mother for their advice and insights when times were difficult, and my two sisters who were always there to listen and help out. I would like to thank my friends Jeffery Butson, Susan Behan, Andrew Croskery, Alex Mullen, Grant Rivard, Veronica Wajda, and many more who have always supported me, listened to my grievances during hard times, and kept me going right to the end.

Lastly, I would like to thank the Panel on Energy Research and Development (PERD) the Clean Energy Fund (CEF) and the ecoEnergy Innovation Initiative (ecoEII) for their funding, and of course, the University of Ottawa for laying the foundations of my knowledge and providing me the opportunity to participate in this very fulfilling program.

Table of Contents

List of Tables

List of Figures

Chapter 1. Introduction

1.1. Motivation

With the rapid expansion of emerging economies such as China and India, global energy demand is projected to grow by more than one-third over the period between 2011 and 2035 [1]. Despite the growth in low-carbon sources of energy, fossil fuels will remain dominant in the global energy mix, with growth in oil consumption by emerging economies outweighing reduced demand in the Organisation for Economic Co-operation and Development (OECD) [1]. These increased demands will push oil use steadily higher, with projected oil demand rising from 87.4 million barrels per day (b/d) in 2011 to 99.7 million b/d in 2035 [1]. It is projected that the Organization of the Petroleum Exporting Countries' (OPEC) share in global oil production will rise to 50% in 2035 from its current share of 42% due to a surge in unconventional oil supplies. These unconventional supplies include: light tight oil in the United States, the oil sands in Canada, natural gas liquids, and deepwater production in Brazil [1].

Canada's unconventional oil sands comprise the vast majority of its proven reserves, which now rank third globally [2]. Production in the oil sands, which consist mainly of bitumen – a form of petroleum in solid or semi-solid state, sand, clay and water – is expected to increase from 1.74 mb/d in 2011 to 4.5 mb/d by 2025 [3].

Extraction of bitumen from the oil sands requires unconventional techniques which use two predominant methods: traditional pit mining on the surface, in which bitumen-rich earth is shovelled into trucks for separation at a processing facility; and *in-situ* production, in which steam is injected into underground bitumen formations to soften it so it can be pumped to the surface through wells [2]. *In-situ* techniques, which comprise mainly of Steam Assisted Gravity Drainage (SAGD) and to a lesser extent, Cyclic Steam Stimulation (CSS), are projected to make up 57% of total oil sands production by 2025, compared to 49% in 2011 [3].

Environmental concerns regarding oil sands development mainly center upon the relatively energy-intensive and carbon-intensive extraction and processing methods required [2]. Although calculations surrounding the climate impacts of oil sands development often yield different results, well-to-tank greenhouse gas (GHG) emissions are typically higher compared to conventional oil extraction methods [2]. In addition to production of GHGs, land use, water use, water quality, the impacts of toxic tailings ponds and the possibility of oil spills from pipelines are also cause for concern [2].

In-situ extraction methods such as SAGD are less invasive than mining, but will result in more greenhouse gas (GHG) emissions per barrel [4] and require large amounts of water that needs to be treated and recycled, with around a 10% make-up water requirement [5].

With energy demands increasing, the climate goal of having a 50% chance of limiting the global increase in average temperature to 2 °C in the long term, compared with pre-industrial levels is becoming more difficult and more costly with each year that passes [1]. If the world is to achieve this goal, no more than one-third of proven fossil fuel reserves can be consumed prior to 2050, unless carbon capture and storage (CCS) technology is widely developed [1]. With 22% of carbon reserves related to oil and 15% to gas these findings underline the importance of CCS as a key option to mitigate CO_2 emissions [1].

Oil sands development is inevitably going to increase in order to keep up with the world's growing energy demand, with SAGD projected to comprise the majority of production in the future. The motivation for this study is to propose and investigate the feasibility of a technology that will reduce GHG emissions and water requirements of the SAGD process to help ensure that oil sands development proceeds in an environmentally responsible manner.

1.2. Relevant Technologies

1.2.1. Steam Assisted Gravity Drainage (SAGD)

SAGD is a process in which steam is injected into a horizontal well to deliver heat to bitumen deep underground. The heat reduces the bitumen viscosity so that it can flow

more easily. Gravity then causes the bitumen to flow down to a second horizontal well positioned below the injector so it can be produced to the surface [6]. The SAGD horizontal well pairs are illustrated in **Figure 1.1**. The produced fluids are separated into bitumen, water, and non-condensable gases. The water is treated and then recycled back to the steam generator to once again produce steam [7].

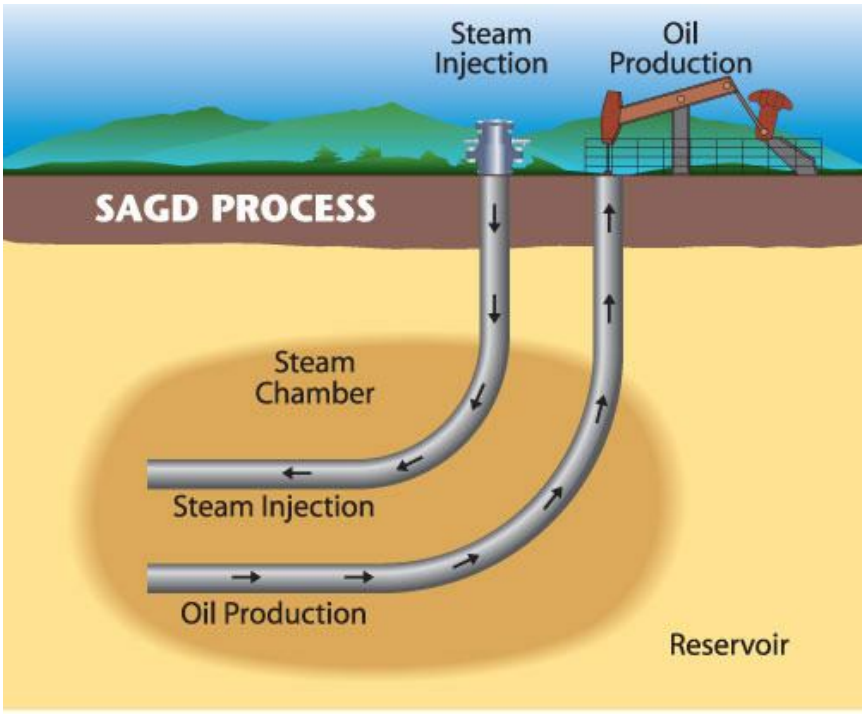

Figure 1.1. – SAGD horizontal well pairs [8]

There are two predominant types of steam generators encountered in SAGD facilities: once through steam generators (OTSGs) and circulating drum boilers [9]. This study focuses on the facilities using OTSGs. These boilers are typically natural gas fired and thus emit significant amounts of GHGs [4]. OTSGs typically operate at 10, 000 kPa [10] and produce steam with a vapour phase fraction of around 0.8 [7]. The OTSGs require certain feed water specifications resulting in the need for water treatment plants [7]. The combined water losses associated with the low vapour phase fraction and water treatment plants result in disposal requirements of around 3-5% [11] and make-up water requirements of 10-20% [5]. Further details regarding the SAGD process are presented in **Chapter 2**.

A technology designed to reduce the environmental impacts of SAGD should incorporate CCS, reduce water treatment requirements, reduce disposal requirements, and reduce make-up water requirements. The steam generator is thus an ideal unit operation to be replaced because it is the piece of equipment that dictates the emissions, treatment requirements and disposal requirements of the SAGD process.

1.2.2. High Pressure Oxy-fired (HiPrOx) Direct Contact Steam Generation (DCSG)

With regards to CCS, traditional air-fired combustion systems produce low flue gas CO_2 concentrations, making them unsuitable for direct sequestration. Oxy-fired combustion, in which a mixture of O_2/CO_2 is used instead of air to produce a CO_2 rich stream (as high as 95 %) has emerged as a promising new technology [12]. The enriched CO_2 stream is achieved by feeding the combustor with an oxygen-rich stream and recycled flue gases [13]. An in-depth discussion of oxy-fuel combustion will not be included here, but relevant information can be found in the book entitled "Oxy-fuel combustion for power generation and carbon dioxide capture" [14].

Pressurized oxy-fuel combustion systems offer better energy performance over conventional atmospheric oxy-fuel combustion power cycles [13]. Clements *et al.* [15,16], performed process simulations of a high pressure oxy-fired (HiPrOx) system, known as the ThermoEnergy Integrated Power System (TIPS). They found that pressurized combustion at 8000 kPa leads to a 5% absolute increase in net efficiency over ambient CO_2 capture-ready oxy-fired systems (24% and 29% net efficiencies for ambient and HiPrOx systems, respectively) [15,16]. Ente Nazionale per l'Energia Electrica (ENEL) has suggested that combustion at high pressures may increase both the burning rate of coal and heat transfer rates in the convective sections of the heat transfer equipment. A series of tests on a 5 MW_{th} scale combustor, working at 400 kPa, was undertaken to demonstrate these benefits [17-19]. Hong *et al.* performed a numerical analysis of a pressurized oxy-fuel combustion power cycle which included a flue gas purification and compression process. Compared to a base case of 110 kPa they found

that the use of pressurized combustion at 1000 kPa led to a 3% increase in net efficiency [13].

An alternative steam generation technology is known as direct contact steam generation. Direct contact steam generation (DCSG) is a process in which steam is produced by directly contacting water with a hot gas in order to cause it to evaporate without the use of boiler tubes. Direct contact air-fired steam generators produce steam by evaporating the water in a high pressure, high temperature flue gas stream [21]. One of the disadvantages of using air is it produces a lower quality steam due to dilution with nitrogen because the nitrogen acts to moderate the flame temperature, reducing the heat available for evaporation of water.

Since the product steam for SAGD applications goes directly into a well, the pressurized oxy-fuel combustion concept can be extended to include direct contact steam generation (DCSG). Similar to oxy-fuel, pure oxygen will be combusted with a solid, liquid, or gaseous fuel, but H_2O is used instead of CO_2 as a moderator. The use of pure oxygen will eliminate the moderation effect of nitrogen for air fired DCSG. If the combustion products are quenched to saturation temperature a product gas consisting of around 90% H_2O with the balance consisting of CO_2 with some impurities can be achieved. If this is applied to SAGD, the CO_2 will be injected directly underground with some being sequestered [21]. Since the combustion products of this technology are all converted to the useable product that is injected into the well, the thermal efficiency of this device will be close to 95-98%.

CanmetENERGY is developing a new steam generation technology known as the High Pressure Oxy-fired Direct Contact Steam Generator (HiPrOx/DCSG or simply DCSG) [22]. Further details regarding how this technology will be implemented in a SAGD process are provided in **Chapter 2**.

1.3. Thesis Objectives and Outline

The objective of this thesis is to evaluate the technical feasibility of CanmetENERGY's high pressure oxy-fired direct contact steam generator. This will be achieved by evaluating its feasibility from an energy perspective using process simulations; investigating whether the high steam environment will impede solid fuel combustion at the bench scale; evaluating the combustion performance of liquid fuels at the pilot-scale; and evaluating the combustion performance of solid fuels at the pilot-scale. These studies will provide insight into potential technical flaws that may exist in the system and suggest necessary future steps to commercialize this process.

In **Chapter 2** of the thesis, details regarding the existing SAGD process and the HiPrOx/DCSG will be discussed. A method in which to integrate the DCSG into the SAGD process will be presented. The SAGD/DCSG process will be evaluated using AspenTech HYSYS® 2006 and compared to the base SAGD case with and without CCS. The objective of this study will be to evaluate the energy intensity, total water requirements, make-up water requirements, water treatment requirements, equivalent natural gas requirements (i.e., energy requirements converted to an equivalent consumption of natural gas), and CO_2 emissions for DCSG firing natural gas, and petroleum coke compared to SAGD. These parameters will be used to compare DCSG against SAGD with and without combustion capture technology. These results will provide insight into the impacts DCSG will have on reducing the environmental footprint of oil sands development if it is adopted.

The second study (**Chapter 3**) investigates the reactivity of a Canadian lignite coal char in different HiPrOx environments (including DCSG) using a pressurized thermogravimetric analyzer (PTGA). Lignite was selected because it was a common solid fuel that could be used for both DCSG and another HiPrOx technology designed for power generation. Although this thesis does not focus on the HiPrOx power generation technology it was a subject of interest for CanmetENERGY at the time of this study. The objectives of the study were to investigate whether the high H_2O environments used in the DCSG process will significantly affect the combustion efficiency of the char; and to

determine how this effect will change with pressure. Specific background literature and theory regarding factors that affect coal char reactivity are presented. PTGA results of char combustion in different $O_2/CO_2/H_2O$ environments at various pressures are also presented. Further background theory regarding regimes of combustion and other related solid fuel combustion theory relevant to this study is provided elsewhere [23, 24].

The study performed in **Chapter 4** involves pilot-scale testing of DCSG with n-butanol. Butanol was selected as a suitable fuel for proof-of-concept due to its high volatility and the simplicity of liquid fuel injection systems compared to compressed gases. The objectives of the study were: to obtain operating data for the development of a HiPrOx/DCSG system as a proof-of-concept, to determine the maximum theoretical H_2O content that could be achieved in the product gas, to establish how low of an O_2 concentration in the product gas could be achieved without significantly affecting flame stability and formation of CO, and to study the effect of nitrogen in the oxidant on the formation of NO_x. It was also important to maximize the attainable H_2O content in the product gas in order to minimize energy intensity (latent heat produced per unit of fuel consumed) and to maximize the partial pressure of H_2O because lower partial pressure will reduce the saturation temperature, and thus, reservoir temperature, which may reduce bitumen production [21]. Flame stability and CO formation were investigated because they indicate the conversion efficiency of the process and provide insight into how easily the process can be controlled at the commercial scale. The formation of NO_x was studied because it has the potential to condense and form nitric acid in downstream piping which may lead to corrosion issues.

The fourth study (**Chapter 5**), investigates the combustion of graphite and graphite/butanol mixtures at the pilot-scale. Graphite/butanol mixtures were selected because certain combinations can represent the range of proximate analyses of waste fuels and it serves as a proof-of-concept that fuels with very little volatile matter and relatively inert chars, such as graphite and petroleum coke, can be used within the HiPrOx/DCSG environment. The objectives of this study were: to obtain operating data for the development of a high pressure oxy-fired direct contact steam generator system using low volatile fuels, to examine the effect of hydrogen-to-carbon ratio in the fuel on

the saturated gas product composition, to determine the effect of volatile content on flame stability and CO formation, and to measure any residual fuel as an indication of the combustion efficiency. These trends were studied to provide insight into the effect of fuel on operating conditions and to prove that highly unreactive fuels will combust in this environment.

Following the four main studies performed in this thesis, the results are summarized and conclusions are drawn about the feasibility of this process in **Chapter 6**. Recommendations regarding desired operating conditions and factors that require further investigation are also made.

1.4. References

[1] International Energy Agency. World Energy Outlook 2012, Paris, France: IEA Publications; November 2012. p. 23-35.

[2] Canada – Analysis [internet]. Washington DC, USA: U.S. Energy Information Administration – [cited 2013 Apr]. Available from: http://www.eia.gov/countries/cab.cfm?fips=CA.

[3] Canadian Association of Petroleum Producers. Crude oil: forecast, markets & pipelines. 2012 June. 7 p.

[4] Bohm M, Goold S, Laux S, Neu B, Sharma A, Aasen K. Application of oxy-fuel CO_2 capture for in-situ bitumen extraction from Canada's oil sands. Energy Proc. 2011;4:958-965.

[5] Alberta Government. In-situ process steam assisted gravity drainage. 2013 Feb. 1 p.

[6] Learn about energy regulation: in-situ impacts. [internet]. Calgary, Alberta, Canada: Energy Resources Conservation Board (ERCB) – [cited 2013 Apr]. Available from: http://www.ercb.ca/learn-about-energy/oilsands/insitu.

[7] Pedenaud P, Michaud P, Goulay C. Oily-water treatment schemes for steam generation in SAGD heavy-oil developments. Proceedings of the 2005 International Thermal Operations and Heavy Oil Symposium; 2005 Nov 1-3; Calgary, Alberta, Canada.

[8] Steam assisted gravity drainage (SAGD) [internet]. Calgary, Alberta, Canada: The Oil Sands Developers Group – [cited 2013 Apr]. Available from: http://www.oilsandsdevelopers.ca/index.php/oil-sands-technologies/in-situ/the-process-2/steam-assisted-gravity-drainage-sagd/.
[9] Heins, WF. Operational data from the world's first SAGD facilities using evaporators to treat produced water for boiler feedwater. J Can Pet Tech. 2008;47(9):32-39.
[10] Butler RM. Steam recovery equipment and facilities (Chapter 8). In: Butler RM, editor. Thermal recovery of oil & bitumen. New Jersey: Prentice-Hall, Inc.; 1991. p. 368
[11] Central processing facility (Part C5). In: Application for approval of the Devon Jackfish 3 project volume 1 – project description. 2010 Aug; p. 35–73 [internet]. Calgary, Alberta, Canada: Devon NEC Corporation – [cited 2013 Mar]. Available from: http://www.devonenergy.com/downloads/mainmenu.pdf
[12] Tan R, Santos S, Spliethoff H, G23/y/2. IFRF Report 2006.
[13] Hong J, Chaudry G, Brisson JG, Field R, Gazzino M, Ghoniem AF. Analysis of oxy-fuel combustion power cycle utilizing a pressurized coal combustor. Energy. 2009;34:1332.
[14] Zheng L, editor. Oxy-fuel combustion for power generation and carbon dioxide (CO2) capture, Cambridge: Woodhead Publishing; 2011. p. 207, 211.
[15] Clements BR, Zheng L, Pomalis R, Next generation oxy-fired systems: potential for energy efficiency improvement through pressurization. Proceedings of the 3rd international conference on energy sustainability: San Fransisco, California, USA; 2009.
[16] Zheng L, Pomalis R, Clements BR. Technical feasibility study of TIPS process and comparison with other CO2 capture power generation processes. Proceeding from the 32nd international technical conference on coal utilization and fuel systems: Clearwater, FL, USA; 2007.
[17] Benelli G, Malavasi M, Girardi G. Oxy-coal combustion process suitable for future and more efficient zero emission power plants. Proceeding from the PowerGen Europe conference and exhibition: Madrid, Spain; 2007.
[18] Benelli G, Girardi G, Malavasi M, Saponaro A. ISOTHERM®: a new oxy-combustion process to match the zero emission challenge in power generation.

Proceeding from the 7th high temperature air combustion and gasification international symposium: Phuket, Thailand; 2008.
[19] Gazzino M, Benelli G. Pressurized oxy-fuel combustion for future zero emission power plants: process design and energy analysis. Proceedings from the 2nd international conference on energy sustainability: Jacksonville, FL, USA; 2008.
[20] Clements B, Pomalis R, Zheng L, Herage T. High pressure oxy-fuel (HiPrOx) combustion system (Chapter 13). In: Zheng L, editor. Oxy-fuel combustion for power generation and carbon dioxide (CO_2) capture, Cambridge: Woodhead Publishing; 2011. p. 273–292.
[21] Gates ID, Bunio G, Wang J, Robinson B. Impact of carbon dioxide co-injection on the performance of SAGD. Proceedings of the 2011 World Heavy Oil Congress; 2011 Mar 14 -17; Edmonton, Alberta, Canada.
[22] Clements B, inventor; Her Majesty the Queen in Right of Canada as Represented by the Minister of Natural Resources, assignee. High pressure direct contact oxy-fired steam generator. Unites States patent US 20110232545A1. 2011 Aug 29.
[23] Roberts DG. Intrinsic reaction kinetics of coal chars with oxygen, carbon dioxide and steam at elevated pressure [dissertation]. Newcastle, Australia: University of New Castle; 2000.
[24] Field MA, Gill DW, Morgan BB, Hawksley PGW. Combustion of coal. Surrey, England: Cheney & Sons Ltd.; 1967.

Chapter 2. Direct Contact Steam Generation (DCSG) using High Pressure Oxy-firing (HiPrOx) for Steam Assisted Gravity Drainage (SAGD) Application

Bruce R. Clements[a,*], Paul Emanuel Cairns[a], Ted Herage[a], Robin Hughes[a], Ligang Zheng[a], Arturo Macchi[b], Edward J. Anthony[c]

[a]Natural Resources Canada, CanmetENERGY, 1 Haanel Dr., Ottawa, Ontario, Canada, K1M 1M1

[b]Faculty of Chemical and Biological Engineering, University of Ottawa, 161 Louis Paster St., Ottawa, Ontario, Canada, K1N 6N5

[c]School of Applied Sciences, Cranfield University, College Rd., Cranfield, Bedford MK43 0AL, United Kingdom

In submission to the Journal for Canadian Petroleum Technology (JCPT) 2013

2.1. Abstract

High pressure direct contact steam generation can be attained by the oxy-combustion of hydrocarbon fuels with the injection of liquid water. This process can produce streams of about 90% steam with the remainder being CO_2, for processes where the steam purity is less important, such as steam assisted gravity drainage (SAGD) for *in-situ* oil production within the Canadian oil sands. The thermal efficiency for this type of technology is close to 100% because the combustion products are all injected into the reservoir with potentially positive effects on reservoir behaviour. Using this process, any CO_2 that does not stay in the bitumen reservoir can be separated through flashing of the produced fluids after they have come to the surface and recycled back to the combustor with the produced gas. Water used within this system can have high solids content and hydrocarbon contamination because the equipment is relatively insensitive to the quality of the water used. The material presented in this document includes: process modeling of expected system performance and aspects of a process design approach for which this equipment could be applied to SAGD. The process simulations indicated that for DCSG using petroleum coke and DCSG using natural gas, respectively: produced oily water treatment can be reduced by about 56.3% and 52.1%, produced water treatment is eliminated for both cases, total water-to-oil ratio is decreased by around 2.9% and 7.7%, and make-up water requirements per barrel of oil are reduced by 37.5% and 100%. Energy intensity decreased by 3.6% and 7.6% compared to the base SAGD case without CCS, and by 8.2% and 12.0% compared to the base SAGD case with CCS. A sensitivity analysis found that the results were not sensitive to changes in the assumed fraction of CO_2 sequestered in the well.

Keywords: Heavy Oil, Bitumen, Steam generation, Oxy-fuel, SAGD, CCS

2.2. Introduction

2.2.1. Canadian Oil Sands

The Canadian oil sands located in Alberta consist of deposits of bitumen with sand, clay and water. This resource is the largest portion of the total Canadian oil reserves. Canada has the third largest oil reserves in the world, with 95% associated with the oil sands [1].

The recovery, extraction and processing of oil sand bitumen to usable product is an energy intensive process resulting in large associated greenhouse gas (GHG) emissions. These deposits are currently processed using either surface mining, which produces approximately 55% of the bitumen, or *in-situ* techniques, producing the remaining 45%. There are pros and cons to each approach from an environmental perspective. Surface mining requires less energy and therefore has lower CO_2 emissions. *In-situ* techniques have a smaller direct-land footprint [2].

Typical *in-situ* production methods include steam assisted gravity drainage (SAGD) and cyclic steam stimulation (CSS). The extraction of bitumen with either of these methods requires the use of steam. *In-situ* techniques such as SAGD require vast quantities of high pressure steam supplied by either Once Through Steam Generator (OTSG) boilers or conventional circulating boilers [3]. OTSG boilers are an adaptation of the industrial boiler that allows water of lower quality to be used as feed water. These OTSGs generally produce steam with a vapour phase fraction of 80%, meaning that there may be 20% saturated water included in the product [4]. Traditional, indirectly heated boiler systems require extensive water treatment to remove impurities. The thermal efficiency of these devices is typically between 75-80%. The thermal losses consist mostly of sensible heat associated with the dry flue gases and the latent heat associated with the uncondensed moisture exiting through the stack.

The net fresh water requirement for mining processes is on average 3.1 barrels of fresh water per barrel of oil produced but can range from 2-6. *In-situ* production methods require 0.4 barrels of fresh water per barrel of oil because over 90% of the water is

reclaimed and recycled. Given the high production rates, this still amounts to large quantities of fresh water make-up using traditional steam generation methods [5].

Conventional oil sands processing generates wastewater tailing ponds which are usually contaminated with hydrocarbons and solids, present in both suspended and dissolved forms. Although boilers require very large amounts of water, water from process waste water streams and waste water ponds are not suitable due to their poor quality. The result is that clean water sources are consumed and more contaminated water is produced, exacerbating the problem. In addition, boilers exhaust air pollution including large amounts of greenhouse gas emissions and other emissions.

2.2.2. Direct Contact Steam Generation

Direct contact steam generation (DCSG) is an attractive technological pathway to perform greenhouse gas control through carbon sequestration in the oil sands using either *in-situ* or mining operations. It has the potential to address many of the other associated oil sands environmental issues related to water use, wet tailings and acid gas emissions. Early publications regarding direct contact steam generation [6] noted its advantages as being the production of economic steam, low water treatment requirements, the ability to fire all types of hydrocarbon slurries, fewer water treatment requirements and co-production of CO_2 that can reduce oil viscosity further.

Direct contact air-fired steam generators and downhole steam generators produce steam by evaporating water in a high pressure, high temperature flue gas stream without the use of boiler tubes. They have been available for a number of years with several demonstrations having been carried out with relatively positive results [7]. The major advantages of the air-fired DCSG systems compared with traditional steam generation include smaller and more portable units, lower capital costs, higher energy efficiency and the ability to use lower quality water. The disadvantages include the production of lower purity steam due to dilution with nitrogen, non-condensability of the nitrogen fraction and production of carbonic acid leading to potential corrosion problems [8-10].

The use of oxygen in place of air for combustion in DCSG addresses the nitrogen related issues allowing production of higher purity steam while maintaining the advantages of the air-fired units. The additional benefits of oxy-fired DCSG technologies over air fired DCSG technologies are: smaller equipment size, greater portability, ability to more easily separate and capture CO_2, higher purity steam production and the ability to use waste water. The disadvantage is the requirement for oxygen supply, including the need for an air separation unit (ASU).

Many configurations of DCSG are oriented towards the use of natural gas as opposed to solid fuels [11]. It is believed that the economics of direct contact steam generation can be improved with the use of solid fuels. Solid fuels including asphaltene, petroleum coke, bitumen and coal, have been suggested as possible replacements of predominantly natural gas used within the oil sands industry [12]. CanmetENERGY uses a reactor design based on slagging gasifiers so that it can more easily handle solid fuels and waste water having large quantities of solids [13].

The flue gas stream, mainly H_2O and CO_2, will be injected underground, resulting in the sequestration of a portion of the CO_2. The thermal efficiency of this device will be close to 100% because the combustion products are directly injected down-hole as a useable product stream, eliminating thermal losses associated with the flue gas that would go out the stack with conventional boilers. There is some evidence that CO_2 in the liquid phase assists with the oil reclamation [6], however, CO_2 in the gaseous phase is considered a non-condensable gas which may impede bitumen recovery [14, 15]. Further investigation into the effects of CO_2 injection into the reservoir is required.

2.3. Steam Assisted Gravity Drainage (SAGD) Process

2.3.1. The Conventional Steam Assisted Gravity Drainage Process Description

A simplified block flow diagram of a conventional SAGD process is presented in **Figure 2.1** The water cycle in the SAGD process has five (5) main sub-processes including steam generation, injection of steam into the bitumen reservoir, produced fluids separation, produced water de-oiling, and produced water treatment.

In the first stage, steam is created by combusting natural gas with air in an OTSG for plants that use traditional water treatment methods, or a conventional circulating drum boiler for plants using evaporators [16]. This study will focus on the OTSG style of plant. Within the OTSG, boiler feed water is converted into saturated steam (~80% vapour phase fraction). The required boiler feedwater specifications are shown in **Table 2.1**. The saturated steam is sent to a flash separation train where the vapour phase fraction is increased to 100%. The steam is then injected into the well in order to produce oil [4, 17].

Table 2.1 – OTSG Boiler Feed Water Specification [4]

Item	Spec
Total hardness (mg/L $CaCO_3$)	<1
Barium (mg/L)	<0.1
Iron (mg/L)	<0.25
Free chlorine (mg/L)	<0.1
Oxygen (mg/L)	<0.02
pH	7.0-9.5
Silica (mg/L)	< 100
Total dissolved solids (mg/L)	< 12000
Free and emulsified oil and grease (mg/L)	<0.5

In the second stage, the steam enters the well and begins to heat up the bitumen, causing a reduction in viscosity. The condensed water and hydrocarbons then flow by gravity to the production well located 3-5 m below the injection well. The produced fluids are pumped up to the surface using progressive cavity pumps [4, 17].

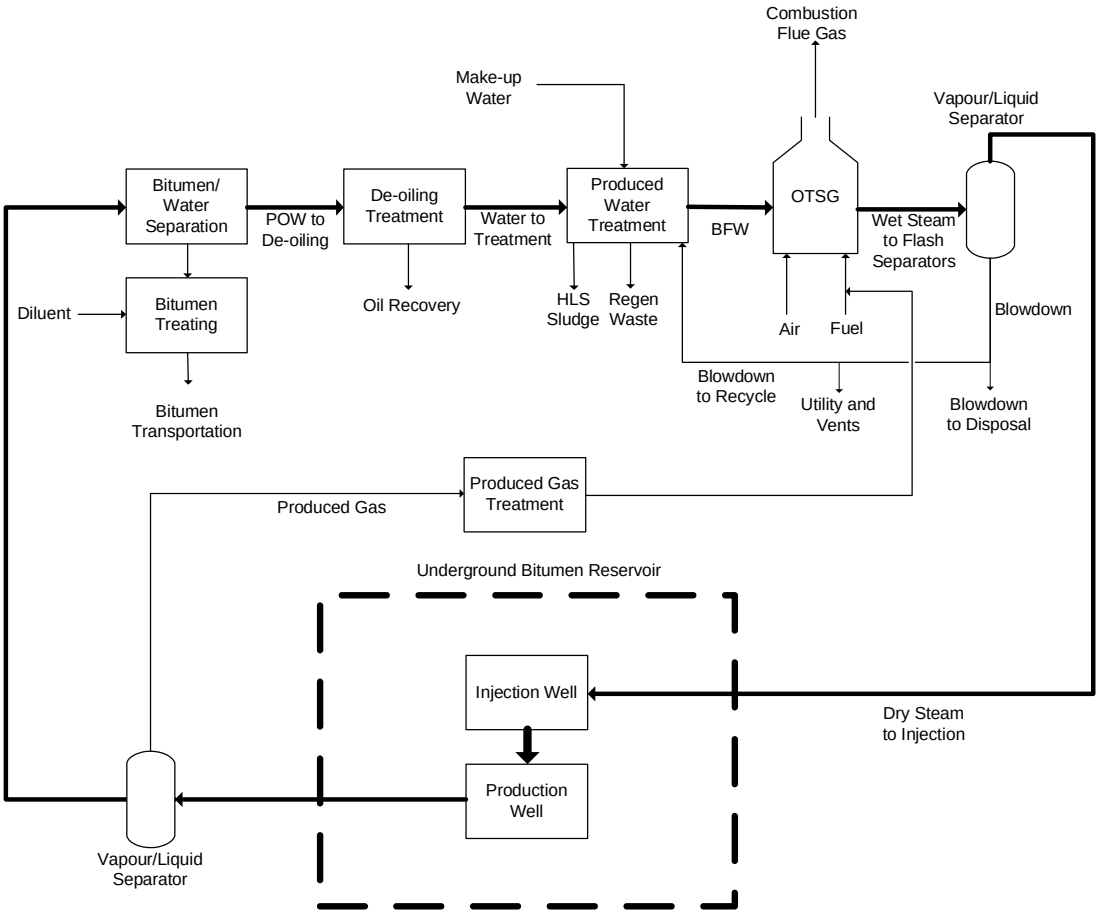

Figure 2.1 – Existing SAGD Block Flow Diagram

In the third stage of this process, the produced fluids are separated into produced gas, water and bitumen. The produced gas is flashed off, treated, and recycled back to the steam generator. The bitumen is sent to the bitumen treatment process where a diluent is added and it is treated to the required specifications for delivery to the upgrading facilities. The remaining water, typically containing around 1000 mg/L of oil [17], referred to as produced oily water (POW) is then sent to the fourth process known as de-oiling [4, 17].

In the fourth, de-oiling, stage of this process the POW undergoes treatment in order to reduce the concentration of hydrocarbons in the water. The de-oiled produced water (PW) typically leaves the de-oiling process with a hydrocarbon content of less than 5 mg/L [17]. Two examples of produced water composition are shown in **Table 2.2**.

Table 2.2 – Two Examples of Produced Water Composition [4]

Item	Example 1	Example 2
Free and emulsified oil and grease (mg/L)	<5[a]-1000[b]	<5[a]-1000[b]
Cations (mg/L)		
Na	1615.9	706.0
Ca	23.2	3.9
Mg	13.1	0.3
Ba	2.0	0.2
K	68.0	28.7
Fe	0	0.7
Anions (mg/L)		
Cl	1395.0	930.0
SO_4	2.0	1.0
CO_3	0.0	1.0
HCO_3	2130.0	332.0
Total dissolved solids (mg/L)	5249.3	2370.0
Total suspended solids (mg/L)	164.0	100.0
Hardness (mg/L $CaCO_3$)	112.0	11
pH (25 ºC)	7.9	8
Density (kg/m^3)	1003.2	1001
Silica (mg/L)	260	260

a - Design amount for PW [17], b – Design amount for POW [17]

In the fifth stage of this process, entitled produced water treatment, the PW is treated to remove the silica content, reduce the total suspended and dissolved solids (TSS and TDS, respectively), reduce the total hardness, and remove any remaining minerals and dissolved oxygen. The result is boiler feed water (BFW) suitable for steam generation in an OTSG [4]. Produced water treatment can be performed using either traditional methods (lime softening, filtration, ion exchange) or an evaporator [16]. This study only considers comparison with the traditional methods and not systems including evaporators.

2.3.2. SAGD process using High Pressure Oxy-fired (HiPrOx) Direct Contact Steam Generation (HiPrOx/DCSG)

A block flow diagram of the HiPrOx/DCSG process is presented in **Figure 2.2**. The combustor consists of a vessel that combusts a gaseous, liquid, or slurried solid fuel with pure oxygen and water. POW is injected into the combustor in order to generate steam and act as a temperature moderator to maintain flame temperatures below those required for material constraints. Combustor staging POW is injected downstream of the burner to quench the flue gas to around 850 °C and increase the steam concentration. It is expected that the high temperatures within this vessel will destroy any hydrocarbon contamination

within the POW, but this needs to be proven experimentally. The fuel ash and mineral matter in the water will deposit on the internal hot face of the combustor, melt, and flow out of the bottom as a mineral melt. The internals of the combustor are based on equipment used for slagging gasification and are thus expected to be highly tolerant to high solids from the fuel as well as in the injected water.

The flue gas leaving the combustor vessel enters the steam generator where PW, make-up water and the blowdown recycle are injected to further quench the flue gas to a desired vapour phase fraction. The latent heat of the flue gas vaporizes most of the quench water to produce a product gas of approximately 90% H_2O with the balance consisting mainly of CO_2 and some impurities. The gas passes through a demister and enters a flash drum in order to remove the liquid fraction. The product gas is injected into the well via a horizontal injector in order to produce oil.

The produced fluids are separated into produced gas, bitumen, and water. For this case, the produced gas will contain any CO_2 that was not sequestered in the well. Similar to the OTSG case the produced gas and produced CO_2 are re-compressed and injected back into the combustor as fuel. This recycle of the produced CO_2 means that this is a zero emission technology. For the purpose of this study, the produced CO_2 was treated as a separate stream to ease the analysis of its effect on the product gas.

Following the produced fluids separation, a portion of the POW is diverted to the combustor and the remainder is sent to de-oiling. This will result in a reduction of de-oiling treatment requirements. After de-oiling, the PW, blowdown recycle, and make-up water are directly injected into the steam generator, which completely eliminates the water treatment required for those streams. The use of tailings water as make-up water may be possible if it is injected into the combustor, but this will need to be demonstrated experimentally.

An ASU is added to the system, which will result in additional power requirements, but the combined effect of increased thermal efficiency and increased production of steam

from the hydrogen in the fuel will act to reduce overall fuel consumption which may possibly offset this energy penalty. Process simulations of the DCSG process were performed to quantify these competing effects on the energy intensity of this process.

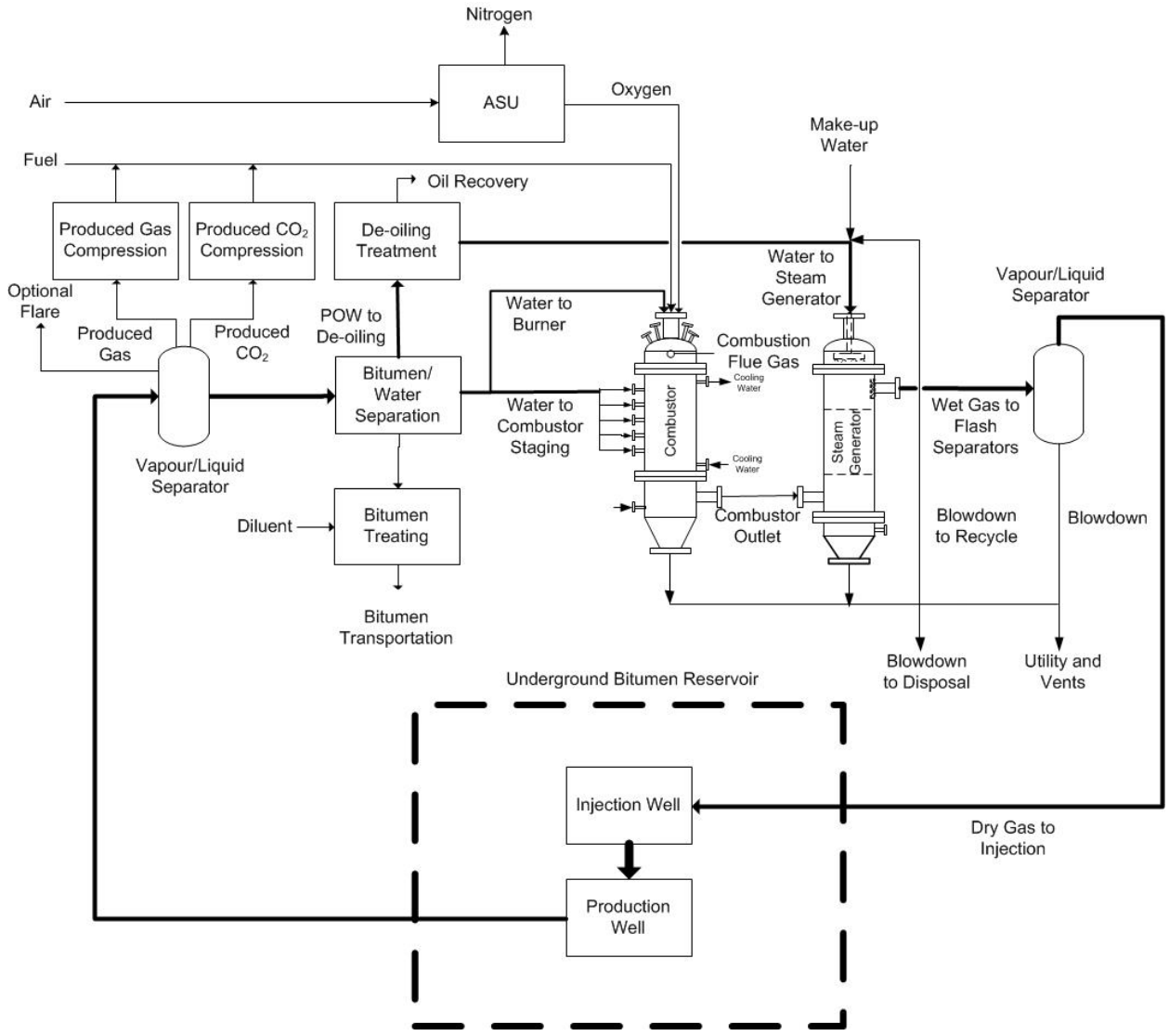

Figure 2.2 – Oxy-fired Direct Contact Steam Generation Block Flow Diagram

2.4. Methodology

Process simulations for three cases were performed using ApenTech HYSYS® 2006. The three cases include: a base OTSG SAGD case using the Devon NEC Corporation's Jackfish 3 application data [17,18], a HiPrOx/DCSG case using petroleum coke slurry as a fuel, and a HiPrOx/DCSG case using natural gas as a fuel. The purpose of the simulations was to compare: the water treatment capacity requirements for each stage (de-oiling, produced water treatment), the energy intensity, the equivalent natural gas consumption per barrel of oil produced, the total water requirements per barrel of oil produced, and the make-up water requirements per barrel of oil produced of the two DCSG cases against the base case with and without amine scrubbing. Since the DCSG process does not emit CO_2, the carbon capture requirement for the base case (% CO_2 captured) was determined by setting the net CO_2 emissions equal based on the CO_2 emitted from the process (OTSG) plus the CO_2 emitted from the utility requirements. This was done to account for CO_2 emissions associated with the electrical utility requirements of the ASU. The CO_2 emissions associated with utilities were calculated assuming the current Alberta energy mix (approximately 90% of electricity is derived from fossil fuels [19]) with CO_2 emissions per MW_e calculated using default settings in IECM-cs©. IECM-cs© (Integrated Environmental Control Model) is a computer-modeling program that performs systematic cost and performance analyses of emission control equipment at thermal power plants.

To determine the comparison basis for the three cases, it is necessary to take into account the effect that the non-condensable gases have on the latent heat of the product gas as the water condenses in the reservoir. A comparison that sets the mass flow of water into the OTSG and DCSG equal to one another would be inaccurate because it does not account for the down-hole thermal input of the non-condensable gases plus the additional creation of steam obtained from the hydrogen in the fuel. With these considerations in mind, the basis for comparison was to set the flow rate of steam down the well equal for all cases. Since the majority of the heat used to warm up the bitumen in the well is associated with the latent heat of steam in the injected gas, this basis of comparison is approximately the

same as making the thermal duty to the bitumen equal for all cases. Although a comparison based on thermal duty to the bitumen in the well would be ideal, the added complications of the well characteristics would make the material balance more difficult to close. This method allows the amount of water produced vs. the amount injected to remain constant for all cases, which eliminates unknowns involved with retention of water in the well and production of water from the well.

Using this basis, it was possible to calculate the fuel and oxidant requirements and perform a water mass balance on the process water. The energy requirements for the ASU and fuel pressurization were added to the total energy requirement as electrical utility requirements for the DCSG cases.

2.4.1. Modeling Assumptions

Table 2.3 presents the modeling assumptions used for this study. The data used for the base case process was based on the data presented in Devon NEC Corporation's Jackfish 3 application [17] to the Energy Resources Conservation Board (ERCB) unless otherwise specified. The Jackfish 3 plant is a typical SAGD plant using OTSG boilers. Regarding the effects of CO_2 in the well, it is difficult to quantify the solvent tendencies of the CO_2 that lower bitumen viscosity [14, 20], the effects of non-condensable gas on the total pressure in the well, and the migration of the gases to the top of the well that act as an insulating layer against the loss of heat which may result in more favourable steam-to-oil ratios [21]. When a reservoir modelling study of co-injection of methane with steam was performed, it was found that there was a significant decrease in oil production rates [15]. However, a recent modelling based study performed by Gates *et al*. [20] in which CO_2 was co-injected indicated that oil production rates and cumulative steam-to-oil ratio were only marginally lower. One of the main differences was the study by Gates *et al.* [20] allowed CO_2 to dissolve into both the oil and water phases in the reservoir. An experimental investigation into the effects of non-condensable gas (NCG) co-injection with steam in conditions typical for the field found that co-injection of NCG with steam (known as steam and gas push, or SAGP) can achieve oil rates comparable to or higher than those for SAGD, and with much lower steam requirements [21]. Furthermore, field

testing done by Yee and Stroich [22], in which they co-injected natural gas and steam during the wind down of a well found that the actual performance was substantially higher than the simulation prediction and the bitumen rates were even better than those predicted for the steam only cases. As a result of these findings, this study takes the middle ground between reservoir simulations and field testing and assumes that any effects of CO_2 injection on bitumen production will be negligible.

Table 2.3 – Modeling assumptions used

Parameter	SAGD	DCSG (Pet. Coke)	DCSG (Natural Gas)
Fuel supply pressure (kPag)[23]	6,200	0	6,200
Oxygen purity (mole%)	-	95.0	95.0
Combustor reactant delivery pressures (kPag)	0	12,500	12,500
DCSG heat losses to actively cooled wall (%)	-	5	5
Oxygen in combustion flue gas (mole%)	3.00	1.00[a]	0.01[a]
OTSG BFW delivery pressure (kPag)	12,000	-	-
Steam generator operating pressure (kPag)	11,000	11,000	11,000
Steam pressure to flash separator (kPag)	9,500	9,500	9,500
Reservoir pressure (kPag)	2,700	2,700	2,700
Reservoir temperature (°C)	15	15	15
Portion of injected CO_2 that is produced (%)[20]	-	20	20
Bitumen production (sm^3/h)	232	232	232

a – based on O_2 required for complete conversion from pilot-scale testing [24, 25]

2.4.2. Fuel Analyses

Table 2.4 presents the natural gas and produced gas compositions used for this study [26]. The natural gas delivery pressure was based on typical Alberta & Southern pipeline pressure delivery requirements [23]. **Table 2.5** presents the delayed petroleum coke fuel analysis that was used for this study [27].

Table 2.4 – Natural gas and produced gas specifications [26]

Property	Natural Gas	Produced Gas
Higher Heating Value (MJ/sm^3)	36.8	37.4
Lower Heating Value (MJ/sm^3)	33.4	33.9
Delivery Temperature (°C)	21.0	15.0
Delivery Pressure (kPag)	6200[23]	2700.0
Composition (mol%)		
N_2	1.21	1.21
CO_2	0.98	2.99
H_2O	-	4.58
C_1	97.63	89.56
C_2	0.07	0.06
C_3	0.03	0.03
i-C_4	0.02	0.02
n-C_4	0.02	0.02
i-C_5	0.02	0.15
n-C_5	0.03	0.25
C_6	-	1.18
H_2S	-	0.05
Total	100	100

Table 2.5 – Typical delayed petroleum coke fuel analysis [27]

Property	Value
Higher Heating Value (MJ/kg dry)	34.7
Lower Heating Value (MJ/kg dry)	34.0
Proximate Analysis (wt% d.b.)	
Volatile Matter	11.5
Fixed Carbon	87.5
Ash	1.0
Ultimate Analysis (wt% d.b.)	
Carbon	86.9
Hydrogen	3.2
Nitrogen	1.8
Oxygen	1.2
Sulfur	5.9
Ash	1.0

2.5. Results and Discussion

2.5.1. Simulation Results

The fuel requirements, oxidant requirements, product gas data associated with the DCSG, and steam data associated with the OTSG are presented in **Table 2.6**. The water mass balance for the three cases is presented in **Table 2.7**. All of the stream names used in

Table 2.6 and **Table 2.7** are based on those illustrated in **Figure 2.1** for the OTSG case and **Figure 2.2** for the DCSG cases.

Compared to the base case, both DCSG cases decreased fuel consumption because of the higher thermal efficiency and steam production from the hydrogen in the fuel. The H_2O content in the injected steam was higher for the DCSG natural gas case (95.0 mol% wet) than the petroleum coke case (91.1 mole% wet) because of the lower required excess oxygen and the higher hydrogen-to-carbon ratio in natural gas (33 wt%) compared to petroleum coke (4 wt%). The saturation temperature was lowest for petroleum coke because it produced the lowest partial pressure of H_2O. The base case had the highest saturation temperature because it is pure steam at the same total pressure.

A reservoir modeling study performed by Gates *et al.* [20] concluded that co-injection of up to around 15 mole% CO_2 in steam does not impact oil production rates significantly. They found that the cumulative oil volume produced remained unchanged for the first three years, with a drop of only about 10% at the end of the operation for a co-injected fraction of 15 mole%, and a drop of only 5% for a co-injected fraction of 5 mole%. They outlined that the similarity in cumulative oil volume produced is due to the solvent impact of carbon dioxide, which offsets the reduced saturation temperature caused by the partial pressure of CO_2 [20]. Their findings indicate that DCSG with natural gas will have less of an effect on cumulative oil production than DCSG with petroleum coke because it results in a product gas with a higher H_2O concentration and saturation temperature. The reduced fuel costs for the DCSG case will likely offset the lost revenue from decreased production over the life of the plant, especially considering that petroleum coke is currently considered a waste fuel that would be essentially costless [12]. A detailed economic analysis is not performed here and will be the subject of future work.

Table 2.6 – Product gas/steam data

Parameter	OTSG	DCSG (Pet-coke)	DCSG (Natural Gas)
Fuel	Natural Gas	Petroleum coke	Natural Gas
Fuel flow rate (kg/h)	-	36,680	-
Fuel flow rate (sm^3/h)	45,176	-	34,142
Produced gas flow rate (sm^3/h)	1,995	1,995	1,995
Produced CO_2 flow rate (kg/h)	-	23,359	12,710
Air flow rate (kg/h)	641,794	-	-
Oxygen flow rate (kg/h)	-	111,675	101,540
Combustion flue gas composition			
N_2 (mole%)	71.63	0.69	0.63
H_2O (mole%)	16.19	73.01	84.80
CO_2 (mole%)	8.20	24.04	13.84
O_2 (mole%)	3.06	1.00	0.01
SO_2 (ppm)	2	4963	3
Combustor outlet temperature	204[28]	850	850
Combustor outlet composition			
N_2 (mole%)	71.63	0.37	0.34
H_2O (mole%)	16.19	85.43	91.81
CO_2 (mole%)	8.20	12.98	7.46
O_2 (mole%)	3.06	0.54	0.01
SO_2 (ppm)	2	2679	2
Wet steam/gas vapour fraction	0.78	0.78	0.78
Wet steam/gas composition			
N_2 (mole%)	-	0.18	0.16
H_2O (mole%)	100.00	92.94	96.02
CO_2 (mole%)	-	6.29	3.62
O_2 (mole%)	-	0.26	0.00
SO_2 (ppm)	-	1298	1
Dry steam/gas to injection temperature (°C)	308	298	302
Dry steam/gas to injection pressure (kPag)	9500	9500	9500
Dry steam/gas vapour fraction	1.00	1.00	1.00
Dry steam/gas composition			
N_2 (mole%)	-	0.23	0.21
H_2O (mole%)	100.00	91.07	94.96
CO_2 (mole%)	-	7.95	4.58
O_2 (mole%)	-	0.33	0.00
SO_2 (ppm)	-	1556	1

The study performed by Gates *et al.* [20] also found that the produced CO_2 from the well is less than 20% of the injected amount, with the remainder being sequestered in the gas, oil, and water phases in the reservoir. They also stated that the amount of carbon dioxide

sequestered will be higher than that found in their simulations because they did not take mineral reactions into account. Based on this assumption it was found that DCSG using petroleum coke resulted in a higher amount of produced CO_2 from the well because of the high carbon content in the fuel that combusts to produce CO_2 compared to natural gas. This greater amount of CO_2 produced is recycled back to the combustor which also played a role in the lower H_2O concentration in the injected product gas because it increases the partial pressure of CO_2.

The water mass balance for the three cases is given in

Table 2.7. The de-oiling requirements are reduced by 52.1% and 56.3% for the DCSG natural gas and petroleum coke cases, respectively. De-oiling requirements are reduced most for the pet-coke case because its lower hydrogen-to-carbon ratio requires a larger portion of the steam in the injected product gas to come from evaporation of waste water as opposed to combustion products. Therefore, it will consume more water in the burner and combustion staging compared to natural gas.

Due to the steam created by combustion of the fuel, make-up water requirements were reduced by 100% and 38.8% for the DCSG natural gas and petroleum coke cases, respectively. For the natural gas case, the steam produced by combustion exceeded the make-up water requirements leading to a surplus of water (assuming blowdown to disposal is equal for all cases). Since it can be drawn from any part of the process, the implications of this surplus water are unclear. If a DCSG is constructed at an existing SAGD facility this surplus water could be used to provide make-up water for the conventional steam generators by diverting some of the POW from primary separation. If the DCSG is constructed at a new plant, it could be flashed to produce utility steam, some of the POW from primary separation could be treated to drinking water standards and sold, or it may be disposed of with the rest of the blowdown to disposal. Regardless of the fate of the surplus water, this case may eliminate make-up water requirements entirely, depending on the natural gas, produced gas, and reservoir characteristics.

The water cooling duty for the ASU can be estimated with the duty of the compressors (ASU power requirement) plus the duty associated with condensing any humidity in the inlet air. If it is assumed that an evaporator cooled ASU with a 2% make-up water requirement is used [29], the make-up water flow rate will range from approximately 50,000 - 70,000 kg/h. If an air-cooled closed-loop cooling system for the ASU is used there will be no make-up water requirements but there will be a marginal increase in power requirements mainly as a result of increased coolant temperature (1% per 3°C increase in coolant temperature) [30]. This study assumes that an air-cooled ASU is used. The condensed water from the inlet air is the major source of ASU water disposal requirements [30]. For this study, air at 21 °C and a relative humidity of 50% is assumed.

Table 2.7 – Water mass balance

Parameter	OTSG	DCSG (Pet-coke)	DCSG (Natural Gas)
POW from primary separation (kg/h)	665,580	665,580	665,580
Water from combustion of fuel (kg/h)	-	13,450	53,966
Water to burner (kg/h)	-	165,525	145,568
Water to combustor staging (kg/h)	-	208,961	201,354
POW to de-oiling (kg/h)	665,580	291,094	318,658
Make-up water (kg/h)	55,417	33,902	-6,615[a]
Blowdown (kg/h)	186,951	206,920	197,770
Blowdown to recycle (kg/h)	143,784	163,753	154,603
Water to treatment (kg/h)	865,580	-	-
PW to steam generator (kg/h)	-	483,060	462,031
Water losses			
Blowdown to disposal (kg/h)	43,167	43,167	43,167
HLS sludge (kg/h)	375	-	-
Regen Waste (kg/h)	8,333	-	-
Utility and Vents (kg/h)	3,542	3,542	3,542
ASU water disposal[b]	-	3,342	3,039
BFW (kg/h)	853,330	-	-
Wet steam/product gas to flash seperators (kg/h)	853,330	1,030,429	948,596
Dry steam/product gas to injection (kg/h)	666,379	823,509	750,826
Steam down well (kg/h)	666,379	666,223	666,223

a – This process case provides a surplus of water, b – Based on water condensation from air inlet to ASU, assuming 50% relative humidity for air at 20 °C.

An energy balance for the three cases is given in **Table 2.8**. For the reasons previously mentioned, the fuel heat input requirements were reduced by 23.4% and 22.6% for the DCSG natural gas and pet-coke cases, respectively. The additional heat from the CO_2 in the dry product gas slightly increased the amount of energy used to produce bitumen by

about 0.98% and 1.96% for natural gas and pet-coke, respectively. The increase is slightly higher for the pet-coke because of the larger fraction of CO_2. This increase in downhole heat may act to offset the lower saturation temperature of the diluted steam mixtures, but the net effect is unknown. For the case with CCS, the electrical utility combustion requirements increased by 66.8% for the natural gas case and 91.2% for the pet-coke case over the base case using amine scrubbing. Both of these utility requirements are associated with the ASU. The petroleum coke case had the highest ASU requirement because of the excess O_2 requirements that were assumed. The electrical requirements were converted to thermal requirements based on 35% of Alberta's electricity coming from natural gas and 55% from coal [19], with CO_2 emissions per MJ fuel consumed being 0.051 $kgCO_2/MJ$ (results from IECM-cs©) for natural gas and 0.091 $kgCO_2/MJ$ (results from IECM-cs©) for a sub-bituminous coal, both fired using a 33% efficient sub-critical Rankine Cycle. When all of the energy requirements are accounted for, the DCSG pet-coke case results in a 3.6% decrease and the natural gas case results in a 7.6% decrease in thermal energy compared to the base case without CCS. When CCS on the base case is considered, these numbers become 8.2% and 12.0%, respectively.

In summary, the zero emission DCSG process will have a similar energy requirement compared to the base SAGD case without CO_2 capture requirements and will be less energy intensive if CO_2 capture is added to a SAGD facility because of the major reductions in fuel requirements associated with the increased thermal efficiency and the additional steam produced from the combustion of the fuel.

Table 2.8 – Energy balance

Parameter	SAGD	DCSG (Pet-coke)	DCSG (Natural Gas)
Fuel heat input (MW_{th})	483	374	370
Integrated heat from produced fluids (MW_{th})[a]	122	122	122
Integrated heat from blowdown recycle (MW_{th})	54	58	56
Heat to well to produce bitumen (MW_{th})	511	521	516
Energy losses (MW_{th})[b]	108	23	17
Electricity for water treatment and utilities (MW_e)[c]	15	6	3
Electricity for ASU (MW_e)[d]	-	41	38
Electricity for natural gas compression (MW_e)	-	-	0.8
Electricity for produced gas compression (MW_e)	-	0.15	0.2
Electricity for produced CO_2 compression (MW_e)	-	0.61	0.3
Total electrical requirements, no CCS (MW_e)	15.0	47.8	41.7
Electricity for CO_2 capture (MW_e)	10.0	-	-
Total electrical requirements, with CCS (MW_e)[e]	25.0	47.8	41.7
Total base plant thermal energy required (MW_{th})	524	505	484
Total thermal energy required with CCS (MW_{th})	550	505	484

a – From reference heat balance, assuming produced fluids are the same for all cases [18], b – Includes input electrical energy for case with no CCS, c – Includes energy for pressurization of water, d – Based on an energy consumption of 371.2 kWh/tonne O_2 (95% pure at 125 bar) which was extrapolated from various references [31-33], e – Assuming MEA scrubbing using IECM-cs™ to determine kW_e/tonne of CO_2 captured

The CO_2 mass balance for the three cases is presented in **Table 2.9**. Both DCSG cases had zero CO_2 emissions from the process. The DCSG pet-coke case had the greatest CO_2 emissions from utilities at 35,429 kg/h because of the higher O_2 requirements for the ASU. The CO_2 capture requirements for the base case were determined such that its net CO_2 emissions were equal to the CO_2 emissions associated with utility requirements for the higher oxygen consuming DCSG petroleum coke case. In other words, the capture requirements for the OTSG case were set equal to the difference between the CO_2 emissions associated with the base SAGD plant plus its utility requirements and the CO_2 emitted as a result of the DCSG's utility requirements.

Table 2.9 – CO_2 mass balance

Parameter	OTSG	DCSG (Pet-coke)	DCSG (Natural Gas)
CO_2 from steam generators (kg/h)	87,198	142,124	78,508
Produced CO_2 from well (kg/h)	-	23,359	12,710
CO_2 emitted from process (kg/h)	87,198	0[a]	0[a]
CO_2 generated by process utilities[b] (kg/h)	11,147	35,429	30,930
CO_2 generated by CCS utilities[c] (kg/h)	7,241	-	-
OTSG CO_2 capture requirements[d] (kg/h)	70,158	-	-
Net CO_2 emissions (kg/h)	35,429	35,429	30,930

a – Produced CO_2 is re-compressed and directed back to the steam generator, b – Based on 35% of Alberta's electricity coming from natural gas and 55% from coal [19] with CO_2 emissions per MJ fuel consumed being 0.051 $kgCO_2/MJ$ (calculated using IECM-cs™) for natural gas and 0.091 $kgCO_2/MJ$ (calculated using IECM-cs™) for a sub-bituminous coal, both fired using a 33% efficient sub-critical Rankine Cycle, c – Solved iteratively based on OTSG capture requirements d - Amount of CO2 capture required from OTSGs to break even with DCSG using petroleum coke

The key parameters are presented in **Table 2.10**. When compared to the base case without CCS, the energy intensity was reduced by 3.6% for the DCSG pet-coke case and 7.7% for the DCSG natural gas case. When CCS was added to the base plant, these figures increased to 8.2% and 12.1%, respectively. Even if the cumulative bitumen production loss of 5% for the natural gas calculated by Gates *et al.* [20] were included, the energy intensity of this zero emission process will be very competitive on an energy intensity basis with the status quo and most competitive if CCS is implemented.

The total water to oil ratio is decreased by 2.9% and 7.7% for the pet-coke and natural gas cases, respectively, and the make-up water-to-oil ratio are reduced by 37.5% and 100% as well. Both of these findings result from the water produced by the combustion of the fuel, and the reduction in treatment losses due to reduced treatment capacity.

When the total thermal energy requirements are converted to equivalent natural gas consumption, both the pet-coke process and natural gas process are lower than the status quo. When CCS is considered, the natural gas case is up to 12.1% lower.

Table 2.10 – Key parameters

Parameter	SAGD	DCSG (Pet-coke)	DCSG (Natural Gas)
Equivalent sales oil thermal output (MW_{th})	3144	3144	3144
Energy intensity x 100, no CCS (MW_{th}in/MW_{th}out)[a]	16.66	16.06	15.38
Energy intensity x 100, with CCS (MW_{th}in/MW_{th}out)[a]	17.50	16.06	15.38
Water to oil ratio (sm^3 water/sm^3 bitumen)	3.11	3.02	2.87
Make-up water to oil ratio (sm^3 water/sm^3 bitumen)	0.24	0.15	0
Equivalent NG consumption, no CCS (sm^3/sm^3 bitumen)[a]	220.9	212.9	204.0
Equivalent NG consumption, with CCS (sm^3/sm^3 bitumen)[a]	232.1	212.9	204.0

a – includes thermal energy requirements for utilities

In summary, the DCSG process is very competitive from an energy intensity and material balance basis. To further evaluate this technology, pilot-scale testing using POW and PW is required to investigate scaling and corrosion issues as well as laboratory and field testing to confirm the effects of down-hole injection of CO_2 on bitumen recovery.

2.5.2. Sensitivity Analysis

In the HiPrOx/DCSG process, the produced CO_2 that comes up with the produced gas is compressed and re-injected into the combustor. Based on the reservoir modelling work performed by Gates *et al.* [20], it was assumed for this study that 20% of the CO_2 injected into the well would be produced. Since this assumption is based on a simulation rather than experimental evidence, and the fraction of produced CO_2 will affect the product gas composition, a sensitivity analysis in which the fraction of injected CO_2 that is not sequestered was varied from 10% to 65% was performed.

Figure 2.3 illustrates the effect of the fraction of injected CO_2 that is produced on the overall process energy intensity. The results indicate that an increase in the fraction of produced CO_2 will result in a range of energy intensity of approximately 0.1602 – 0.1623 (MW_{th}in/MW_{th}out) for the petroleum coke and 0.1535-0.1554 (MW_{th}in/MW_{th}out) for the natural gas. The rise is a result of increased fuel heat requirements to evaporate more water and increased utility requirements to compress the produced gas. Even if a produced fraction of 65% is assumed, the energy intensity for the petroleum coke is still less than the base case (0.1666) without CCS, indicating that this process scheme is very competitive no matter what fraction of injected CO_2 is produced.

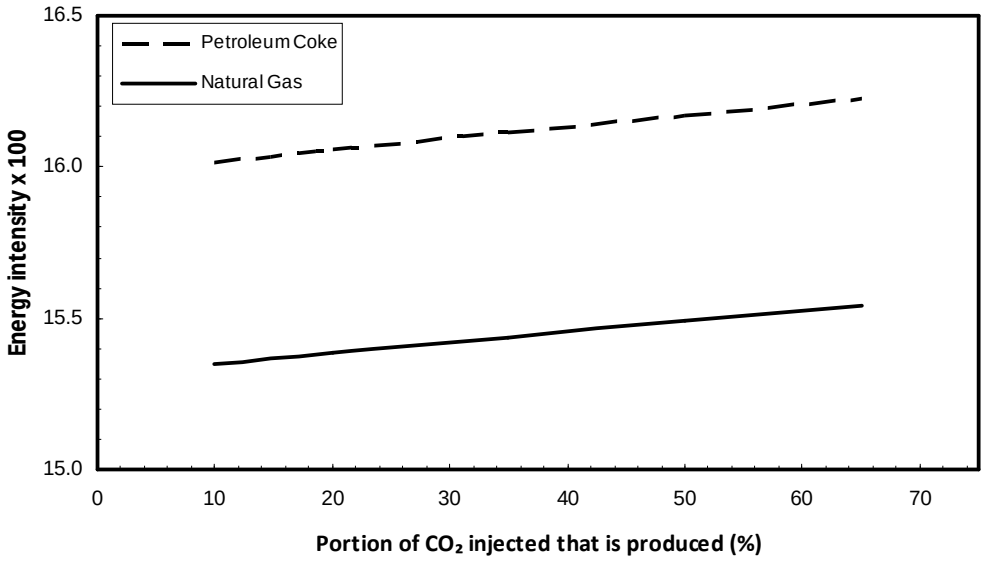

Figure 2.3 – Effect of produced CO_2 on process energy intensity

When the fraction of produced CO_2 is increased, the concentration of H_2O in the injected gas will decrease (**Figure 2.4**), causing the partial pressure and thus the saturation temperature to decrease. This will decrease the amount of latent heat contained in the injected gas that is used to produce the bitumen. The fraction of the heat delivered to the well, at a specific well temperature, is also affected by the produced CO_2 fraction as shown in **Figure 2.5**.

Figure 2.5 indicates that increasing the fraction of CO_2 produced resulted in a small increase in heat of approximately 2.06 MW_{th} or 0.40% for the natural gas and 3.68 MW_{th} or 0.71% for the petroleum coke. The fraction of produced CO_2 has a greater effect on the pet-coke process than the natural gas process because the petroleum coke has a higher carbon content, which produces more CO_2 per kg of fuel, which in turn, increases the amount of produced CO_2 that is recycled thus further increasing the partial pressure of CO_2 in the injected product gas.

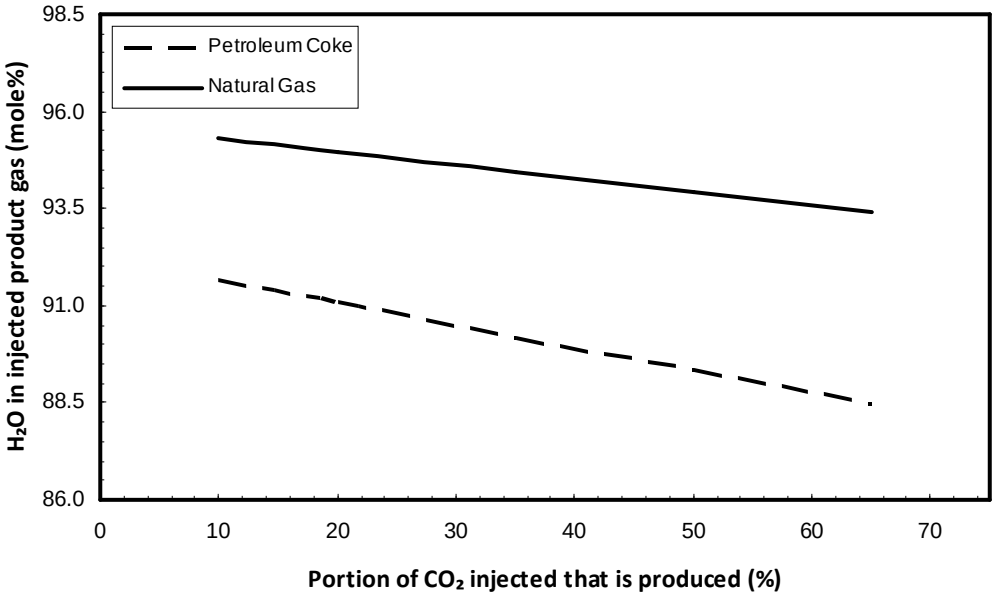

Figure 2.4 – Effect of produced CO_2 on the dry product gas composition

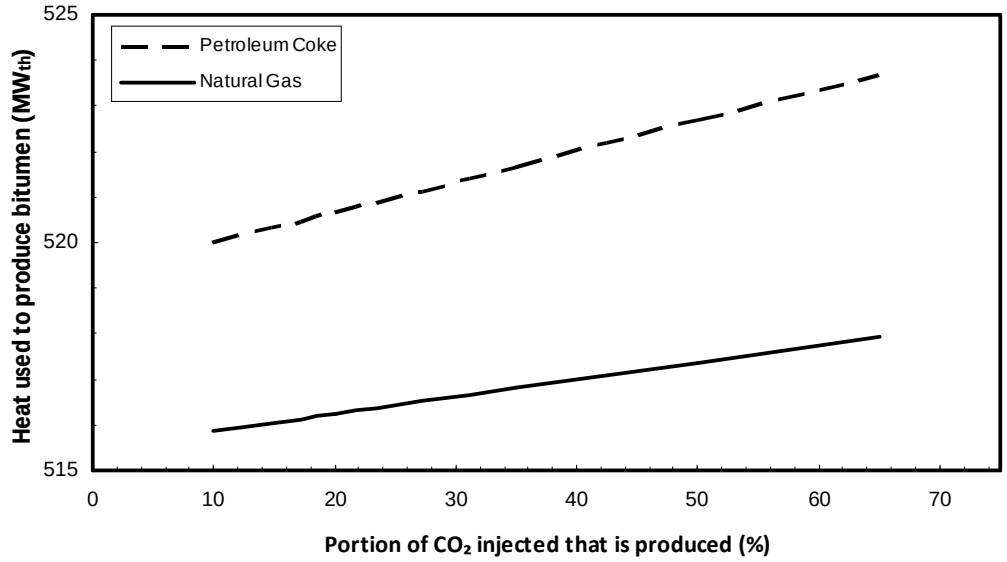

Figure 2.5 – Effect of produced CO_2 on the portion of heat in the injected stream used to produce bitumen for reservoir temperature assumed in this study

Figure 2.6 illustrates the effect of reservoir temperature on the heat used to produce bitumen for the pet-coke case normalized to the base case. Although it is not shown here, it is intuitive that as the reservoir temperature rises the heat released to the bitumen

becomes lower for all cases because the product gas is cooled less and the latent heat contribution drops as temperature rises (e.g. for base case reservoir temperatures of 15 °C and 150 °C, heat is around 511 MW_{th} and 409 MW_{th}, respectively). In order to isolate the effect of produced CO_2, the heat release was shown as a relative value by normalizing to the base case at the corresponding reservoir temperature as opposed to showing the absolute heat release.

From **Figure 2.6**, as the reservoir temperature increases, the portion of heat from the CO_2 becomes less significant compared to the latent heat of the condensing steam. Once the temperature exceeds around 110 °C, increasing produced CO_2 fraction results in decreased heat delivery to the well due to reduced latent heat of the steam fraction. Although these effects occur, they only seem to result in an approximate ±2% deviation indicating that they will not significantly impact the results.

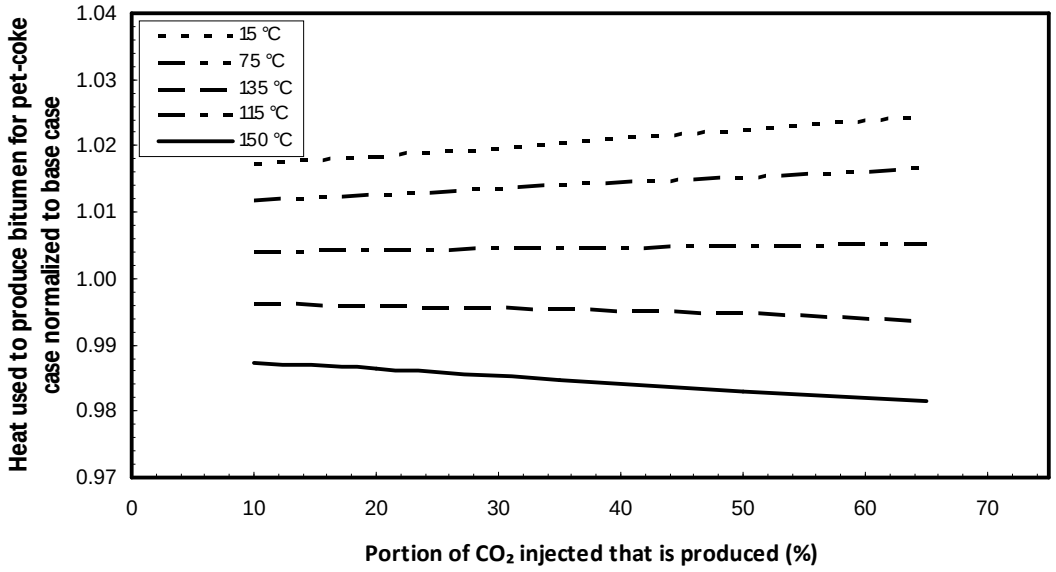

Figure 2.6 – Effect of produced CO_2 on the portion of heat in the injected stream used to produce bitumen normalized to the base case with varying reservoir temperatures

In summary, the effect of changing the produced CO_2 fraction has a negligible effect on the overall performance characteristics of the DCSG process.

2.6. Summary and Conclusions

1. A HiPrOx DCSG system has been presented that can replace a conventional steam generator in the SAGD process.
2. The steam generator component is based on the design of coal gasifiers and is therefore expected to be tolerant of high solids from fuel ash or solids in water.
3. The water treatment requirements were reduced significantly. Produced oily water treatment was reduced by ~56% for the petroleum coke case and ~52% for the natural gas. Produced water treatment is not necessary for either case, therefore the reduction is 100% for both.
4. Total water to oil ratio was decreased by around 2.9% and 7.7% for the DCSG petroleum coke and natural gas cases, respectively.
5. Make-up water requirements per barrel of oil were reduced by 37.5% and 100% for the DCSG pet-coke and natural gas cases, respectively.
6. Natural gas produced a higher steam concentration in the product gas (~95 mole% wet) than the petroleum coke (~91 mole% wet) due to its higher hydrogen to carbon ratio.
7. Energy intensity is decreased by 3.6% for the DCSG pet-coke case and 7.6% for the DCSG natural gas case compared to the base SAGD case without CCS.
8. When CCS is included in the base case, the energy intensity is decreased by 8.2% and 12.0% for the DCSG pet-coke and natural gas cases, respectively.
9. Pilot-scale tests of the DCSG are required to investigate scaling issues and corrosion issues caused by acid.
10. More laboratory and field data is required to elucidate the effects of down-hole injection of CO_2 and its effects on bitumen recovery.

2.7. Acknowledgements

The authors would like to acknowledge support received for this project through the Panel on Energy R&D (PERD), technical assistance from Todd Pugsley, at Suncor and the Oil Sands Leadership Initiative (OSLI).

2.8. References

[1] Analysis Brief: Canada [Internet]. Washington, DC, USA: U.S. Energy Information Administration – [cited 2013 Feb 27]. Available from: http://www.eia.gov/countries/cab.cfm?fips=CA

[2] Bergerson J, Keith D. The truth about dirty oil: is CCS the answer?. Env Sci. 2010;44:6010-6015.

[3] In-situ extraction method [internet]. Calgary, Alberta, Canada: The oil sands developers group – [cited 2013 Mar] Available from: http://www.oilsandsdevelopers.ca/index.php/thank-you/oil-sands-facts/extracting-oil-sands-in-situ-and-mining-methods/in-situ-extraction/.

[4] Pedenaud P, Michaud P, Goulay C. Oily-water treatment schemes for steam generation in SAGD heavy-oil developments. Proceedings of the 2005 International Thermal Operations and Heavy Oil Symposium; 2005 Nov 1-3; Calgary, Alberta, Canada.

[5] Water Supply for Canada's Oil Sands [internet]. Ottawa, Ontario, Canada: Government of Canada, Natural Resources Canada – [cited 2013 Mar]. Available from: http://www.nrcan.gc.ca/earth-sciences/climate-change/landscape-ecosystem/by-theme/3483

[6] Havlena Z. Some innovative approaches which may facilitate production of heavy crudes. Proceedings of the 1st International Conference on the Future of Heavy Crude Oils and Tar Sands; 1979 Jun 4-12; Edmonton, Alberta, Canada.

[7] Clements B, Pomalis R, Zheng L, Herage T. High pressure oxy-fuel (HiPrOx) combustion system (Chapter 13). In: Zheng L, editor. Oxy-fuel combustion for power generation and carbon dioxide (CO_2) capture, Cambridge: Woodhead Publishing; 2011. p. 273–292.

[8] Sarkar S. Direct contact steam generation by opposed jet flame stabilization. Can J Chem Eng. 1988;68:55-58.
[9] Alamatsaz A, Moore R, Mehta S, Ursenbach M. Experimental investigation of in-situ combustion at low air fluxes. J Can Pet Tech. 2011:48-67.
[10] Mohtadi M, Sarkar S. Use of opposed jet flame stabilization in a downhole steam generator. Can J Chem Eng. 1985;63:674-680.
[11] Betzer-Tsilevich M. Integrated steam generation process and system for enhanced oil recovery. Proceedings of the 2010 Canadian Unconventional Resources & International Petroleum Conference; 2010 Oct 19-21; Calgary, Alberta, Canada.
[12] McKellar J, Bergerson J, MacLean H. Replacing natural gas in Alberta's oil sands: trade-offs associated with alternative fossil fuels. Energy Fuel. 2010;24(3):1687-1695.
[13] Clements B, inventor; Her Majesty the Queen in Right of Canada as Represented by the Minister of Natural Resources, assignee. High pressure direct contact oxy-fired steam generator. United States patent US 20110232545A1. 2011 Aug 29.
[14] Al-Murayri M, Harding T, Maini, B. Solubility of methane, nitrogen and carbon dioxide in bitumen and water for SAGD modeling, J Can Pet Tech. 2011:34-45.
[15] Al-Murayri M, Harding T, Maini B. Impact of noncondensable gas on performace of steam-assisted gravity drainage. J Can Pet Tech. 2011:46-54.
[16] Heins, WF. Operational data from the world's first SAGD facilities using evaporators to treat produced water for boiler feedwater. J Can Pet Tech. 2008;47(9):32-39.
[17] Central processing facility (Part C5). In: Application for approval of the Devon Jackfish 3 project volume 1 – project description. 2010 Aug; p. 35–73 [internet]. Calgary, Alberta, Canada: Devon NEC Corporation – [cited 2013 Mar]. Available from: http://www.devonenergy.com/downloads/mainmenu.pdf
[18] ERCB Responses: Facilities. In: Application for approval of the Devon Jackfish 3 project volume 1 – project description. 2010 Aug; p.ERCB-73 to ERCB-113 [internet]. Calgary, Alberta, Canada: Devon NEC Corporation – [cited 2013 Mar]. Available from: http://www.devonenergy.com/downloads/mainmenu.pdf

[19] Alberta's installed generation and interconnections capacity [internet]. Calgary, Alberta, Canada: Government of Alberta, Alberta Energy – [cited 2013 Mar]. Available from: http://www.energy.alberta.ca/Electricity/682.asp
[20] Gates ID, Bunio G, Wang J, Robinson B. Impact of carbon dioxide co-injection on the performance of SAGD. Proceedings of the 2011 World Heavy Oil Congress; 2011 Mar 14 -17; Edmonton, Alberta, Canada.
[21] Butler RM, Jiang Q, Yee CT. Steam and gas push (SAGP) – 3; recent theoretical developments and laboratory results. J Can Pet Tech. 2000;39(8):51-60.
[22] Yee CT, Stroich A. Flue gas injection into a mature SAGD steam chamber at the dover project (formerly UTF). J Can Pet Tech. 2004;43(1):54-61.
[23] Younger AH. Natural gas processing principles and technology – part I [report]. Calgary, Alberta, Canada: University of Calgary; 2004, p. 1-1 to 1-8.
[24] Cairns P, Hughes R, Clements B, Herage T, Zheng L, Macchi A, et al. High pressure direct contact oxy-firing (HiPrOx) of fuel with water for the purpose of direct contact steam generation – part 1: butanol. Fuel. Forthcoming 2013.
[25] Cairns P, Clements B, Hughes R, Herage T, Zheng L, Macchi A, et al. High pressure oxy-fureing (HiPrOx) of fuels with water for the purpose of direct contact steam generation – part 2: graphite and mixtures of butanl/graphite. Fuel. Forthcoming 2013.
[26] Appendix B1. In: Application for approval of the Devon Jackfish 3 project volume 3 – EIA Appendices. 2010 Aug; p. 37 [internet]. Calgary, Alberta, Canada: Devon NEC Corporation – [cited 2013 Mar]. Available from: http://www.devonenergy.com/downloads/mainmenu.pdf
[27] Clements B, Zhuang Q, Pomalis R, Wong J, Campbell D. Ignition characteristics of co-fired mixtures of petroleum coke and bituminous coal in a pilot-scale furnace. Fuel. 2012;97:315-320.
[28] Butler RM. Steam recovery equipment and facilities (Chapter 8). In: Butler RM, editor. Thermal recovery of oil & bitumen. New Jersey: Prentice-Hall, Inc.; 1991. p. 368
[29] Greene DW, Maloney JO, editors. Perry's chemical engineers' handbook 6th ed. United States: McGraw-Hill, Inc.: 1984. p. 12-17
[30] Higginbotham p. Air Products and Chemicals Inc. personal communication. 2013.
[31] Fogash K. Air Products and Chemicals Inc. personal communication. 1995.

[32] Kerry FG. Industrial Gas Handbook: Gas Separation and Purification. New York: CRC Press, 2007. p. 468-469.
[33] Prosser NM, Shah MM. Current and future oxygen (O_2) supply technologies for oxy-fuel combustion (Chapter 10). In: Zheng L, editor. Oxy-fuel combustion for power generation and carbon dioxide (CO_2) capture, Cambridge: Woodhead Publishing; 2011. p. 207, 211.

Chapter 3. Pressurized TGA Study on the Reactivity of Canadian Lignite Coal Char under Different High Pressure Oxy-fired (HiPrOx) Environments

Paul Emanuel Cairns[a], Bruce R. Clements[a], Arturo Macchi[b], Edward J. Anthony[c]

[a]Natural Resources Canada, CanmetENERGY, 1 Haanel Dr., Ottawa, Ontario, Canada, K1M 1M1

[b]Faculty of Chemical and Biological Engineering, University of Ottawa, 161 Louis Paster St., Ottawa, Ontario, Canada, K1N 6N5

[c]School of Applied Sciences, Cranfield University, College Rd., Cranfield, Bedford MK43 0AL, United Kingdom

Presented at the 28th Annual International Pittsburgh Coal Conference. Pittsburgh, PA, USA; 2011 Sept 12-15.

Revised: 2013 Apr.

3.1. Abstract

High Pressure Oxy-firing of solid fuels has been proposed for direct contact steam generation (DCSG) for use in industrial applications such as *in-situ* heavy oil extraction processes like steam assisted gravity drainage (SAGD). These firing scenarios present unique operating conditions and chemical species concentrations that affect the combustion characteristics of solid fuel chars. TGA experiments were performed to study the effects of steam on a Canadian lignite coal char's reactivity in different oxy-fuel ($O_2/CO_2/H_2O$) environment as a proof-of-concept of DCSG at the bench scale. It was found that under reaction-kinetic controlled conditions at atmospheric pressure, the increased addition of steam led to a reduction in burnout time and temperature. The findings appear to have resulted from the lower heat capacity and higher thermal conductivity of steam compared to CO_2. At increased pressures CO_2 inhibited burnout due to its higher heat capacity, lower thermal conductivity, and its effect on C(O) concentrations on the particle surface. When steam was added, the inhibiting effects of CO_2 were counteracted, resulting in burning rates similar to pressurized O_2/N_2 environments. Future work using the realistic, reactive and hydrodynamic environment of an entrained flow reactor is recommended.

Keywords: Pressurized combustion, Char reactivity, Steam, Oxy-fuel, SAGD, CCS

3.2. Introduction

Recent estimates have shown that Canada has the third largest oil reserves in the world with 95% associated with the Alberta oil sands [1]. In Alberta, 80% (135 billion barrels) of the oil sands can only be accessed through *in-situ* methods such as Steam Assisted Gravity Drainage (SAGD) [2]. In 2011, total oil sands raw bitumen production was 1.74 million barrels per day (b/d) with *in-situ* techniques making up about 49% of this production. By 2025, *in-situ* production is forecast to make up 57% of a total 4.5 million b/d [3]. Although *in-situ* extraction methods such as SAGD are less invasive than mining, they will result in more greenhouse gas (GHG) emissions per barrel [4] and require large amounts of water that need to be treated and recycled with around a 10% make-up water requirement [2].

CanmetENERGY has patented [5] a pressurized oxy-fuel combustion process using direct contact steam generation (DCSG) to produce high quality steam. It is proposed that the DCSG system be applied for use in steam reforming, and of most interest for this paper, steam assisted gravity drainage (SAGD) for *in situ* bitumen extraction from the oil sands [5,6].

CanmetENERGY's DCSG system produces steam by combusting a low grade slurried fuel such as lignite coal or petroleum coke, with upwards of 95% pure oxygen at high pressure. In this case, water is used as the quench mechanism instead of the flue gas recirculation (FGR) scheme used in typical oxy-fuel applications. After the combustor, the products pass into a second vessel called the steam generator, in which additional water is injected and converted to steam via direct contact with the flue gas. The use of DCSG may make it possible to use waste water for the production of steam to reduce tailings pond pollution and simultaneously capture and store CO_2.

Another application of interest for pressurized oxy-fuel combustion is power generation. Pressurized oxy-fuel combustion systems offer better energy performance over conventional atmospheric oxy-fuel combustion power cycles [7]. Clements *et al.* [8,9],

performed process simulations of a high pressure oxy-fired (HiPrOx) system, known as the ThermoEnergy Integrated Power System (TIPS). They found that pressurized combustion at 8000 kPa lead to a 5% absolute increase in net efficiency over ambient CO_2 capture-ready oxy-fired systems (24% and 29% net efficiencies for ambient and HiPrOx systems, respectively) [8,9]. Ente Nazionale per l'Energia Electrica (ENEL) has suggested that combustion at high pressures may increase both the burning rate of coal and heat transfer rates in the convective sections of the heat transfer equipment. A series of tests on a 5 MW_{th} scale combustor, working at 400 kPa, has been undertaken to demonstrate these benefits [10-12]. Hong *et al.* performed a numerical analysis of a pressurized oxy-fuel combustion power cycle which included a flue gas purification and compression process. Compared to a base case of 110 kPa, they found that the use of pressurized combustion at 1000 kPa led to a 3% increase in net efficiency [7].

Under pressurized firing conditions, the physical properties of the bulk combustor gas are different from those for conventional air-fired and ambient oxy-fired technologies. One difference arises from the effect of total pressure, and another, from the use of a slurry-fed system as opposed to a dry fed system. The latter will result in increased steam concentrations in the combustion gas (up to 80% water for the DCSG firing mode) and varying CO_2 concentrations. These differences will affect combustion gas properties such as: heat capacity, thermal conductivity, radiation characteristics, and density. Design of DCSG systems requires a better understanding of fuel reactivity under these conditions. This study will investigate the reactivity of a Canadian lignite coal char subjected to various pressurized oxy-fired scenarios to provide insight into the effects of elevated steam concentrations and total pressures on combustion.

3.3. Factors that affect char reactivity in various atmospheres

Rathnam *et al.* [13] reported a number of factors which affect char reactivity in O_2/CO_2 atmospheres when compared to the reactivity in O_2/N_2 atmospheres. These factors are detailed below and include char particle temperature, oxygen diffusivity through the boundary layer gas, pressure, and char structure. The current paper will examine

previous studies in terms of these factors and look at the implications of employing high steam concentrations and elevated pressures.

3.3.1. Char particle temperature

The char particle temperature is an important factor, especially when burning in Regime I or Regime II conditions (chemically controlled and pore diffusion controlled, respectively). The higher molar specific heat of CO_2 compared to N_2 causes lower boundary layer gas temperatures and therefore reduced fuel particle temperatures [13]. Bejarano and Levendis [14] measured the volatile flame and char particle temperatures during single particle combustion of bituminous coal and lignite coal for various O_2 levels in N_2 and CO_2. For the bituminous coal, the flame temperatures were about 150 °C lower in systems where the combustion gases consisted of only O_2/CO_2 for various O_2 levels. They found that a higher O_2 level (30% O_2 in CO_2) for the oxy-fired combustion case was required to match the char particle temperatures in the air case, and the O_2 level required to match the char burnout time in air was 35% O_2 in CO_2. In summary, under these regimes, the higher molar heat capacity of CO_2 lowers the boundary layer gas temperature and subsequently, the char particle temperature, resulting in lower reactivity.

In $O_2/CO_2/H_2O$ fired conditions, the lower molar heat capacity of H_2O compared to CO_2 (**Figure 3.1**), leads to comparatively higher boundary layer gas temperatures. This will increase the char particle temperature resulting in increased particle temperatures. These effects are demonstrated by a recent TGA study performed by Gil *et al*. [15] in which steam (10% and 20%) was added to mixtures of O_2 (21% and 30%) and CO_2 (balance). The addition of steam led to an increase in reactivity and a decrease in burnout temperature as compared to the dry gas. The authors concluded that the lower molar heat capacity of steam led to these findings.

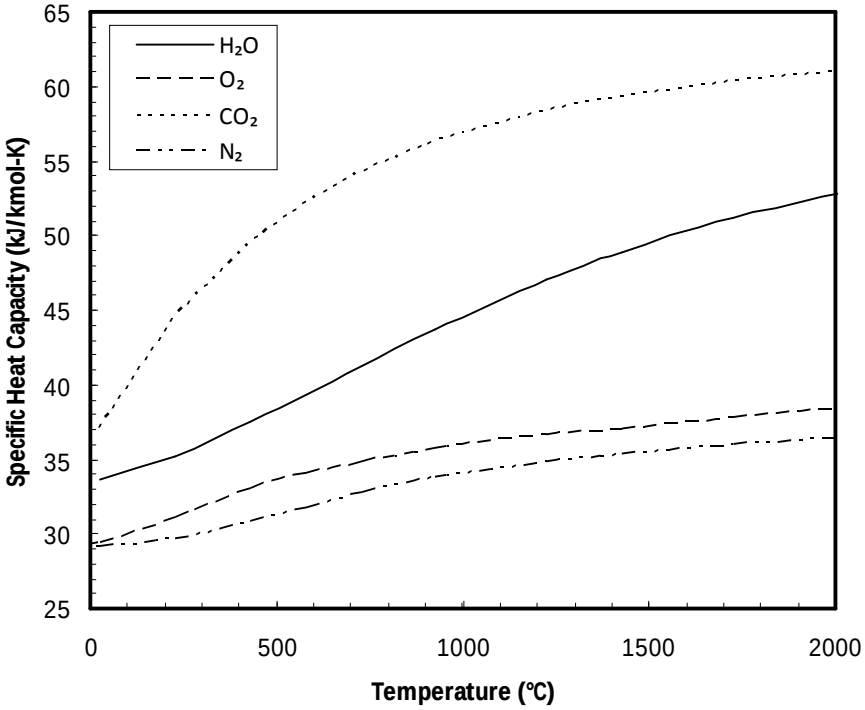

Figure 3.1 – Molar specific heat capacity for H_2O, CO_2, and N_2 at constant pressure of 100 kPa [16]

Another factor affecting particle temperature which was not discussed by Rathnam *et al.* [13] or Gil *et al.* [15] is the boundary layer gas thermal conductivity [17]. Shaddix and Molina [17] calculated the particle temperature of a spherical 100 μm coal particle in selected gas environments at 1227 °C and found that oxy-fuel environments containing steam produce higher particle temperatures than O_2/CO_2 environments (**Figure 3.2**) due to the higher thermal conductivity of H_2O than CO_2 (**Figure 3.3**). They stated that the higher heat capacities of CO_2 and H_2O will cause them to absorb heat released from the oxidation of CO in the boundary layer, reducing peak boundary layer gas temperature and therefore the heat transfer back to the particle which will reduce the burning rate. However, the higher thermal conductivity of H_2O will tend to increase heat transfer back to the particle, making the net effect of H_2O on this phenomenon unclear [17].

Therefore, the increased burnout observed by Gil *et al.* [15] may also be a result of the higher H_2O thermal conductivity. In summary, under Regime I and Regime II conditions, the higher thermal conductivity and lower molar heat capacity of H_2O

compared to CO_2 should lead to higher particle temperatures and an observed increase in burning rate. This study will perform atmospheric and pressurized TGA testing to confirm and expand upon the findings found by Gil *et al.* [15].

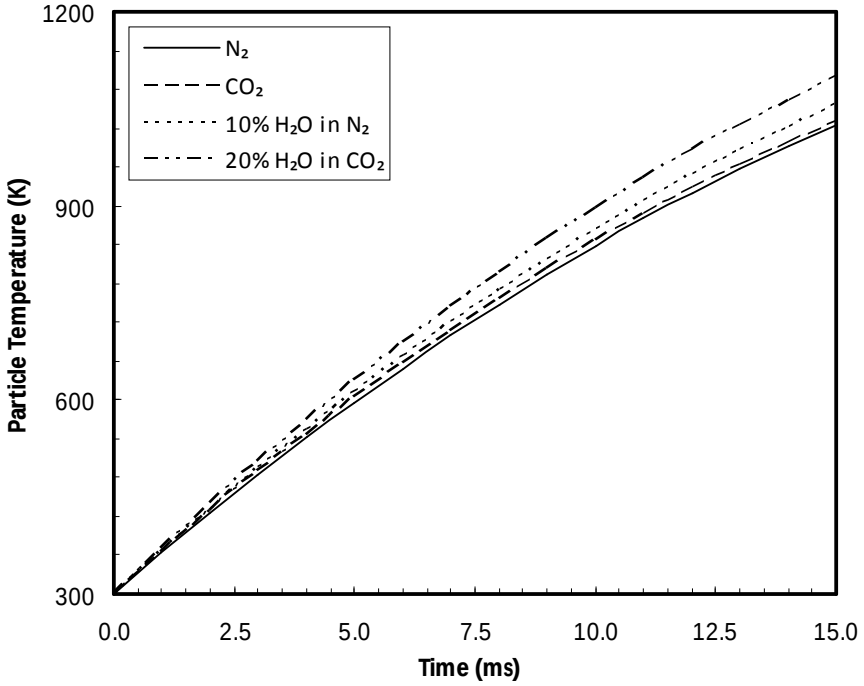

Figure 3.2 – Calculated particle temperature of a spherical 100 um coal particle in selected gas environments at 1227 °C, with radiative boundary at 1000 °C and a Nusselt number of 2.0. Gas thermal conductivities are those indicated in **Figure 3.3**, with gas mixture conductivity estimated according to simple molar mixing ratios, adapted from [17]

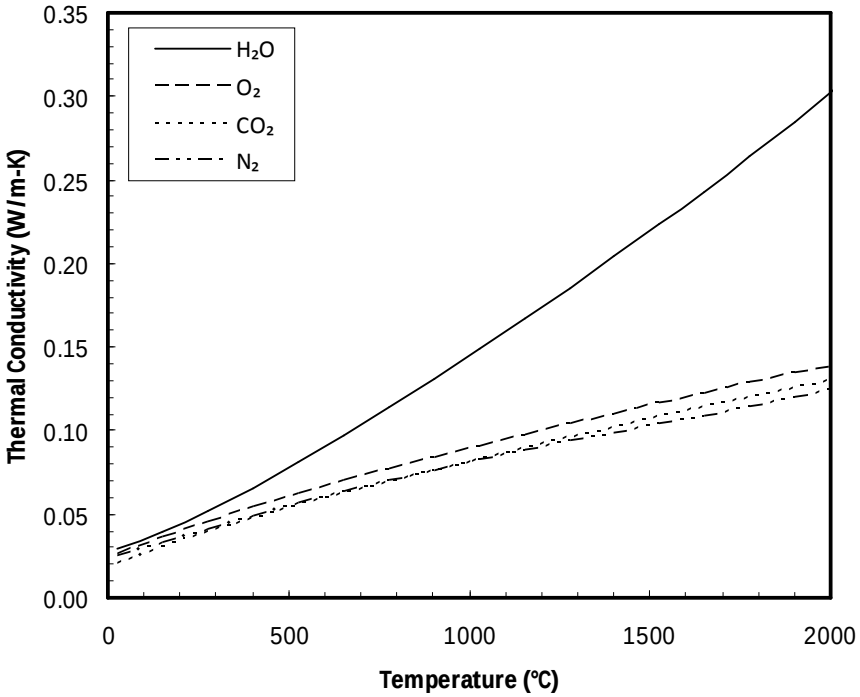

Figure 3.3 – Thermal conductivity of selected gases as a function of temperature, adapted from [17]

3.3.2. Diffusivity of O_2 through boundary layer gas

Practical combustor conditions, generally lead to char combustion being controlled by diffusion of O_2 through the gas boundary layer at very high temperatures (mass transfer limited Regime III conditions) or limited by a combination of reaction kinetics and diffusion through the porous char at moderately high temperatures (pore diffusion limited Regime II conditions) [13]. The diffusivity of O_2 is greater in H_2O than it is in N_2 and is the lowest in CO_2 (**Figure 3.4)**. Rathnam *et al.* [13] reported on the findings of a study [18] that investigated the influence of CO_2 on coal char combustion kinetics in oxy-fuel conditions. The study (6 to 36 % O_2 in N_2 or CO_2) revealed that the lower observed overall burning rate in O_2/CO_2 conditions was attributed to the lower diffusivity of O_2 in CO_2 than the diffusivity of O_2 in N_2 [13].

The effect of O_2 diffusion to the char surface in CO_2 and H_2O gases was discussed by Shaddix and Molina [17]. They stated that, in all but reaction-kinetic controlled burning

conditions (Regime I), elevated H_2O concentrations may promote combustion by augmenting oxygen diffusion because the diffusivity of oxygen is 20% higher in H_2O than in N_2 at temperatures in which combustion is mass transfer limited. In summary, the higher diffusivity of O_2 in H_2O than O_2 in CO_2 should lead to increased reactivity of the char in Regime III conditions.

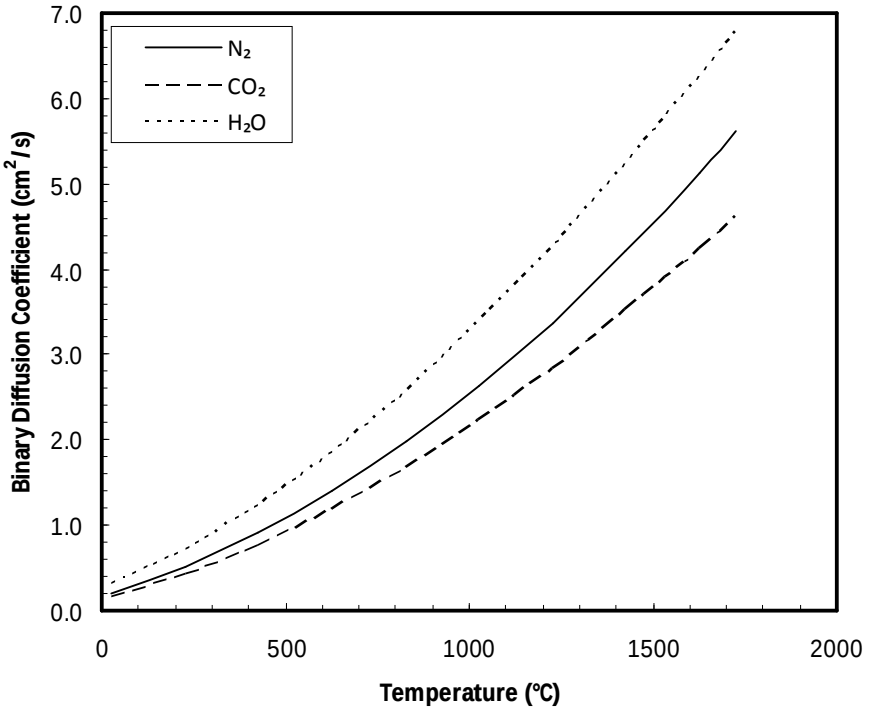

Figure 3.4 – Binary diffusion coefficient of O_2 in N_2, CO_2, and H_2O as a function of temperature, adapted from [17]

3.3.3. Pressure

The combustor pressure is another factor that affects char reactivity and more importantly the char structure [13]. Saastamoinen *et al.* [19] performed experiments in a pressurized entrained flow reactor where they varied the O_2 and CO_2 partial pressures between 25-100 kPa and 50-200 kPa, respectively. The balance gas was N_2 and the total pressure was varied between 200 kPa and 800 kPa with temperatures between 800 °C and 1200 °C. They found that at a fixed volume fraction of 10 % O_2 the reactivity increased with increase in total pressure from 200 to 500 kPa and then leveled off with further increases

in total pressure. Monson *et al.* [20] performed oxidation experiments at atmospheric and elevated pressures (100-1500 kPa) in a drop tube reactor with 5-21% oxygen and N_2 balance gas. They found that increasing total pressure from 100 to 500 kPa in an environment of constant gas composition led to a modest increase in reaction rate, whereas the reaction rate decreased with further increases in pressure. Lester *et al.* [21] performed experiments in a shock tube reactor over a particle temperature range of 1427-1927 °C, with a total pressure range of 550-1000 kPa and oxygen mole fraction of 0.1-0.5. They found that as total pressure increased from 550 to 1000 kPa, the oxidation rates for chars in air decreases. They explained the reduced rate in terms of the decreasing pore area available for reaction with oxygen with increasing total pressure. This effect may also explain the results found by Saastamoinen *et al.* [19] and Monson *et al.* [20].

The previously mentioned study by Saastamoinen et al. [19] also revealed that at high pressures and temperatures, when the combustion rate becomes increasingly controlled by diffusion of O_2 to the surface, high CO_2 concentrations may increase the char-CO_2 gasification rate resulting in a higher total combustion rate. Messenbock *et al.* [22] studied the effect of pressure on the extent of steam and CO_2 gasification in a wire mesh reactor in a pressure range of 100 to 3000 kPa. Their studies were performed in pure CO_2 environments and mixtures of 80 % steam and 20 % helium. At reaction times applicable to this study (10 seconds or less), the extent of steam gasification was about 2 to 3 times higher than those for CO_2. They also found that the reactivity of the chars decreased with increasing pressure. Deactivation of the char caused by secondary char deposition was said to have led to an un-reactive layer of re-polymerised tar. Roberts and Harris [23] measured the apparent and intrinsic reaction rate of Australian bituminous coal chars with O_2, CO_2, or H_2O in an N_2 balance at pressures up to 3000 kPa using a pressurized TGA (PTGA). It was found that the reaction order in CO_2 and H_2O was not constant over the pressure range investigated, varying from 0.5 to 0.8 at atmospheric pressure and decreasing at pressures above approximately 1000 kPa. The intrinsic reaction of oxygen was less affected by pressure over the range 100 to 1600 kPa while the apparent reaction increased with increasing pressure [23]. Changes in physical structure (shown by

apparent reaction), not chemical rates (shown by intrinsic reaction) were explained to be the cause of the observed trends.

In summary, previous studies have shown that with increasing pressure the O_2 reaction increases up to around 5 bar where it begins to level off or decreases [19-21,23]. This was attributed to physical changes in the char structure with increasing pressure [21,23]. In H_2O and CO_2 gasification studies, it was found that increasing pressure led to a decrease in reaction rate [22,23]. This was attributed to char deactivation caused by secondary char deposition of volatiles [22]. Since all of these studies were conducted with pure gases only, it is still unclear what the net effect on char reactivity will be in a mixture of these gases.

3.3.4. Char structure

Another factor that affects the coal reactivity results from the char structure formed throughout the combustion process. Rathnam *et al.* [13] performed devolatilization experiments in N_2 and CO_2 in a drop tube furnace and characterized the char formed using SEM and BET analyses. Increased swelling of the char particles and an increase in BET surface area were observed for the CO_2 chars, when compared to the N_2 chars. The char-CO_2 gasification reaction during devolatilization was suggested to be the cause of the observed results.

Using SEM Messenbock *et al.* [22] examined the effects of CO_2 and H_2O on char structure after devolatilization in a pressurized wire mesh reactor. At atmospheric pressure, the authors observed that chars from steam gasification did not agglomerate, indicating that they did not soften or melt to the same degree as their N_2 and CO_2 devolatilized counterparts, but a structure with large pore size had evolved. An increased reactivity of the char gasified in steam compared to N_2 and CO_2 was observed. It was concluded that the more reactive steam gasification reaction compared to CO_2 and N_2 led to the better observed char structure. In summary, it is expected that the char structure formed in the presence of steam should lead to a higher reactivity because it will increase pore size and cause swelling.

3.4. Motivation for current study

Past work has focused on the effect of an O_2/CO_2 environment on the reactivity of coal char at ambient pressure [24-34]. As mentioned in the previous section, most of these studies have shown that the gasification reaction has less of an effect on char burnout than the higher specific molar heat capacity of CO_2 and the lower diffusivity of O_2 in CO_2 in comparison to combustion in air at the same oxygen concentration (21%). However, little work has been done that includes the effect of steam.

Regarding the effects of pressure, most studies have been performed in environments where only one reactant was present with the balance of the gas being inert (He, N_2 or Ar) [19,21]. To the best of our knowledge, very little work has been done to examine the effect of the gas environment, and its properties (specific heat capacity, thermal conductivity) on the coal reactivity in these pressurized studies.

In a pressurized reactor it is likely that the fuel will be slurry fed [6]. This will lead to high steam concentrations in the bulk gas. At present, it is unclear what affect these firing scenarios will have on the coal combustion [6]. Therefore, this study aims to examine the effects of pressure, and increased H_2O concentration on solid fuel combustion.

3.5. Experimental Methodology

This paper looks at char reactivity using a pressurized TGA (PTGA), with low heating rates and prepared chars. The experimental conditions are designed to result in combustion occurring in Regime I and perhaps Regime II. Therefore, char structure, diffusivity of O_2 through the product gas, and condensation of tars during devolatilization should not be rate-limiting, or affect the results.

3.5.1. Char preparation

Chars from a Canadian lignite coal were used in this study. Lignite was chosen for this study because it was a common solid fuel that is widely available in Western Canada and could be used for HiPrOx/DCSG and HiPrOx power generation. Future work will be undertaken using low grade, high sulphur fuels such as petroleum coke and asphaltenes

for DCSG focused studies, and higher ranks of coals for power generation related studies. Chars were made under laboratory conditions by heating sized coal samples (38-75 μm) in a horizontal tube furnace to 1000 °C at 10 °C/min under dry nitrogen (about 500 mL/min), and maintaining that temperature for 1 hour. The resulting chars were again sieved to the 38-75 μm chars to eliminate any agglomerated particles. While it is understood that coal chars made under such conditions are not true representations of chars produced in combustion technologies, such a pyrolysis technique can be used to produce the amount of sample required that is also free from variations between particles which can arise from high heating-rates and reactive atmospheres.

3.5.2. Thermogravimetric Analyses (TGA)

Non-isothermal pressurized TGA (Linseis^{TM} High Pressure HP TGA-DCS) experiments were performed on the chars prepared above. Samples weighing approximately 5 to 10 mg were placed in the TGA. In a nitrogen atmosphere, the pressure was increased to the desired test pressure. Following pressurization, the temperature was increased at a rate of 25 °C/min to 250 °C and then to 300 °C at a rate of 5 °C/min. Gas flow through the chamber was set at a rate of 100 mL/min for all test cases. Therefore, the delivery flow rates had to be increased proportionally with pressure. After allowing the temperature and weight to stabilize for 7.5 minutes, the gas flow was switched to the desired mixture at the same flow rate. The temperature was held constant for another 7.5 minutes. Following the 15 minutes hold in temperature, the temperature was again raised at a rate of 25 °C/min to 1000 °C and held for 3 minutes to ensure full burnout. Duplicate runs for each test point were performed.

Based on the final and initial mass readings, the conversion was calculated as a function of time and temperature. Since the higher pressures coupled with steam injection caused noise in the data, the duplicate conversion curves were curve fit using the SYSTAT TableCurve 2D^{TM} software. The error bars on the curve fit are included in the analysis. Using the curve fit for the conversion function, it was possible to numerically differentiate using Simpson's rule in order to obtain char reactivity curves.

The char reactivity in TGA experiments is given by [14]:

$$R = \frac{-1}{(m_O - m_f)} \frac{dm}{dt} = \frac{dX}{dt}$$

where, m_o is the initial dry mass of char sample, m_f final mass of the sample after reaction, *dm/dt* is the measured mass loss rate, and *dX/dt* is the measured conversion rate, determined through numerical differentiation of the conversion vs. time curve.

3.5.3. Test Conditions

Table 3.1 outlines the experimental matrix. The experimental gas compositions were selected to represent the bulk gas composition in a reactor after devolatilization with typical HiPrOx power generation feed gas compositions (30 mol% O_2, 50 mol% CO_2, 20 mol% H_2O) and HiPrOx/DCSG feed gas compositions (30 mol% O_2, 70 mol% H_2O), assuming CH_4 as the volatiles that are combusted. **Table 3.2** gives the proximate and ultimate analyses of the Canadian lignite coal used for this study. Due to difficulties with reliably injecting high quantities of steam at the higher pressures, the 80% H_2O runs at 1500 kPag and 2500 kPag are not included.

Table 3.1 – Experimental matrix

Description	**Dry N_2**	**Dry CO_2**	**HiPrOx Power Gen**	**HiPrOx DCSG**
101.325 kPa				
O_2	10	10	10	10
N_2	90	-	-	-
CO_2	-	90	55	10
H_2O	-	-	35	80
1601.325 kPa				
O_2	10	10	10	N/A
N_2	90	-	-	N/A
CO_2	-	90	55	N/A
H_2O	-	-	35	N/A
2601.325 kPa				
O_2	10	10	10	N/A
N_2	90	-	-	N/A
CO_2	-	90	55	N/A
H_2O	-	-	35	N/A

Table 3.2 – Canadian lignite coal proximate and ultimate analyses

Parameter	As Received	Dry at 105 °C	Dry Ash Free	Method
Proximate analysis (wt%)				
Ash	14.20	16.64	-	ASTM D7582
Volatile matter	31.96	37.45	44.93	ISO 562
Fixed carbon	39.18	45.91	55.07	ASTM D7582
Moisture	14.66	-	-	ASTM D7582
Total	100.00	100.00	100.00	
Ultimate analysis (wt%)				
C	51.01	59.78	71.15	ASTM D5373
H	3.24	3.80	4.53	ASTM D5373
N	0.85	1.00	1.19	ASTM D5373
O	15.47	18.12	22.35	By difference
S	0.56	0.66	0.78	ASTM D4239
Ash	14.20	16.64	-	ASTM D7582
Moisture	14.66	-	-	ASTM D7582
Total	100.00	100.00	100.00	

3.6. Results and discussion

Figure 3.5 presents the curve fit results of the conversion data obtained from the experiments. The error bars, based on the 1st standard deviation of duplicates, have been included to show the error associated with noise in the data and variability between experiments. Burnout occurred much earlier with increasing pressure because of the increased partial pressure of oxygen driving the reaction faster. The change became less distinct between the higher two pressures. The effect of steam was more prominent at atmospheric pressure than at 1500 kPag and 2500 kPag because the increased reaction with oxygen at higher pressures becomes the dominating factor as pressure is increased. The dry CO_2 runs resulted in a decrease in burning rate with increasing pressure because of its higher heat capacity and lower thermal conductivity. When the steam is added, it counteracts the inhibition cause by CO_2 because it reduces its partial pressure, reducing its inhibiting effects, increasing the thermal conductivity and lowering the heat capacity of the gas mixture.

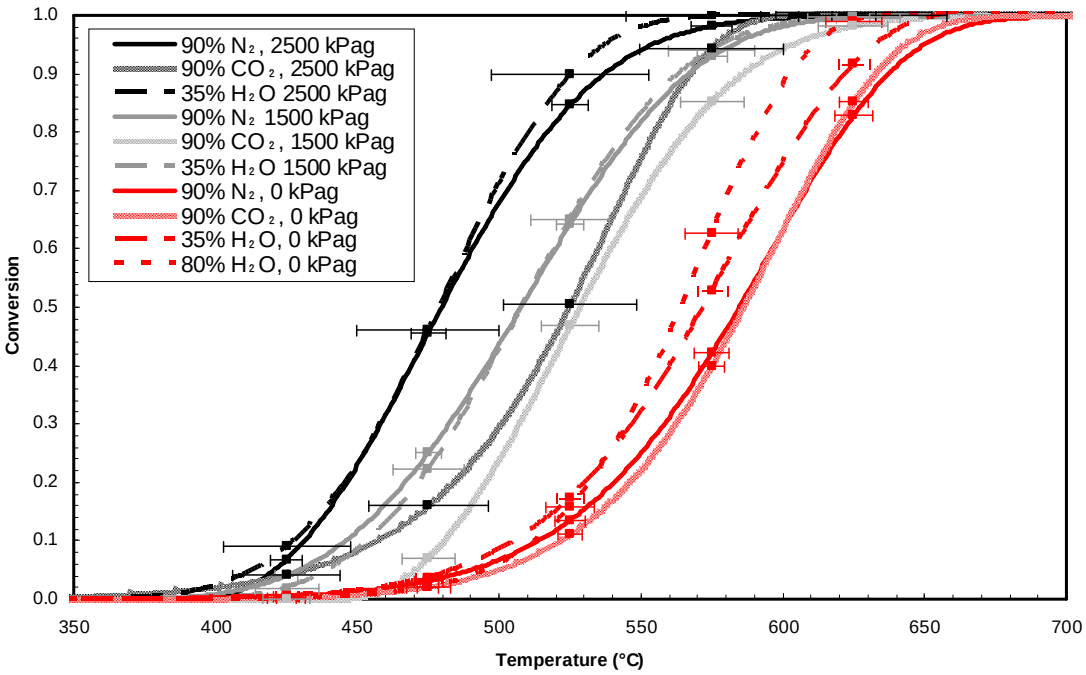

Figure 3.5 – Curve fit of experimental conversion including error bars against temperature

Figure 3.6, **Figure 3.7**, and **Figure 3.8** compare the reactivity of the Canadian lignite char in each gas environment at 101.3 kPa, 1601.3 kPa, and 2601.3 kPa, respectively. At 101.325 kPa, the increased addition of steam shifted the curves to lower temperatures as a result of increased particle temperature caused by the lower heat capacity and higher thermal conductivity of steam compared to CO_2. Therefore, in Regime I conditions the addition of steam should act to increase the combustion rate. Similar results were reported by Gil *et al.* [17] for their experiments.

As pressure increased, the effect of steam became less significant because the increased particle temperature had less of an effect on the reactivity compared to the higher partial pressure of O_2 (**Figure 3.7** and **Figure 3.8**). As previously mentioned, the CO_2 reduces the burnout because of its higher heat capacity and lower thermal conductivity. Furthermore, the increased partial pressure of CO_2 may act to shift the equilibrium of the following reaction: $C(O) + CO_2 \leftrightarrow C(O) + CO$ [35] toward higher C(O) and CO concentrations on the surface of the char and boundary layer gas, which will occupy active sites leading to decreased reactivity. At the 2601.3 kPa pressure, the 90% CO_2

mixture reacts at around the same rate as the 1601.325 kPa runs. Therefore, the inhibition effect of CO_2 becomes even stronger as the pressure is increased. However, a completely dry O_2/CO_2 mixture would never be encountered in a real solid fuel combustion application because the hydrogen in the fuel and volatiles would react to produce some H_2O.

When the steam is added, this effect is counteracted because the partial pressure of the CO_2 is reduced to a point where the inhibition becomes negligible. Furthermore, steam will catalyze the oxidation of CO [36], reducing its concentration which will allow C(O)→ CO, resulting in further oxidation of carbon via the following mechanisms: $2C + O_2 \rightarrow C(O) + CO$ and $C + C(O) + O_2 \rightarrow CO_2 + C(O)$ [35]. The steam presence may also be acting to increase the particle temperature through increased thermal conductivity and decreased heat capacity of the gas, but the net effect is not quantifiable due to the experimental error associated with the injection of steam.

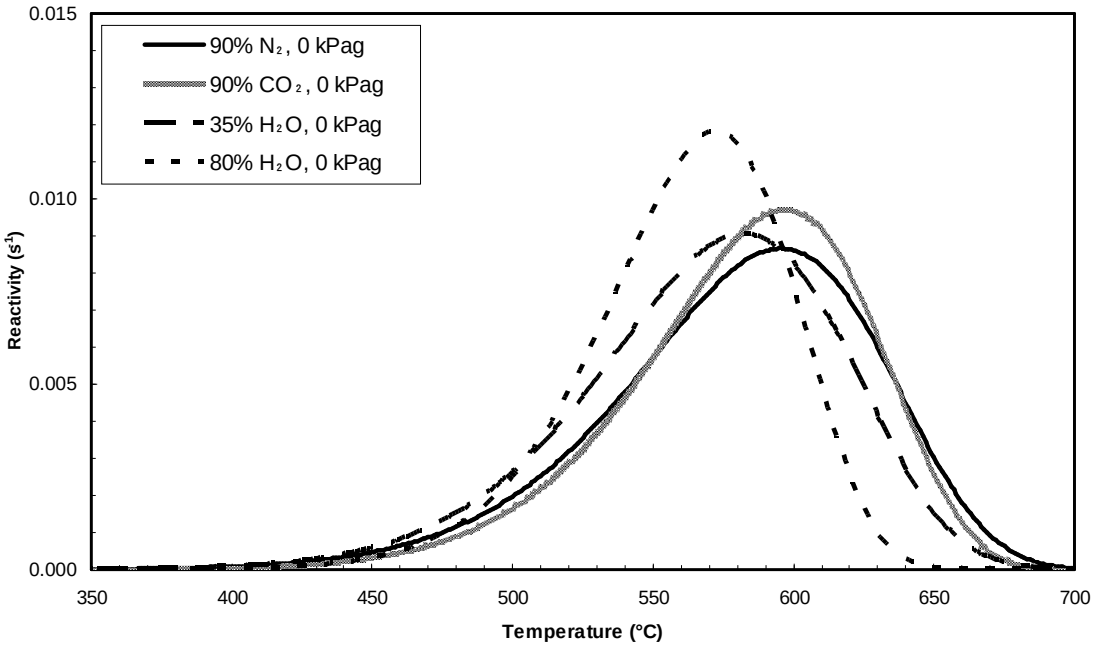

Figure 3.6 – Char reactivity against temperature at 101.3 kPa

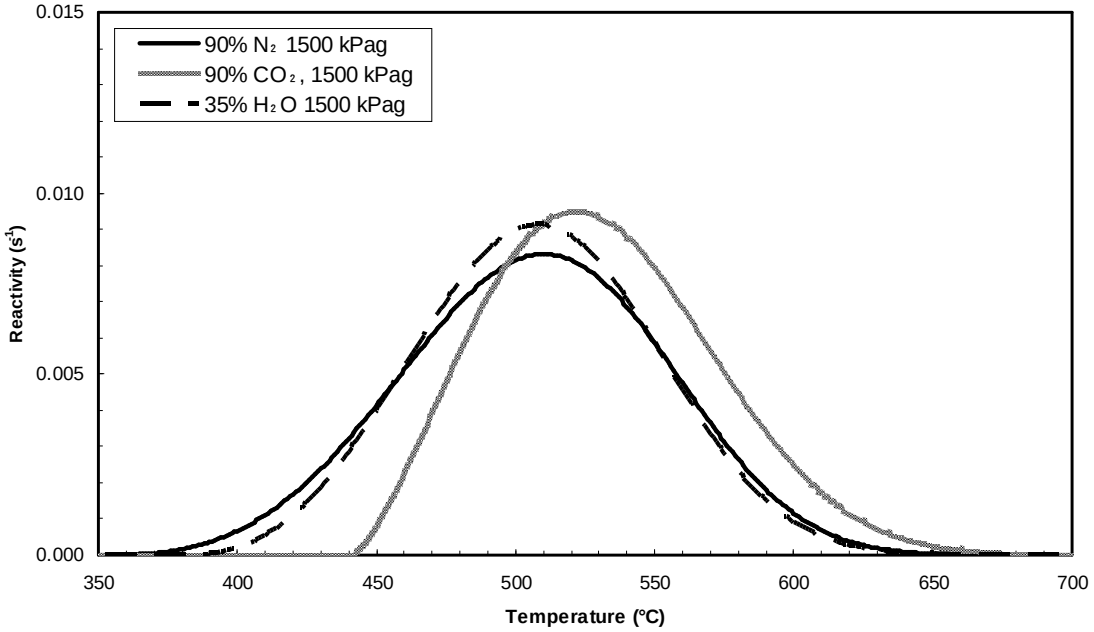

Figure 3.7 – Char reactivity against temperature at 1601.3 kPa

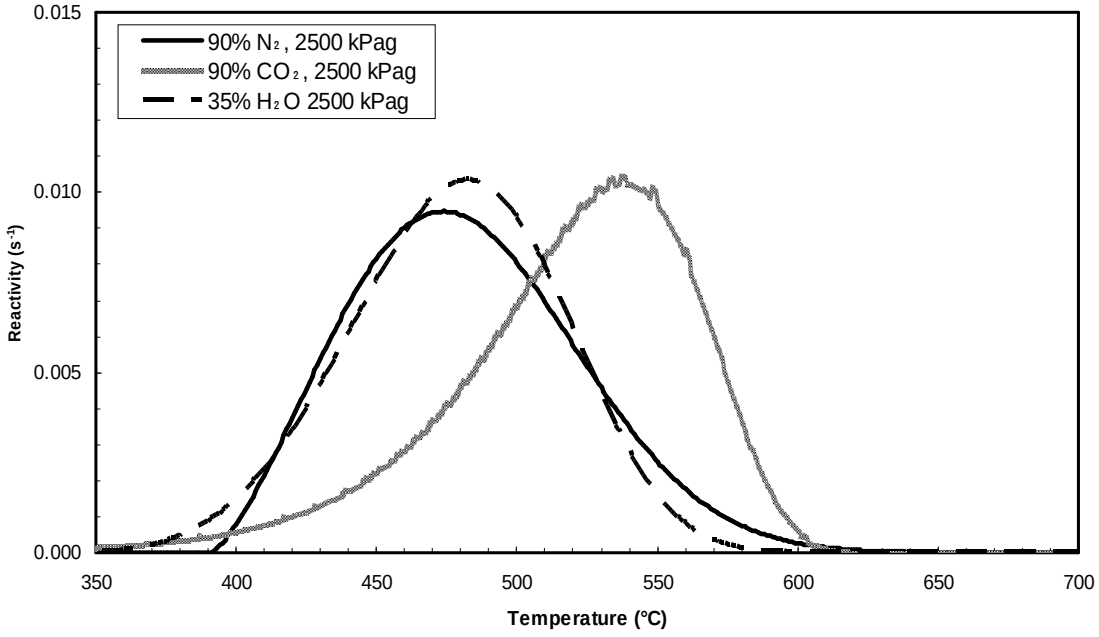

Figure 3.8 – Char reactivity against temperature at 2601.3 kPa

Although these results show decrease in burnout time caused by the presence of steam in Regime I conditions at atmospheric pressure, with the net effect becoming less significant with increasing pressure, they do not indicate whether the presence of steam will lead to

better burnout in large scale applications. For example, Nozaki *et al.* [37] found that gas temperatures near the burner were about 150 °C lower when using a wet flue gas recycle as compared to a dry flue gas recycle (**Figure 3.9**). This will adversely affect char particle temperature and thus burnout because the bulk gas temperature will be lower, comparatively.

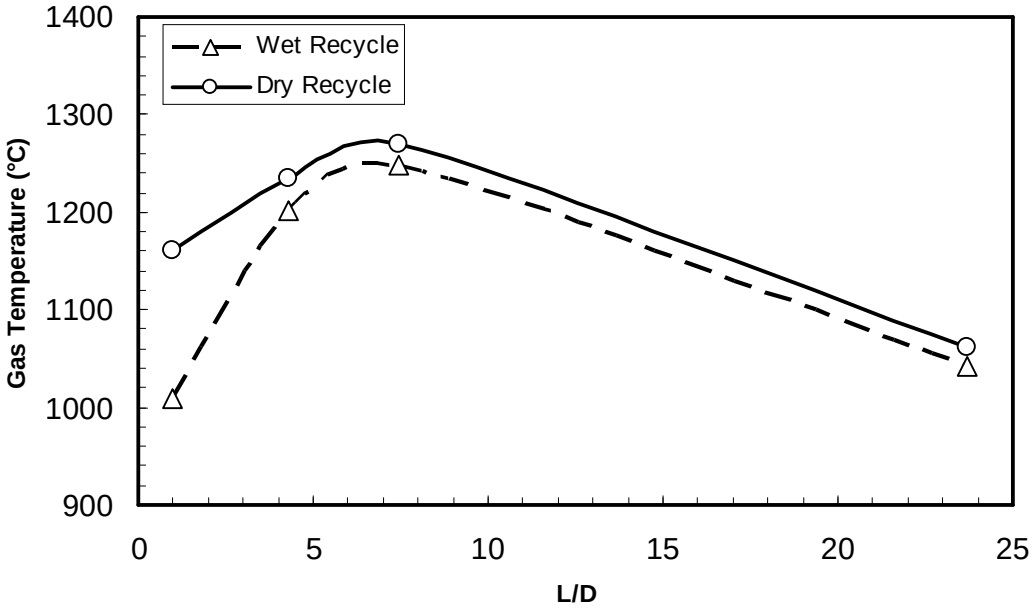

Figure 3.9 – Gas temperatures for wet and dry recycles of primary gas, adapted from [37]

The results obtained by Nozaki *et al.* [37] are unexpected because as previously discussed, the presence of H_2O should: increase particle temperature in Regimes I and II due to its higher thermal conductivity and lower heat capacity, increase O_2 diffusion to the particle surface in Regimes II and III due to its higher binary diffusion coefficient, and lead to more favourable particle structures because of the higher reactivity of H_2O during coal devolatilization. This indicates that there must be another factor that is having a greater effect on coal burnout than those reported in previous studies. Toftegaard *et al.*[38] noted that these findings suggest that factors such as radiation and endothermic dissociation reactions with radical formation (O·, OH·, H·, etc.) dominate the temperature effect of water vapour in the recycle.

Shaddix and Molina [17] reported that the presence of CO_2 and H_2O may suppress radical concentrations by promoting the backward reaction ($CO + OH\cdot \leftrightarrow CO_2 + H\cdot$) of the highly reactive and mobile $H\cdot$ radical in the case of CO_2, and the recombination ($H\cdot + O_2 + M \leftrightarrow HO_2\cdot + M$) of the $H\cdot$ radical in the case of H_2O. In fact, they reported that the chaperon efficiency of CO_2 and H_2O in these recombination reactions are 2 to 3 and 11 times that of N_2, respectively. Therefore, for elevated H_2O concentration, some chemical inhibition of homogeneous particle ignition can be expected [17]. In a TGA, the slow heating rate, high particle loading, and small particle size all favor heterogeneous ignition. For those conditions favoring heterogeneous ignition, the only gas property (other than O_2 concentration) expected to be important is thermal conductivity [17]. Shaddix and Molina [17] also report that pulverized coal ignition generally occurs via a homogeneous or heterogeneous-homogeneous mechanism. The difference in ignition mechanism between experiments performed in the TGA versus experiments performed at the pilot scale may explain why the gas thermal conductivity and specific heat capacity don't have as significant an effect on the char burnout and particle temperature compared to effects such as endothermic radical formation that would be present at the pilot scale.

3.7. Conclusion

TGA experiments were performed to study the effects of steam on a Canadian lignite coal char's reactivity in high steam oxy-fuel ($O_2/CO_2/H_2O$) environment. At atmospheric pressure the higher thermal conductivity and lower molar heat capacity of H_2O compared to CO_2 lead to higher burnout temperatures in Regime I conditions with heterogeneous ignition. However, factors such as radiation and the suppression of radical concentrations resulting from the presence of H_2O and CO_2 during homogeneous ignition may potentially have a greater effect at the pilot scale. With increased pressure the net effect of a higher H_2O gas mixture similar to that for DCSG seemed to have the same reactivity as a pressurized air fired case and worked to counteract the inhibiting effect caused by the presence of CO_2. This helps prove the feasibility of this technology at the bench-scale because it indicates that burnout times will decrease with pressure and a high presence of

steam will not greatly effect combustion efficiency and burnout compared to air at high pressure.

The TGA data is not a proper representation of the high temperatures, homogeneous ignition, and char structures that would be found in full scale applications, therefore work at the pilot-scale will be needed to truly prove the feasibility of this technology.

3.8. Acknowledgements

The authors would like to thank the Clean Energy Fund of Canada for supporting this work, CanmetENERGY for providing the facilities required for the experiments performed, the Combustion Optimization and the Fluidized Bed and Gasification groups at CanmetENERGY for their input into much of the research done for this paper and Francie Verdon for her help with the experiments.

3.9. References

[1] Analysis Brief: Canada [Internet]. Washington (DC): U.S. Energy Information Administration – [cited 2013 Feb 27]. Available from: http://www.eia.gov/countries/cab.cfm?fips=CA.

[2] Alberta Government. In-situ process steam assisted gravity drainage. 2013 Feb. 1 p.

[3] Canadian Association of Petroleum Producers. Crude oil: forecast, markets & pipelines. 2012 June. 7 p.

[4] Bohm M, Goold S, Laux S, Neu B, Sharma A, Aasen K. Application of oxy-fuel CO2 capture for in-situ bitumen extraction from Canada's oil sands. Energy Proc. 2011;4:958-965.

[5] Clements B, inventor; Her Majesty the Queen in Right of Canada as Represented by the Minister of Natural Resources, assignee. High pressure direct contact oxy-fired steam generator. Unites States patent US 20110232545A1. 2011 Aug 29.

[6] Clements BR, Zheng L, Pomalis R. Next generation oxy-fired systems: potential for energy efficiency improvement through pressurization. Proceedings of the 3rd international conference on energy sustainability; 2009; San Francisco, California, USA.

[7] Hong J, Chaudry G, Brisson JG, Field R, Gazzino M, Ghoniem AF. Analysis of oxy-fuel combustion power cycle utilizing a pressurized coal combustor. Energy. 2009;34:1332.
[8] Clements BR, Zheng L, Pomalis R, Next generation oxy-fired systems: potential for energy efficiency improvement through pressurization. Proceedings of the 3rd international conference on energy sustainability: San Fransisco, California, USA; 2009.
[9] Zheng L, Pomalis R, Clements BR. Technical feasibility study of TIPS process and comparison with other CO2 capture power generation processes. Proceeding from the 32nd international technical conference on coal utilization and fuel systems: Clearwater, FL, USA; 2007.
[10] Benelli G, Malavasi M, Girardi G. Oxy-coal combustion process suitable for future and more efficient zero emission power plants. Proceeding from the PowerGen Europe conference and exhibition: Madrid, Spain; 2007.
[11] Benelli G, Girardi G, Malavasi M, Saponaro A. ISOTHERM®: a new oxy-combustion process to match the zero emission challenge in power generation. Proceeding from the 7th high temperature air combustion and gasification international symposium: Phuket, Thailand; 2008.
[12] Gazzino M, Benelli G. Pressurized oxy-fuel combustion for future zero emission power plants: process design and energy analysis. Proceedings from the 2nd international conference on energy sustainability: Jacksonville, FL, USA; 2008.
[13] Rathnam RK, Elliot LK, Wall TF, Liu Y, Moghtaderi B. Differences in reactivity of pulverised coal in air (O2/N2) and oxy-fuel (O2/CO2) conditions. Fuel Proc Techol. 2009;90:797.
[14] Bejarano PA, Levendis YA, Single-coal-particle combustion in O2/N2 and O2/CO2 environments. Combust and Flame. 2008;153:270.
[15] Gil MV, Riaza J, Alvarez L, Pevida C, Pis JJ, Rubiera F. A study of oxy-coal combustion with steam addition and biomass blending by thermogravimetric analysis. J Therm Anal Calorim. 2011;109:49-55.
[16] Nist Chemistry Webbook: thermophysical properties of fluid systems [internet]. USA: National Institute of Standards and Technology, US DOE – [cited 2013 Apr] Available from: http://webbook.nist.gov/chemistry/fluid/.

[17] Shaddix C, Molina A. Ignition, flame stability, and char combustion in oxy-fuel combustion (Chapter 6). In: Zheng L, editor. Oxy-fuel combustion for power generation and carbon dioxide (CO2) capture, Cambridge: Woodhead Publishing; 2011. p. 101–125.
[18] Shaddix CR, Molina A. Influence of CO2 on coal char combustion kinetics in oxy-fuel applications. Proceeding of the 5th US Combustion Meeting Organized by the Western States Section of the Combustion Institute; 2007; The University of California, San Diego, USA.
[19] Saastamoinen JJ, Aho MJ, Jouni PH. Pressurized pulverised fuel combustion in different concentration of oxygen and carbon dioxide. Energy Fuels. 1996;10:121.
[20] Monson CR, Germane GJ, Blackham AU, Smoot LD. Char oxidation at elevated pressures. Comb Flame. 1995;100:669.
[21] Lester TW, Seeker WR, Merklin JF. The influence of oxygen and total pressure on surface oxidation rate of bituminous coal. Proceeding from the 18th International Symposium on Combustion form the Combustion Institute. 1981;1257.
[22] Messenbock RC, Dugwell DR, Kandiyoti R. CO2 and steam-gasification in a high-pressure wire-mesh reactor: the reactivity of Daw Mill coal and combustion reactivity of its chars. Fuel. 1999;781.
[23] Roberts DG, Harris DJ. Char gasification with O2, CO2, and H2O: effects of pressure on intrinsic reaction kinetics. Energy & Fuels. 2000;14:483.
[24] Huang X, Jiang X, Han X, Wang H. Combustion characterisetics of fine- and micro-pulverized coal in the mixture of O2/CO2. Energy Fuel. 2008;22:3756.
[25] Rathnam RK, Wall TF, Eriksson K, Stromberg L, Moghtaderi B. Reactivity of pulverised coals in simulated air (O2/N2) and oxy-fuel (O2/CO2) atmospheres. Proceedings from the 25th annual Pittsburgh Coal Conference; 2008; Pittsburgh, PA, USA.
[26] Hecht ES, Shaddix CR, Molina A, Haynes BS. Effect of CO2 gasification reaction on oxy-combustion of pulverized coal char. Proc Comb Inst. 2011;33:1699.
[27] Zhang L, Binner E, Qiao Y, Li CZ. In situ diagnostics of Victorian brown coal combustion in O2/N2 and O2/CO2 mixture in drop-tube furnace. Fuel. 2010;89:2703.
[28] Yuzbasi NS, Selcuk N. Air and oxy-fuel combustion characteristics of biomass/lignite blends in TGA-FTIR. Fuel Proc Tech. 2011;92:1101.

[29] Li Q, Zhao C, Chen X, Wu W, Li Y. Comparison of pulverised coal combustion in air and in O2/CO2 mixtures by thermo-gravimetric analysis. J Anal App Pyrol. 2009:521.
[30] Li X, Rathnam RK, Yu J, Wang Q, Wall T, Meesri C. Pyrolysis and combustion characteristics of an Indonesioan low-rank coal under O2/N2 and O2/CO2 conditions. Energy Fuel. 2009;24:160.
[31] Liu H, Zailani R, Gibbs BM. Comparisons of pulverized coal combustion in air and in mixtures of O2/CO2. Fuel. 2005:833.
[32] Liu H. A comparison of combustion of coal chars in O2/CO2 and O2/N2 mixtures - Isothermal TGA studies. Int J Chem React Eng. 2009;7:A74.
[33] Liu H. Combustion of coal chars in O2/CO2 and O2/N2 mixtures: a comparative study with non-isothermal thermogravimetric analyzer (TGA) tests. Energy Fuel. 2009;23:4278.
[34] Brix J, Jensen PA, Jensen AD. Coal devolatilization and char conversion under suspension fired conditions in O2/N2 and O2/CO2 atmospheres. Fuel. 2010;89:3373.
[35] Liu GS, Niksa S. Coal conversion submodels for design applications at elevated pressures. Part II. Char gasification. Prog En Comb Sci. 2004;30:679-717.
[36] Field MA, Gill DW, Morgan BB, Hawksley PGW. Reacton rate of carbon particles (Chapter 6). In: Combustion of coal. Surrey, England: Cheney & Sons Ltd.; 1967. p. 205
[37] Nozaki T, Takano S, Kiga T, Omata K, Kimura N. Analysis of the flame formed during oxidation of pulverised coal by an O2-CO2 mixture. Energy. 1997;22:199.
[38] Toftegaard MB, Brix J, Jensen PA, Glarborg P, Jensen AD. Oxy-fuel combustion of solid fuels. Prog Energy Comb Sci. 2010;36:581.

Chapter 4. High Pressure Oxy-firing (HiPrOx) of Fuels with Water for the Purpose of Direct Contact Steam Generation – Part 1: Butanol

Bruce R. Clements[a,*], Paul Emanuel Cairns[a], Robin Hughes[a], Ted Herage[a], Ligang Zheng[a], Arturo Macchi[b], Edward J. Anthony[c]

[a]Natural Resources Canada, CanmetENERGY, 1 Haanel Dr., Ottawa, Ontario, Canada, K1M 1M1

[b]Faculty of Chemical and Biological Engineering, University of Ottawa, 161 Louis Pasteur St., Ottawa, Ontario, Canada, K1N 6N5

[c]School of Applied Sciences, Cranfield University, College Rd., Cranfield, Bedford MK43 0AL, United Kingdom

In Submission to Fuel, 2013

4.1. Abstract

High Pressure Oxy-fired Direct Contact Steam Generation (HiPrOx/DCSG) can be achieved by the oxy-combustion of fuels in the presence of water. This process is capable of producing flue gas streams containing approximately 90% steam with the remainder being primarily CO_2. The product flue gas is suitable for processes where the purity of the steam is less important, such as the steam assisted gravity drainage (SAGD) process used for *in-situ* production of bitumen within the Canadian oil sands. This paper describes pilot-scale combustion testing of n-butanol in an atmosphere consisting of oxygen and water at a pressure of 15 bar(g). The tests took place over two days with each test run lasting around an hour and a half in the direct contact steam generation (DCSG) mode. Four test periods at different conditions throughout these runs are presented. Over these test periods, steam content of around 90 mol% at saturation was achieved; the O_2 in the combustion products was between 0.08 and 3.57 mol% with an average of 1.13 mol%. The CO emissions were low, at about 3 ppm in the combustor, with an average of 17.3 ppm (dry gas basis corrected to 3% O_2). The CO levels indicated that high fuel conversion was achieved even with the low O_2 content in the combustion products. The testing also indicated that operation with extremely low O_2 is possible, which will minimize downstream corrosions issues and reduce the energy consumption and costs associated with oxygen production.

Keywords: Heavy oil, bitumen, steam generation, oxy-fuel, SAGD, CCS

4.2. Introduction

Rapid development of Canada's oil sands is expected to continue as a result of high oil prices, concerns surrounding the global supply of oil, and market potential in the U.S. and Asia [1]. In 2011, thermal *in-situ* operations such as steam assisted gravity drainage (SAGD) accounted for 49% of the bitumen production in Alberta [2]. While *in-situ* extraction methods are less invasive than mining and have less local environmental impacts, SAGD results in more greenhouse gas (GHG) emissions per barrel [3] and requires large amounts of water that must be treated and recycled with around a 10% to 20% make-up water requirement [2]. CanmetENERGY is developing a new steam generation technology known as the High Pressure Oxy-fired Direct Contact Steam Generator (HiPrOx/DCSG or simply DCSG) that will reduce water requirements and simultaneously sequester GHGs when extracting heavy oils. The HiPrOx/DCSG technology is described in the CanmetENERGY patent (pending) entitled *"HIGH PRESSURE DIRECT CONTACT OXY-FIRED STEAM GENERATOR"* and is intended to replace the once through steam generators (OTSGs) and drum boilers that are currently used for SAGD [4].

For HiPrOx/DCSG, a fuel is combusted with pure oxygen at high pressure using water, which may be contaminated with hydrocarbons and solids, as a moderator to create the final product, a flue gas stream consisting mainly of steam with a minor portion of CO_2. The product stream can be injected into an underground bitumen reservoir where the heat of the product stream is transferred to the bitumen to reduce its viscosity, allowing it to be pumped to the surface via a production well. It is important that a product gas with a high concentration of H_2O is produced because the latent heat of the water plays the largest role in heating the bitumen. A study performed by Gates *et. al.* [5] found that approximately 80% of the CO_2 that is injected into the reservoir is sequestered, making this technology a competitive CCS technology for the oil sands. Since the combustion products of this technology are all converted to the useable product that is injected into the well, the thermal efficiency of this device will be close to 95-98%.

Direct contact air-fired steam generators and downhole steam generation have been in existence for a number of years. Several demonstrations have been carried out with relatively positive results [6-8] with many configurations of direct contact steam generation oriented towards the use of natural gas as opposed to solid fuels [9]. Work on the combustion and gasification of fuels is mostly focused on solid fuels utilization in power generation systems, with the exception of natural gas combined cycle (NGCC) and oil residue gasification. The main flue gas constituents in these solid fuel systems are typically N_2, CO_2, with some H_2O for combustion and CO, H_2, with some H_2O, and CO_2 for gasification [10–19]. In contrast, CanmetENERGY's DCSG work is targetted to flue gases having concentrations of steam up to 95 mol%. Although our fuel conversion approach is different, previous combustion and gasification work provides a technology base that can be used to work towards the commercialization of the DCSG process with gaseous, liquid and solid fuels. Developments in rocket engines were used to provide designs for highly compact, efficient, and reliable industrial pressurized oxy-fired systems [20]. When applying this technology to industrial combustion systems, the most important criteria are combustion stability, reliability, throttle control, and simplicity of manufacture and maintenance. The pintle injector design used within bipropellant rocket engine designs was adapted for application in HiPrOx/DCSG [21-23]. Mechanical details including injector design [24-26], igniter design [27] and combustion chamber design [28] were considered. Design guidelines and computational fluid dynamics models are currently under development and heavily funded for the purpose of constructing non-toxic reaction control engines, ascent engines, and descent engines for low cost earth orbiters and lunar modules [26, 29]. For the purpose of an initial test of concept, a simpler pintle atomizer design was used for the test work described in this paper than is used in rocket engines.

Steam addition was studied in ambient pressure oxy-fired conditions by Riaza *et. al.* [30] where it was shown that the ignition temperature was increased and burnout was reduced for a reactant oxygen concentration of 21%; however, as the oxygen concentration was increased to 30 and 35% the ignition temperature decreased and burnout improved. They postulated that the results may be related to enhancements in thermal radiation or

endothermic radical formation (O·, OH·, H·, *etc.*). Seepana and Jayanti [31] performed a theoretical study of steam-moderated oxy-fuel combustion of methane. In their study, flame structure analysis using a 325-step reaction mechanism was performed. They determined that higher oxygen content in the oxidant stream was required in order to obtain the same flame structure when moderating with steam compared to CO_2. This resulted in much higher mass fraction of oxygen in the flue gas. For a DCSG process, the need for higher O_2 concentrations in the flue gas may prove to be a disadvantage because higher concentrations of oxygen in the flue gas make corrosion problems a greater issue [32] and the generation of oxygen is energy intensive and expensive. Therefore, reducing the oxygen requirement is beneficial for economic and efficiency reasons.

Although past studies suggest steam addition to oxy-fired flames appears unfavorable, those studies were performed at ambient pressure. Pressurized DCSG may prove to be more favorable due to increased fuel throughput, and enhancements in intensity of reaction [19] which may result in a lower O_2 requirement than ambient systems.

The ultimate goal of CanmetENERGY's HiPrOx/DCSG program is to combust natural gas, low quality liquid fuels, and/or solid fuel slurries such as petroleum coke in the DCSG mode using wastewater containing high solids and hydrocarbon contamination similar to what is found in tailings water produced from mining and upgrading, or SAGD produced oily-water (POW) and produced water (PW). As a first step to proving the feasibility of this technology, this work examines the combustion of n-butanol in a HiPrOx/DCSG system at 15 bar(g) pressure with co-injection of municipal water. Process simulations with AspenTech HYSYS® were also performed using the pilot plant data to determine the steam concentrations throughout the process and to provide insight into the phenomena observed in the process.

The objective of the work presented here was to obtain operating data for the development of a HiPrOx/DCSG system using liquid fuels as a proof-of-concept; to determine the maximum theoretical H_2O content that could be achieved; to establish how low of an O_2 concentration in the product gas could be achieved without significantly

affecting flame stability and formation of CO; and to study the effect of nitrogen in the oxidant on the formation of NO_x. It was important to maximize the attainable H_2O content in the product gas to minimize energy intensity (latent heat produced per unit of fuel consumed) and to maximize the partial pressure of H_2O because lower partial pressure will reduce the saturation temperature, and thus, reservoir temperature, which reduces bitumen production [5]. Flame stability and CO formation were investigated because they indicate the conversion efficiency of the process and provide insight into how easily the process will be controlled at the commercial scale. The formation of NO_x was studied because it has the potential to condense and form nitric acid in downstream piping which may lead to corrosion issues as well as its pollutant potential.

4.3. Experimental

In this study, combustion of n-butanol (C_4H_9OH) with 99.5 mol% pure oxygen and clean city water as a moderator took place at 15 bar(g). The maximum theoretically attainable H_2O contents were determined using process simulations. The effect of low O_2 content in the product gas was determined experimentally by reducing the O_2 flow to the burner. Flame stability was examined by evaluating the fluctuations in the reactor pressure and reactor upper temperature by calculating the standard deviation of both over a certain time period. Formation of CO was determined through dry gas analysis of the experimentally produced product gas. The formation of NO_x was studied through dry gas analysis of the experimental combustion products with and without nitrogen feed.

4.3.1. Fuel Analysis

Although n-butanol is not a practical fuel for this application, it is a suitable research fuel for a trial for proof-of-concept due to its volatility, well defined chemical and physical properties and the inherent simplicity of using liquid fuel delivery compared to compressed gases (*e.g.*, high pressure natural gas) or a solid fuel slurry (*e.g.*, petroleum coke). Typically, n-butanol is used as a solvent, but may be used as a fuel. The analysis of the butanol used in these tests is given in **Table 4.1**.

Table 4.1 – Chemical analysis of n-butanol

Parameter	Value
Specific Gravity @ 25 °C	0.808
Composition	
n-Butanol (wt%)	99.9
Water (wt%)	0.01
Higher Heating Value (MJ/kg)	33.1

4.3.2. Test Matrix

The pilot facility was operated at four conditions (B1 to B4) as summarized in **Table 4.2**.

Table 4.2 – Test condition summary

Description	B1	B2	B3	B4
Butanol flow (kg/h)	11.5	15.2	15.2	15.2
Total heat input (kW_{th})	105.7	139.6	139.6	139.6
Oxygen flow (kg/h)	33.5	40.4	39.8	39.6
Water to burner flow (kg/h)	32.5	50.0	50.0	50.0
Nitrogen to burner flow (kg/h)	0	0	0	2.1

The purpose of condition B1 was to establish that a stable and controllable flame could be achieved while co-injecting liquid water with the fuel. The purpose of conditions B2 and B3 was to evaluate the quality of combustion with little excess oxygen. The purpose of B4 was to gain insight into the potential for NO_x generation in the reactor when low levels of N_2 are present.

4.3.3. Equipment Description

The experimental work was performed at 15 bar(g) pressure in the pilot-scale slagging reactor (**Figure 4.1**) at CanmetENERGY. The refractory lined reactor had an inner diameter of 250 mm and a length of 2135 mm. The fuel was injected into the reactor through a gas-swirl atomizer, shown in **Figure 4.2**, with impinging plate and pintle to provide a hollow cone spray. The n-butanol and burner water (water stream #1) were mixed and sent into the mixing chamber via the fuel supply tube. Oxygen (99.5 mol%) was introduced into the mixing chamber through the fluid conduit identified as “oxygen

jets" in **Figure 4.2**. After impact with the impinging plate, the fluid flowed through the shear region and impacted the pintle to produce the desired hollow cone spray. The atomized liquid mixture was injected downwards into the combustion zone on the central axis of the reactor to produce the flame.

The internal reactor temperatures were measured at 355 mm intervals along the vertical axis using ceramic coated type B thermocouples. Sample Point #1, located near the exit of the reactor, 1660 mm from the top of the reactor, used a nitrogen cooled sample probe to extract flue gas samples. The combustion products left through the bottom of the reactor and entered the quench zone, in which quench water (water stream #2) was introduced via four flat fan spray nozzles located 300 mm below the reactor outlet. The product gas was created within the quench zone but was over-quenched to a temperature below saturation to ensure ease of operation and to protect downstream equipment. The flue gas left the quench vessel near the top of the vessel and entered the scrubber, where the flue gas temperature was further reduced to near ambient temperature and exhausted. A dry gas sample was collected at Sample Point #2 located near the exhaust where O_2 was measured using a HoribaTM MPA-510 gas analyzer, CO_2 and CO were measured using HoribaTM VIA-510 gas analyzers, NO, NO_2 and NO_x were measured using a Thermo ScientificTM 42i-HL gas analyzer and SO_2 was measured using an AmetekTM 9000RM photometric gas analyser. All liquid effluents were filtered through bag filters and sent for water treatment.

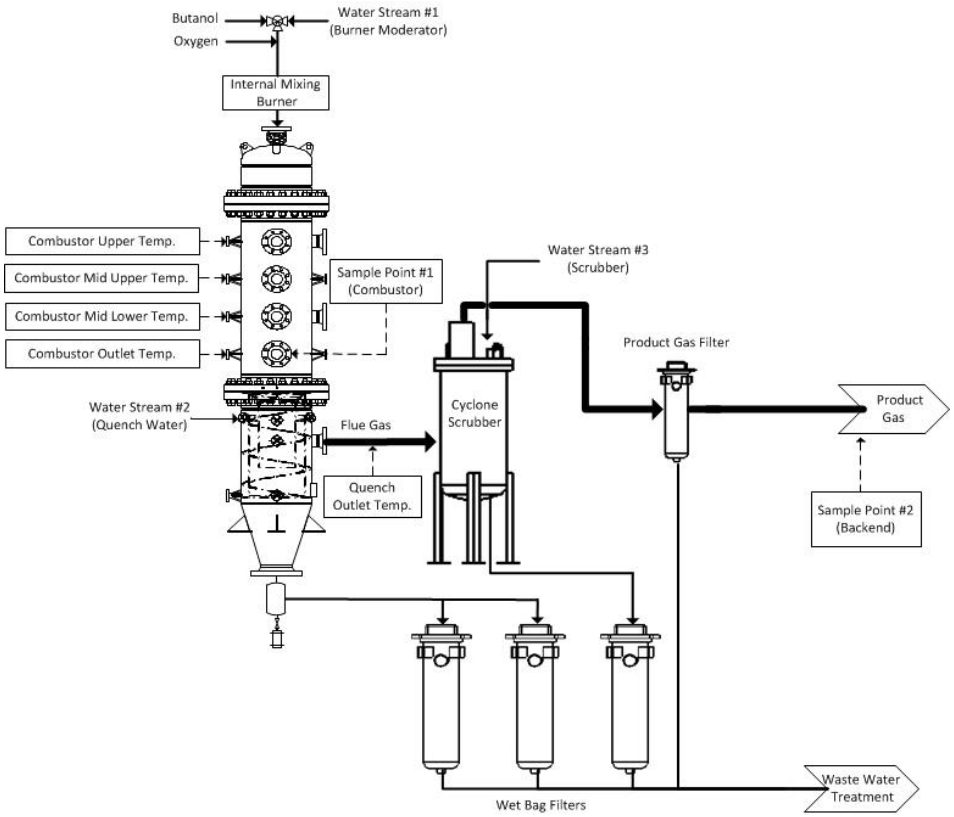

Figure 4.1 – 15 bar(g) pilot scale reactor

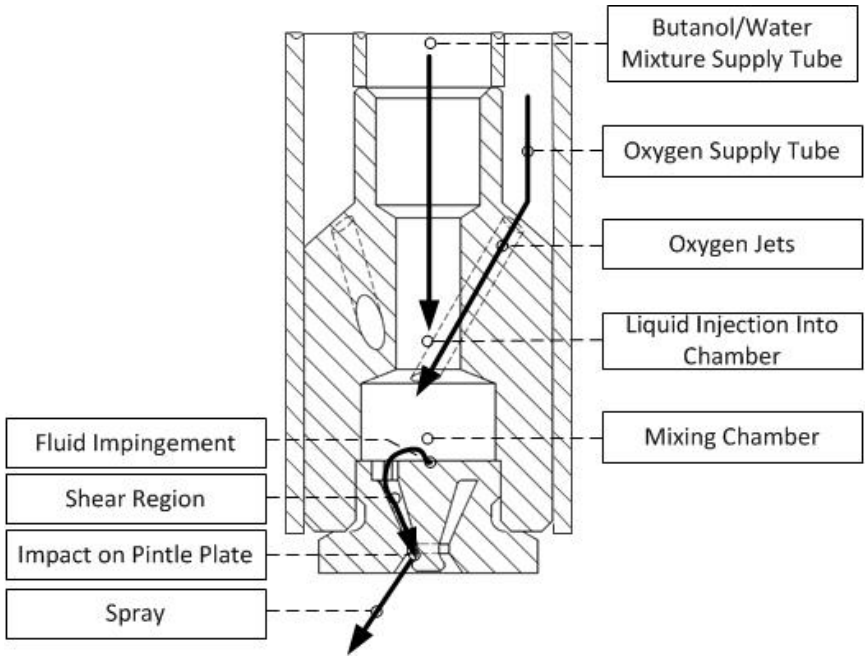

Figure 4.2 – Gas-swirl atomizer used for atomizing butanol/water mixture with oxygen.

4.3.4. Modeling Techniques

The average values from each test period were used to perform AspenTech HYSYS® 2006 simulations to determine the moisture content in the product gas at various intermediate stages within the process. The process flow diagram is shown in **Figure 4.3**.

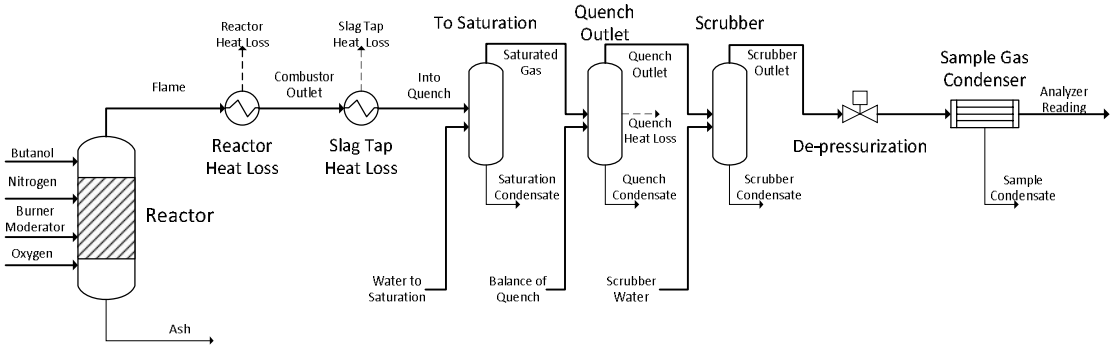

Figure 4.3 – Model process flow diagram

For the model, n-butanol was injected into a conversion reactor along with burner moderator water, oxygen (99.5 mol% pure) and nitrogen when applicable. 100% conversion was assumed as was indicated by the pilot tests. The conversion reactor inlet reactant flow rates were based on the flows measured in the tests, except for the oxygen, which was back calculated from the analyzer readings due to the high level of precision required for the calculations when considering parts per million of carbon monoxide. The flame temperature was based on the Gibbs free energy estimation made by AspenTech HYSYS® for the resulting combustion products. The reactor heat loss was estimated based on the duty required to cool the "flame" stream to the experimentally measured "combustor outlet" temperature. A large portion of the heat loss likely resulted from heat going to the refractory with a portion lost in the burner and sample probe cooling systems. The combustor outlet stream was subjected to a 3 kW heat loss across the slag tap which was determined from other experiments, where the gas temperature drop had been measured across it. The slag tap heat loss was assumed to be constant for all cases.

Experimentally, the flue gas was quenched past the saturation point for ease of operation and to protect downstream equipment. This type of system will eventually be operated near the saturation point because this condition maximizes the latent heat available in the product stream. In the simulations this intermediate saturation condition was determined using the following procedure. The saturated gas composition was defined as the point where the vapour fraction of the gas is completely saturated and any further addition of water would result in condensation of liquid. To determine this condition the "into quench stream" was cooled in the "to saturation" vessel within the simulation. In this vessel, the "water to saturation" was adjusted to the point at which "saturation condensate" was zero. This provided the "saturated gas stream" information.

The intermediate calculated saturated gas stream entered the "quench outlet" vessel where the "balance of quench" water was added as shown in **Figure 4.3**. The "balance of quench" was defined as the experimentally measured quench water flow rate less the "water to saturation" value calculated in the previous vessel. The "quench heat loss" stream was adjusted to match the quench outlet temperature that was measured experimentally. The quench outlet gas entered the "scrubber" vessel where the experimentally measured scrubber water flow rate was applied. After de-pressurization the remaining water in the gas was split using the "sample gas condenser" to confirm the experimental analyzer readings as a check on the mass balance.

4.4. Results

The results from the experiments and modeling are presented in **Section 4.4.1** and **Section 4.4.2**, respectively.

4.4.1. Experimental Results

The test periods took place over two separate runs. Butanol test period 1 (B1) data is shown to span from the time 0:00 to 0:10 (h:mm) beginning after steady-state was achieved. The reactant flows and product compositions over this period are shown in **Figure 4.4** while the process pressures and temperatures are shown in **Figure 4.5**.

Butanol test period 2 (B2) and 3 (B3) data was selected to span from time 0:00 to 0:10 and 0:26 to 0:36 after steady-state was achieved in the second test run, respectively. No data was analyzed for the period between 0:36 and 1:20 because the O_2 flow rate was constantly being adjusted by the operators to determine how close to the stoichiometric point the O_2 content could be controlled. These adjustments resulted in fluctuations in the analyzer readings with no substantial periods of steady state. The lowest O_2 content achieved over that period was less than 0.4 mol% on a dry basis with CO readings of around 50 ppm dry. At time 0:50, N_2 was added to the burner at a rate of 2 kg/h and then increased to 2.1 kg/h at 1:16. After a transient period in the NO_x analyzers, the reactor achieved steady-state at around time 1:20 where the O_2 content was 0.4 mol% on a dry basis which is near the detection limit of the analyzer. Butanol test period 4 (B4) data spanned from 1:25 to 1:35. The reactant flows and product gas compositions throughout the second test run are shown in **Figure 4.6** and the process pressures and temperatures are shown in **Figure 4.7**. A summary of the test data for test points B1-B4 is presented in **Table 4.3**.

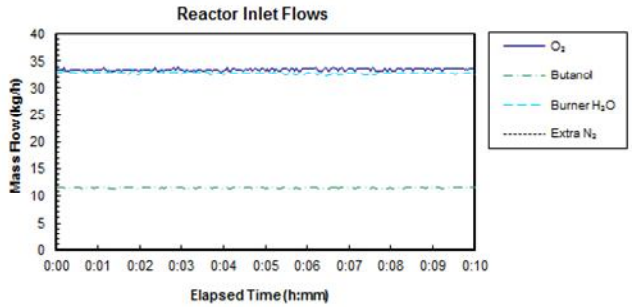

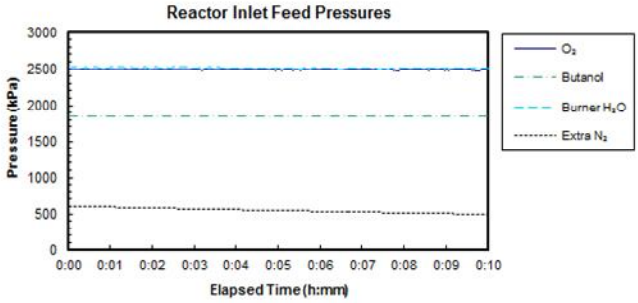

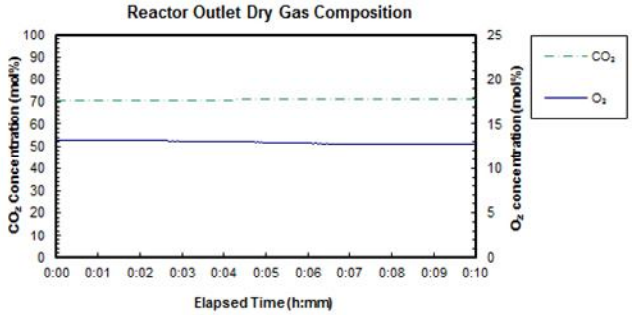

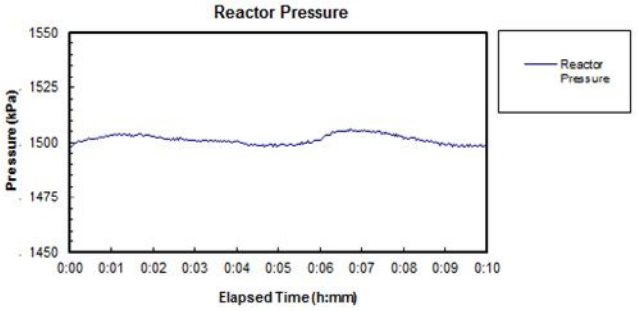

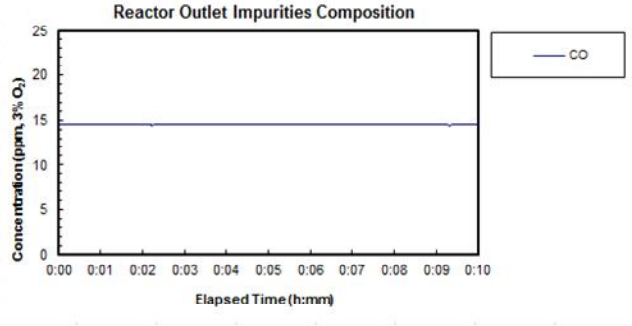

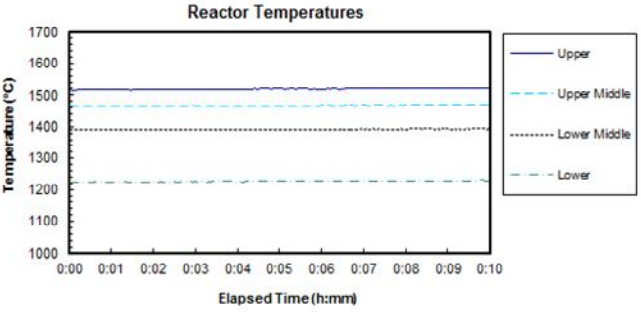

Figure 4.4 – Reactant flows and product gas compositions for the test run that contained test period B1

Figure 4.5 – Process pressures and temperatures for the test run that contained test period B1

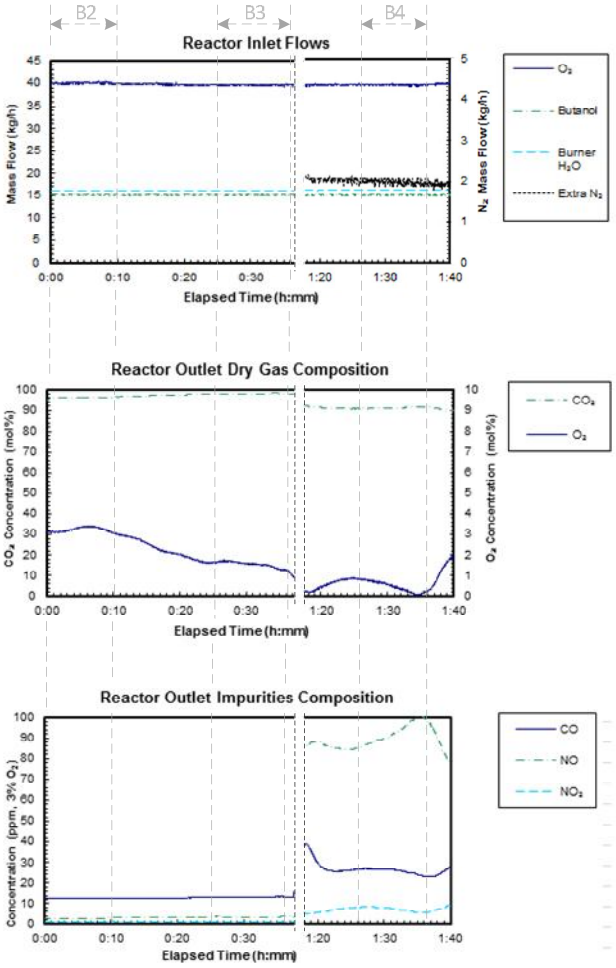

Figure 4.6 – Reactant flows and product gas compositions for the test run that contained test periods B2-B4

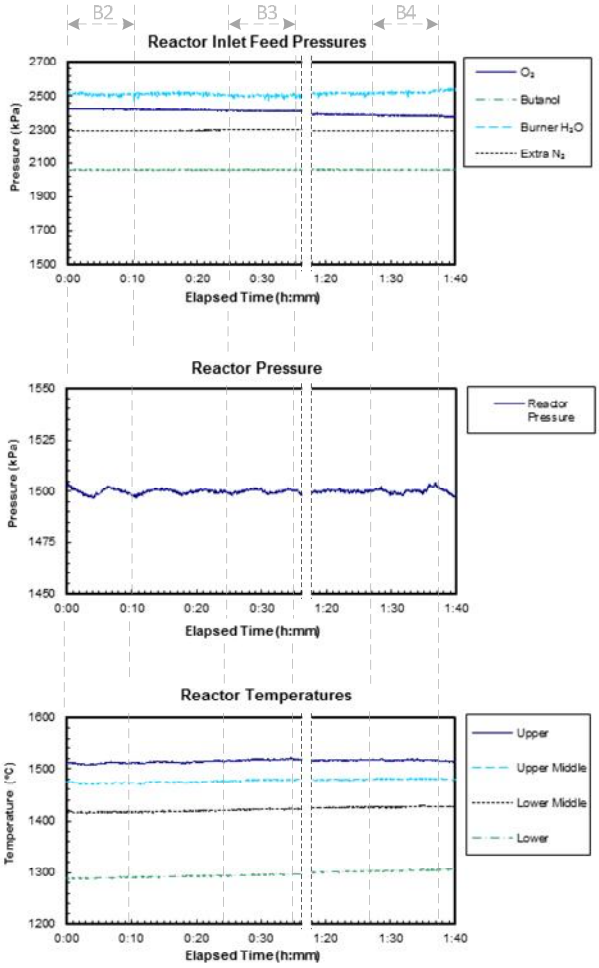

Figure 4.7– Process pressures and temperatures for the test run that contained tetest periods B2-B4

Table 4.3 – Overview of test data

Description	B1	B2	B3	B4
Test run ID	1	2	2	2
Time Period (h:mm - h:mm)	0:00-0:10	0:00-0:10	0:26-0: 36	1:25-1:35
Combustor gauge pressure (bar)	15.013	14.996	15.001	14.999
Standard deviation of pressure (bar)	0.022	0.016	0.008	0.006
Combustor upper temperature (°C)	1540	1510	1518	1514
Standard deviation of upper temperature (°C)	2.1	1.7	1.1	1.7
Combustor outlet temperature (°C)	1230	1291	1297	1427
Combustor heat loss (kW)	37.1	36.4	36.3	27.9
Combustor heat loss (%)	35.1	26.1	26.0	20.0
Quench water flow (kg/h)	230.0	251.5	248.9	248.9
Quench outlet temperature (°C)	125.3	172.5	178.3	190.5
Dry gas composition				
O_2 (mol% dry)	16.1	3.4	1.5	0.4
CO_2 (mol% dry)	83.6 [a]	96.3	98.2	90.6
CO (ppm dry, 3% O_2)	17	13	13	26
NO (ppm dry, 3% O_2)	-	3	3	78
NO_2 (ppm dry, 3% O_2)	-	1	1	5
NO_X (ppm dry, 3% O_2)	-	4	5	84
NO_2/NO	-	0.39	0.29	0.06
SO_2 (ppm dry, 3% O_2)	<10	<10	<10	<10

a – For this single run, CO_2 concentration was determined by difference due to analyzer problems. The impurities in the oxidant were accounted for using a mass balance.

For B1, the O_2 concentration in the product gas was 16 mol% on a dry basis because the objective was a proof-of-concept in which very safe operating conditions were selected. Over this test period CO averaged around 17 ppm (corrected to 3 mol% O_2 dry) indicating excellent conversion to CO_2. For B2 the O_2 concentration was much lower at 3.4 mol% on a dry basis. This was the first test in which attempts to run at low O_2 concentration were made. The CO content was similar at 13 ppm (corrected to 3 mol% O_2 dry) which also indicates significant flame stability and conversion to CO_2. The formation of thermal NO_x caused by nitrogen in the oxidant was less than 5 ppm (corrected to 3 mol% O_2 dry), which is very close to the detection limit of the analyzer. Low NO_x emissions are important to reduce nitric acid formed by condensation of water through the following reaction: $2NO_2 + H_2O + 1/2O_2 \leftrightarrow 2HNO_3$. The O_2 concentration throughout B3 was around 1.52 mol% on a dry basis. The lowest O_2 content was achieved during test period B4 in which it was about 0.4 mol% on a dry basis. The CO fluctuated around 28 ppm which indicates that the conversion of CO to CO_2 was still

high, but less than B1-B3. This is expected because less oxygen was available to complete combustion within the reactor. The most interesting result is that NO_x increased to about 84 ppm from around 5 ppm when nitrogen was added. This indicates that the purity of the oxidant will have an effect on NO_x when a fuel without nitrogen, such as natural gas, is used. For both runs the upper reactor temperature and reactor pressure were very stable (Figures 4 and 6). The standard deviations were no greater than 2.1 °C and 0.022 bar, respectively, indicating both low reaction and gross flow field fluctuations. These low deviations, coupled with the low CO emissions (less than 50 ppm dry corrected to 3% O_2) indicate that the flame was very stable and that the conversion to CO_2 was very high.

4.4.2. Modeling Results

The modeling results are presented in **Table 4.4**. The CO, NO, NO_2 and SO_2 compositions were based on the analyzer readings.

Table 4.4 – Modeling Results Summary

Description	B1	B2	B3	B4
Flame temperature (°C)	1939	1802	1807	1809
Combustion products composition dry				
O_2 (mol% dry)	16.1	3.3	1.5	0.4
CO_2 (mol% dry)	83.6	96.4	98.2	93.6
N_2 (ppm dry, 3% O_2)	592	598	595	5.75[a]
Ar (ppm dry, 3% O_2)	2367	2393	2379	2319
Combustion products composition wet				
H_2O (mol% wet)	77.8	81.7	82.0	81.3
O_2 (mol% wet)	3.57	0.60	0.27	0.08
CO_2 (mol% wet)	18.6	17.7	17.7	17.5
N_2 (ppm wet, 3% O_2)	131	110	107	10729
Ar (ppm wet, 3% O_2)	526	439	429	433
CO (ppm wet, 3% O_2)	3	2	-	5
NO (ppm wet, 3% O_2)	-	<1	<1	14.5
NO_2 (ppm wet, 3% O_2)	-	<1	<1	<1
SO_2 (ppm wet, 3% O_2)	<10	<10	<10	<10
Water to saturation	50.8	77.9	78.3	89.0
Saturation temperature	195.1	196.3	196.9	197.1
Saturated gas composition				
H_2O (mol% wet)	88.0	90.5	90.7	91.0
O_2 (mol% wet)	1.93	0.32	0.14	0.04
CO_2 (mol% wet)	10.0	9.2	9.1	8.5
N_2 (ppm wet, 3% O_2)	15	57	55	5186
Ar (ppm wet, 3% O_2)	284	227	222	209
CO (ppm wet, 3% O_2)	2	1	-	2
NO (ppm wet, 3% O_2)	-	<1	<1	7
NO_2 (ppm wet, 3% O_2)	-	<1	<1	<1
SO_2 (ppm wet, 3% O_2)	<10	<10	<10	<10
Balance of quench (kg/h)	179.2	173.6	170.6	159.9

a – Unit is mol% dry as a result of extra N_2

4.5. Discussion

For B1 the maximum attainable steam content was calculated to be ~88 mol% and ~90.5 mol% for B2. This could be attributed to the significant difference in O_2 content in the flue gas. The O_2 affects the maximum attainable steam concentration because its increased partial pressure will lower the saturation temperature of the mixture since O_2 is non-condensable in these conditions. The maximum attainable steam content calculated for B3 was 90.7 mol%. For B4, the lowest O_2 content, also resulted in the highest maximum attainable steam (91.0 mol%) content. Although the data supports the

hypothesis that O_2 concentration will have an effect on maximum attainable steam concentration, the difference is within experimental error limits making this effect difficult to quantify without further investigation.

In all cases, CO production was minimal peaking at 50 ppm (corrected to 3 mol% O_2 dry) for the period where the O_2 content was lowest on the second test run. This indicates that the fuel was close to fully converted in all cases. This result opens up the possibility of operating the combustor slightly sub-stoichiometric with the goal of producing a product gas with oxygen concentrations less than 100 ppm. This process is ideal for this operating condition because the combustion products are further diluted with water downstream. For example, if the combustion results in a 1 mol% CO concentration in the dry gas, it will be diluted to as low as around 0.1 mol% in a 90 mol% steam product gas. A low concentration of CO is not expected to create corrosion issues in the bitumen reservoir as demonstrated by Yee and Stoich [32] when they injected a dry flue gas containing around 0.71 mol% CO down a SAGD well and found no corrosion issues.

When the standard deviations on the upper reactor temperature and reactor pressure were calculated for B1-B4, it was observed that the deviations were no larger than 2.2 °C and 0.022 bar for temperature and pressure, respectively. These numbers indicate low fluctuations in fuel conversion (temperature) and stable flow fields (pressure) within the reactor. These results, coupled with the low CO emissions indicate that the flame was quite stable throughout the testing. This observed flame stability shows that combustion is not significantly impeded by the high concentration of steam and the energy required to vaporize the water.

It was also observed that thermal NO_x formation increased with the addition of nitrogen. This result is important because it provides insight into the effects that the purity of the oxidant will have on NO_x formation when a fuel that doesn't contain any nitrogen, such as natural gas, is used. Therefore, lower purity oxygen such as 95% pure will lead to higher NOx formation than 99% pure oxygen. It is likely that additional N_2 will reduce the maximum attainable H_2O content, but as previously mentioned, the effect that non-

condensable gases have on bitumen production still remains unclear. It is recommended that further sensitivity analysis on oxygen purity be performed to optimize oxygen purity and minimize commercial operating costs.

Overall, the data indicates that unlike ambient oxy-fired conditions with steam addition, lower O_2 contents are attainable in the combustion products (as low as 0.08 mol%) when pressurized combustion is used. Furthermore, the increased addition of H_2O to attain the product gas composition results in an O_2 content as low as 0.04 mol%, or 4000 ppm (wet basis). Field tests performed by Yee and Stoich [32], in which they injected a flue gas generated by a fuel-rich natural gas fired internal combustion engine into a SAGD well, found that after four months of operation none of the carbon steel corrosion monitoring devices showed signs for concern. The flue gas composition for these field tests was 100 ppm O_2, 16.15 mol% CO_2, 81.5 mol% N_2, 1.34 mol% H_2, and 0.71 mol% CO. Although the O_2 content for the tests performed in this study were higher, it may be possible to run this technology slightly fuel-rich as well without affecting combustion characteristics as evidenced by the flame stability for the low O_2 contents discussed above.

As previously mentioned, the H_2O content in the product gas is important because of the latent heat that it contributes as it condenses in the bitumen reservoir. The test results indicate that a H_2O content in the product gas of around 90 mol% is attainable at the saturation point using n-butanol even at the small pilot scale. Although this is favorable from a thermodynamic standpoint, heat losses in transport pipes may cause condensation and corrosion due to the formation of carbonic acid. Yee and Stoich [32] suggested that if the flue gas is always above its dew point, the potential for corrosion from carbonic acid would be reduced. One method of ensuring this with the HiPrOx/DCSG technology is to operate the scrubber at a vapor phase fraction of around 90% to avoid scaling issues and then to superheat the scrubber outlet gas by 100-200 °C above the dew point. This will result in H_2O contents in the product gas that are below 90 mol% but also well above 80 mol%, which was the H_2O content in the combustion products at 1800 °C (**Table 4.4**), which leaves 1400 °C of temperature that can be quenched through the addition of water. A sensitivity analysis regarding the effect of the product gas outlet temperature on the

water and fuel requirements per barrel of oil produced will be considered to determine the optimal operating conditions.

4.6. Conclusions

The conclusions for this work are as follows:

1. High product gas O_2 concentrations are not required for the HiPrOx/DCSG technology which will reduce corrosion issues in downstream piping, decrease non-condensable gas concentration into the well, and result in increased efficiencies and lower costs at the commercial scale.
2. High concentrations of H_2O in the product gas are attainable which will maintain the latent heat in the product gas at levels similar to those for pure steam.
3. The CO emissions were low, indicating excellent conversion of the fuel and significant flame stability.
4. Low fluctuations in the upper reactor temperature and reactor pressure indicate a stable flame.
5. Thermal NO_x formation was low and increased with further addition of N_2, indicating that O_2 purity will affect formation of NO_x for fuels that do not contain nitrogen such as natural gas. Further investigation into these effects is required.
6. Concerns regarding corrosion can likely be dealt with by operating in fuel-rich environments with superheating of the wet product gas out of the scrubber. A sensitivity analysis on the effects of these operating conditions on the water consumption and fuel requirements is required in order to optimize the process.

4.7. Acknowledgements

The authors would like to acknowledge the financial support received for this project through the Panel on Energy R&D (PERD), as well as technical assistance by Jeff Slater and Ryan Burchat at the pilot-scale facility.

4.8. References

[1] National Energy Board. Canada's oil sands opportunities and challenges to 2015: an update. 2006 June. 2 p.

[2] Alberta Government. In-situ process steam assisted gravity drainage. 2013 Feb. 1 p.

[3] Bohm M, Goold S, Laux S, Neu B, Sharma A. Aasen K. Application of oxy-fuel CO_2 capture for in-situ bitumen extraction from Canada's oil sands. Energy Proc. 2011; 4:958-965.

[4] Clements B, inventor; Her Majesty the Queen in Right of Canada as Represented by the Minister of Natural Resources, assignee. High pressure direct contact oxy-fired steam generator. Unites States patent US 20110232545A1. 2011 Aug 29.

[5] Gates ID, Bunio G, Wang J, Robinson B. Impact of carbon dioxide co-injection on the performance of SAGD. Proceedings of the 2011 World Heavy Oil Congress; 2011 Mar 14-17; Edmonton, Alberta, Canada.

[6] Sarkar S. Direct contact steam generation by opposed jet flame stabilization. J Inst Eng: Chem Eng Div 1988; 68: 55-58.

[7] Alamatsaz A, Moore R, Mehta S, Ursenbach M. Experimental investigation of in-situ combustion at low air fluxes. J Can Pet Tech 2011; 50:48-67.

[8] Mohtadi M, Sarkar S. Use of opposed jet flame stabilization in a downhole steam generator. Can J Chem Eng 1985; 63:674-680.

[9] Betzer-Tsilevich M. Integrated steam generation process and system for enhanced oil recovery. Proceedings of the 2010 Canadian Unconventional Resources & International Petroleum Conference; 2010 Oct 19-21; Calgary, Alberta, Canada.

[10] Sadhukan A, Gupta P, Saha R. Modelling of combustion characteristics of high ash coal char particles at high pressure: shrinking reactive core model. Fuel 2010; 89:162-169.

[11] Goard P, Mulcahy M. A study of the ignition of graphite. Carbon 1967; 5:137-153.

[12] Sun C, Zhang M. Ignition of coal particles at high pressure in a thermogravimetric analyzer. Comb and Flame 1998; 115:267-274.

[13] Toftegaard M, Brix J, Jensen P, Glarborg P, Jensen A. Oxy-fuel combustion of solid fuels. Prog En Comb Sci 2010; 36:1-45.

[14] Hu Y, Nikzat H, Nawata M, Kobayashi N, Hasatani M. The characteristics of coal-char oxidation under high partial pressure of oxygen. Fuel 2010; 80:2111–2116.

[15] Wang C, Lei M, Yan W, Wang S, Jia L. Combustion characteristics and ash formation of a pulverized coal under pressurized oxy-fuel conditions, Energy Fuels 2011; 25:4333-4344.

[16] Yu J, Harris D, Lucas J, Roberts D, Wu H, Wall T. Effect of pressure on char formation during pyrolysis of pulverized coal. Energy and Fuel 2004; 18:1346–1353.

[17] Monson C, Germane G, Blackham A, Smoot D. Char oxidation at elevated pressures. Comb Flame 1994; 100:669-683.

[18] Yang T, Balles E, Lisauskas R, Vitalis B, Hunt P. Pressurized oxycombustion carbon capture power system. Proceedings of the 35th International Technical Conference on Clean Coal & Fuel Systems; 2010 June 6-10; Clearwater, Florida, USA.

[19] Wall T, Lui G, Wu H, Roberts D, Benfell K, Gupta S, et al. The effects of pressure on coal reactions during pulverized coal combustion and gasification. Prog En Comb Sci 2002; 28:405-433.

[20] Fusselman S. Compact gasification development and test status. Proceedings of the 2011 Gasification Technologies Conference; 2011 Oct 9-12; San Francisco, CA, USA.

[21] Elverum G, inventor; TWE Inc., assignee. Combustion apparatus having a coaxial-pintle injector. United States patent US 4206594. 1971 Nov 1.

[22] Betts E, Frederick R. A historical systems study of liquid rocket engine throttling capabilities.

[23] Fisher S, Rahman S; NASA John C Stennis Space Center. Remembering the giants: Apollo rocket propulsion development. 2009 Dec.

[24] Dressler G, Bauer J. TRW pintle engine heritage performance characteristics. Proceedings of the 36th AIAA/ASME/SAE/ASEE Joint Propulsion Conference and Exhibit; 2000 Jul 16-19; Huntsvile Alabama, USA.

[25] Gromski J, Majamaki A, Chianese S, Weinstock V, Kim T. Northrop Grumman TR202 LOX/LH2 deep throttling engine technology project status. Proceedings of the 46th AIAA/ASME/SAE/ASEE Joint Propulsion Conference and Exhibit; 2010 Jul 25-28; Nashville, Tenessee, USA.

[26] Smith T, Klem M, Fisher K; NASA Glenn Research Center. Propulsion risk reduction activities for nontoxic cryogenic propulsion. 2010 Oct.

[27] Breisacher K, Ajmani K; NASA Glenn Research Center. LOX/Methane main engine flow plug igniter tests and modeling. 2009 June.

[28] Calvignac J, Dang L, Tramel T, Paseur L. Design and testing of non-toxic RCS thrusters for second generation reusable launch vehicle. Proceedings of the 46th AIAA/ASME/SAE/ASEE Joint Propulsion Conference and Exhibit; 2010 Jul 25-28; Nashville, Tenessee, USA.

[29] Boettcher P, Damazo J, Shepherd J. Visualization of transverse annular jets – pintle injectors. Bull Am Phys Soc. 2009; 54.

[30] Riaza J, Álvarez L, Gil M, Pevida C, Pis J, Rubiera F. Effect of oxy-fuel combustion with steam addition on coal ignition and burnout in an entrained flow reactor. Energy 2011; 36:5314-5319.

[31] Seepana S, Jayanti S. Steam-moderated oxy-fuel combustion. Energy Conv Mgmt 2010; 51:1981-1988.

[32] Yee C-T, Stroich A. Flue gas injection into a mature SAGD steam chamber at the dover project (formerly UTF). J Can Pet Tech 2004; 43:54-61.

Chapter 5. High Pressure Oxy-firing (HiPrOx) of Fuels with Water for the Purpose of Direct Contact Steam Generation – Part 2: Graphite and Mixtures of Butanol/Graphite

Paul Emanuel Cairns[a], Bruce R. Clements[a,*], Robin Hughes[a], Ted Herage[a], Ligang Zheng[a], Arturo Macchi[b], Edward J. Anthony[c]

[a]Natural Resources Canada, CanmetENERGY, 1 Haanel Dr., Ottawa, Ontario, Canada, K1M 1M1

[b]Faculty of Chemical and Biological Engineering, University of Ottawa, 161 Louis Pasteur St., Ottawa, Ontario, Canada, K1N 6N5

[c]School of Applied Sciences, Cranfield University, College Rd., Cranfield, Bedford MK43 0AL, United Kingdom

In submission to Fuel, 2013

5.1. Abstract

Production in Canada's oil sands has been increasing with a projected production rate of 4.5 million barrels per day by 2025. Two production techniques are currently used, mining and *in-situ* with the latter projected to make up about 57% of all production by that time. Although *in-situ* extraction methods such as Steam Assisted Gravity Drainage (SAGD) are less invasive than mining, they result in more greenhouse gas (GHG) emissions per barrel and require large amounts of water that must be treated and recycled with a make-up water requirement of about 10%. CanmetENERGY is developing a steam generation technology called the High Pressure Oxy-fired Direct Contact Steam Generator (HiPrOx/DCSG, or DCSG for short) that will reduce these water requirements and sequester GHGs. In this study, a series of tests were undertaken where combustion of graphite slurry and graphite slurry/butanol mixtures with oxygen and water were performed. Graphite/butanol mixtures were selected because certain combinations could represent the range of proximate analyses of waste fuels and to indicate whether fuels that are difficult to burn, such as petroleum coke, will ignite in the high moisture environment. Unassisted combustion of slurried graphite was achieved for a period of 20 minutes until problems were encountered due to burner plugging with the slurry after which the burner was stopped. It was found that the maximum attainable H_2O content in the saturation gas increased with increasing hydrogen to carbon ratio with around 80 mol% being achieved with the graphite, 81 mol% with a 25% butanol in graphite mixture and around 86.5% in a 40% butanol in graphite mixture. It was observed that flame stability decreased with decreasing volatile content in the fuel. No measurable carbon containing residues were found after testing, indicating that high conversion was achieved.

Keywords: Heavy Oil, Bitumen, Steam generation, Oxy-fuel, SAGD, CCS

5.2. Introduction

Recent estimates have shown that Canada has the third largest oil reserves in the world with 95% associated with the Alberta oil sands [1]. In Alberta, 80% (135 billion barrels) of the oil sands can only be accessed through *in-situ* methods such as Steam Assisted Gravity Drainage (SAGD) [2]. In 2011, total oil sands raw bitumen production was 1.74 million barrels per day (b/d) with *in-situ* techniques making up about 49% of this production. By 2025, *in-situ* production is forecast to make up 57% of a total 4.5 million b/d [3]. Although *in-situ* extraction methods such as SAGD are less invasive than mining, they result in more greenhouse gas (GHG) emissions per barrel [4] and require large amounts of water that need to be treated and recycled with make-up water requirement of about 10% [2]. CanmetENERGY is developing a steam generation technology called the High Pressure Oxy-fired Direct Contact Steam Generator (HiPrOx/DCSG) that will reduce these water requirements and sequester GHGs. This technology is described in CanmetENERGY's patent [5].

The ultimate type of fuels intended for use with HiPrOx/DCSG are natural gas and waste fuels that are by-products of oil upgrading such as delayed petroleum coke and asphaltenes. Natural gas would be used in the first implementations of this technology because this infrastructure currently exists in commercial SAGD plants. The waste fuels are identified for the future because they are abundant and essentially free sources of energy [6] within this sector.

Part 1 of the HiPrOx/DCSG pilot-scale campaign [7] studied the combustion of n-butanol with municipal water as a moderator. The objectives were to determine the minimum excess O_2 level that could be achieved while minimizing the formation of CO and maximizing the attainable steam concentration in the product gas. Butanol was selected because it is a volatile fuel that can be injected in liquid form for ease of operation. In the Part 1 testing, an H_2O content of around 90 mol% at saturation was achieved. The O_2 in the combustion products was between 0.08 mol% and 3.57 mol% with an average of 1.13 mol%. The CO emissions were low, at about 3 ppm (wet, corrected to 3% O_2) in the

combustor, with an average of 17.3 ppm (dry gas basis corrected to 3% O_2). The CO levels indicated high conversion regardless of the low O_2 content in the combustion products. The low standard deviation on the combustor temperature and pressure indicated significant flame stability. The testing demonstrated that operation with very low O_2 was possible which will minimize downstream corrosions issues and reduce the energy consumption and costs associated with oxygen production requirements. The results provided insight into the operating conditions that could be attained with another volatile fuel such as natural gas.

In Part 2, a series of tests were undertaken where combustion of graphite slurry and graphite slurry/butanol mixtures in an oxygen and water atmosphere was performed. graphite/butanol mixtures were selected because certain combinations could represent the range of proximate analyses of waste fuels. These tests also served as a proof of concept that fuels with very little volatile matter and relatively inert chars, such as graphite and petroleum coke, can be used within the HiPrOx/DCSG environment. As opposed to more realistic liquid and solid fuels such as oil and petroleum coke, less practical fuels (graphite and butanol) were used due to absence of sulphur, which alleviated concerns over corrosion caused by sulfuric acid for which the pilot-scale reactor was not amenable for at that time. Following this period of initial testing, the inside wall of the reactor was coated with inconel 625 to allow for future experimental programs using more practical fuels.

Graphite is profoundly unreactive and has attractive mechanical and thermophysical properties for which it is typically used as high-temperature, heat-shielding, structural material for atmospheric re-entry, gas turbine blades, scram-jet combustors, *etc.* [8]. As a result, combustion studies involving graphite are typically done in extreme environments. For example, combustion of graphite in high pressure and temperature CO_2 and H_2O environments was studied by Culbertson and Brezinsky [9] to determine whether the post combustion gases were reacting with rocket nozzles and causing erosion. They performed shock-tube testing in pressures ranging from 211.8 to 367.8 bar and temperatures ranging from 1275 and 2420 C in pure CO_2 and pure steam. They found

that the CO_2 and steam were indeed reacting with the graphite and also found that both reactions had the same rate coefficient at those conditions. Makino *et. al.* [8] studied the combustion rate of graphite rods in water vapour flow with the purpose of minimizing hazardous disasters caused by the chemical reaction between overheated graphite moderators and water vapour in nuclear reactors. Their study was performed with pure steam at approximately 8 atmospheres and around 1325 °C to determine the reactivity with steam which was compared to the reactivity in O_2 and CO_2. As expected, they found that H_2O was a weaker oxidizer compared to O_2 and oxidized graphite at about twice the rate observed for CO_2.

Graphite is much more difficult to burn than petroleum coke due to its lower volatility, higher activation energy, highly stable molecular structure, and lack of porosity. A char combustion reactivity study performed by Lang and Hurt [10] found that the reactivity of graphite is around 14 times lower than delayed petroleum coke. Furthermore, its activation energy has been measured at around 165 kJ/mole [11] compared to around 54 kJ/kmole for petroleum coke [12].

In summary, previous studies indicate that combustion of graphite is difficult other than under extreme environments and that graphite is much less reactive than petroleum coke. As a result, combustion of graphite for the tests performed in this study will serve well as a proof of concept and technical feasibility of any solid fuels under these conditions using this technology. Therefore this study measured the flame stability, CO emissions, and maximum attainable steam concentration in the product gas as a function of the fuel mixture.

5.3. Experimental

The tests performed in this study took place at 15 bar(g) with clean city water, 99.5 mol% pure oxygen and different fractions of butanol and graphite slurry. The objective of the work was to obtain operating data for the development of a high pressure oxy-fired direct contact steam generator system using low volatile fuels to prove the feasibility of this technology. The effect of hydrogen to carbon ratio on the saturated gas

product composition was studied by performing process simulations of the test conditions to determine the maximum steam concentration as a function of the fuel mixture. The effect of volatile content on flame stability and CO formation was studied by changing the fuel mixture, measuring the standard deviation of the upper reactor temperature and the reactor pressure as a measure of flame stability, and measuring the resulting CO emissions using online gas analyzers. The bottom and fly ash were collected in liquid and gas bag filters to measure the carbon losses.

5.3.1. Fuel Analyses

The fuel analyses for the graphite and the butanol/graphite mixtures are provided in **Table 5.1**.

Table 5.1 – Fuel mixture analyses

Parameter	BG1	BG2	BG3	BG4	G1 and G2
Fuel Mixture					
Butanol (wt%)	42	41	41	26	0
Graphite (wt%)	58	59	59	74	100
Sum (wt%)	100	100	100	100	100
Ultimate Analysis (d.b.)					
C (wt%)	85.4	85.7	85.6	90.8	99.4
H (wt%)	5.6	5.5	5.5	3.6	0
N (wt%)	0.0	0.0	0.0	0.0	0
O (wt%)	9.0	8.8	8.8	5.7	0.6
S (wt%)	0.0	0.0	0.0	0.0	0
Sum (wt%)	100.0	100.0	100.0	100.0	100
Proximate Analysis					
Moisture (wt%)	0.0	0.0	0.0	0.0	0
Fixed Carbon (wt%)	58.4	59.2	59.1	73.7	99.46
Volatiles (wt%)	41.6	40.8	40.9	26.3	0.54
Ash (wt%)	0.0	0.0	0.0	0.0	0
Calorific Analysis (d.b.)					
HHV (MJ/kg)	33.7	33.7	33.7	33.4	32.77

5.3.2. Test Matrix

The pilot-scale facility was operated at six conditions as summarized in **Table 5.2**. The purpose of BG1 and BG2 was to establish a stable and controllable flame while injecting n-butanol, graphite slurry, municipal water and oxygen. The goal of BG3 was to

examine the effect of a lower excess O_2 on the CO emissions and the flame stability. Test condition BG4 examine the effect that a lower n-butanol fraction in the fuel mixture would have on emissions and flame stability. After tests BG1-BG4 were carried out, the butanol was completely turned off and unassisted combustion of graphite was initiated. The primary goal of these test conditions was to see if a flame could be self-sustained in a stable fashion.

Table 5.2 – Test condition summary

Description	BG1	BG2	BG3	BG4	G1	G2
Butanol flow (kg/h)	8.0	8.0	8.0	4.1	0.0	0.0
Slurry flow (kg/h)	28.1	28.9	28.8	28.5	30.5-36.0	40-43.0
Slurry solids loading (wt%)	40.0	40.0	40.0	40.0	40.0	40.0
Average heat input (kW_{th})	175.7	178.5	178.1	140.9	126.1	150.8
Butanol heat input (%)	41.8	41.0	41.1	26.4	0.0	0.0
Graphite heat input (%)	58.2	59.0	58.9	73.6	100.0	100.0
Oxygen flow (kg/h)	52.1	52.8	51.5	51.5-56.1	50.3	49.6
Burner moderator flow (kg/h)	42.0	41.0	41.1	20-34	3.9	21.0
Total water to burner (kg/h)	58.8	58.3	58.4	37.1-51.1	22.2-25.5	45.0-48.0

5.3.3. . Equipment Description

The experimental work was performed at 15 bar(g) pressure in a pilot-scale slagging gasifier facility (**Figure 5.1**) at the Natural Resources Canada CanmetENERGY facility in Bells Corners, Ontario, Canada. The reactor details are specified in Part 1 [7].

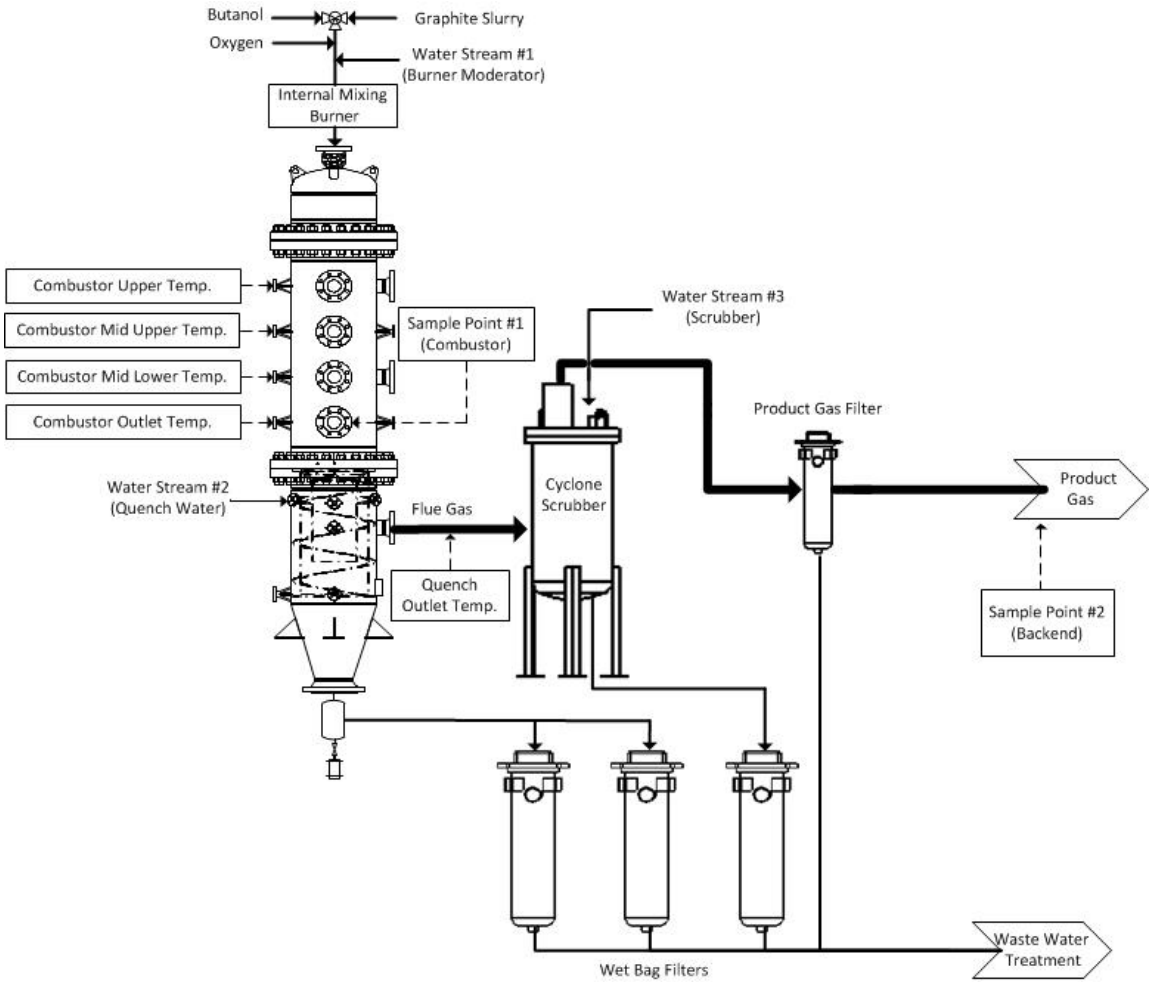

Figure 5.1 – 15 bar pilot-scale reactor

The fuels were injected into the reactor through a gas-swirl atomizer, shown in **Figure 5.2**, with impinging plate and pintle to provide a hollow cone spray. Graphite slurry, butanol and burner water (water stream #1) were mixed and sent into the mixing chamber via the slurry supply tube. For these tests, graphite slurry was initially co-fired with some butanol until the butanol flow was reduced and eventually stopped. The product gas was created within the quench vessel but was further quenched to a temperature below saturation to ensure ease of operation and to protect downstream equipment. A dry gas sample was collected at Sample Point #2 located near the exhaust. All liquid effluents were filtered through bag filters and sent for water treatment.

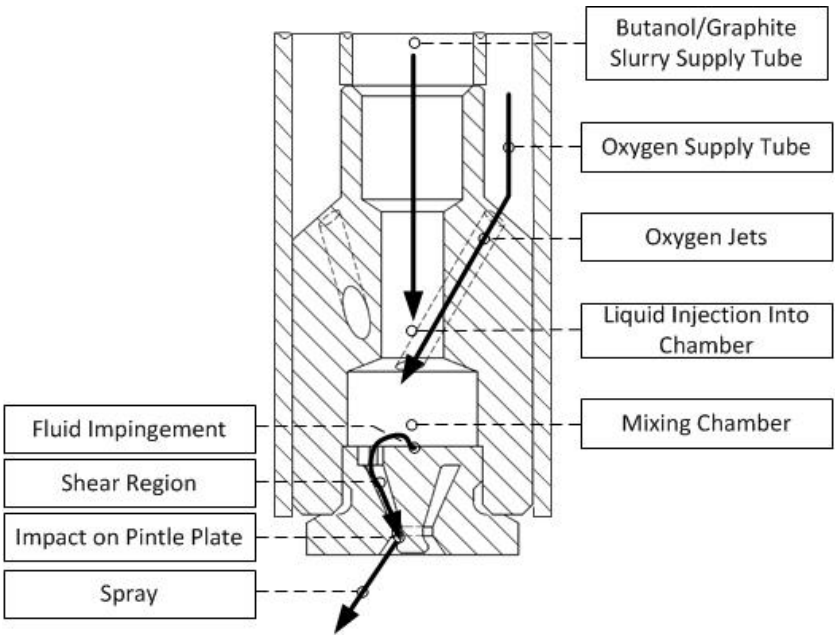

Figure 5.2 – Gas-swirl atomizer used for atomizing slurry with oxygen

5.3.4. Modeling Techniques

The average values from each test period were used to perform AspenTech HYSYS® 2006 simulations to determine the moisture content in the product gas at various intermediate stages within the process. The process flow diagram is shown in **Figure 5.3**.

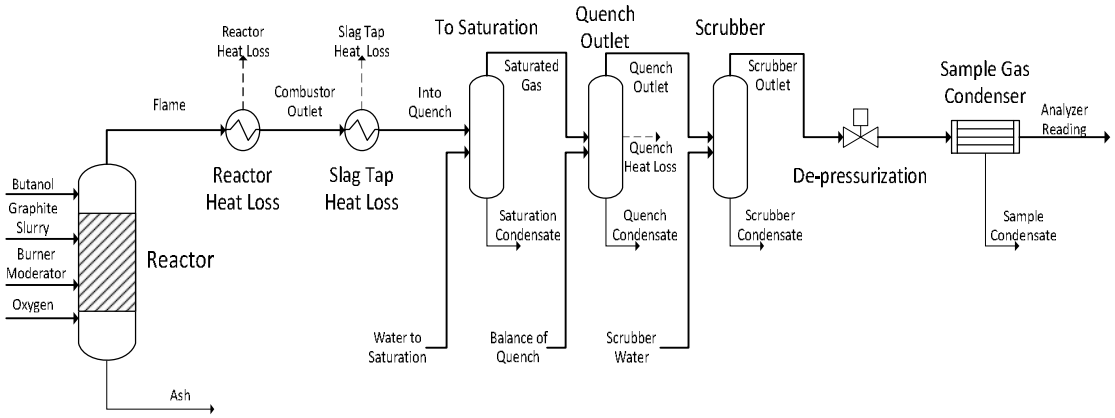

Figure 5.3 – Process flow diagram

For the model, the graphite stream, defined by its ultimate analysis and heating value, was injected into a conversion reactor along with the butanol, water in the slurry, burner moderator water and oxygen (99.5 mol% pure). In the conversion reactor, 100% conversion of the carbon, hydrogen and sulfur in the fuel was assumed. The conversion reactor inlet reactant flow rates were based on the flows measured in the tests, except for the oxygen. The oxygen flow was back calculated from the analyzer readings because of the high level of precision required for the calculations when considering parts per million of carbon monoxide. The flame temperature was based on the Gibbs free energy estimation made by AspenTech HYSYS® for the resulting combustion products exiting the reactor. The reactor heat loss was determined by cooling the flame stream to the measured combustor outlet temperature. A large portion of the heat loss likely resulted from heat going to the refractory and a portion was lost in the burner and sample probe cooling systems. The combustor outlet stream was then subjected to a 3 kW heat loss across the slag tap which was determined based on other experiments, where the gas temperature drop had been measured. The slag tap heat loss was assumed to be constant for all cases.

Experimentally, the flue gas was quenched past the saturation point due to limited control on attaining an exact saturation condition at some point in the process and for ease of operation. This type of system will eventually be operated near the saturation point because this condition maximizes the latent heat available in the product stream. In the simulations this interim saturation condition was determined using the following procedure. The saturated gas composition was defined as the point where the vapour fraction of the gas is completely saturated and any additional water would result in condensation of liquid. To determine this condition the “into quench stream” was cooled in the “to saturation” vessel within the simulation. In this vessel, the “water to saturation” was adjusted to the point at which “saturation condensate” was zero. This provided the “saturated gas stream” information.

The intermediate calculated saturated gas stream entered the “quench outlet” vessel where the “balance of quench” water was added as shown in **Figure 5.3**. The “balance of

quench" was defined as the experimentally measured quench water flow rate less the "water to saturation" value calculated in the previous vessel. The "quench heat loss" stream was adjusted to match the quench outlet temperature that was measured experimentally. The quench outlet gas entered the "scrubber" vessel where the experimentally measured scrubber water flow rate was applied. After de-pressurization the remaining water in the gas was split using the "sample gas condenser" to confirm the experimental analyzer readings as a check on the mass balance.

5.4. Results

The results from the experiments and modelling are presented in **Section 5.4.1** and **Section 5.4.2**, respectively. The nature of the testing and the difficulty in combusting graphite resulted in greater fluctuations in temperature and gas compositions compared to the results in Part I. Furthermore, feeding issues with the graphite slurry caused by graphite settling and plugging the feed lines, resulted in the need for sudden and dramatic operating changes in the reactant flows. As a result, the tests period time spans were shorter, more transient, and of varying lengths compared to the simpler operation of the butanol tests performed in Part I. Although the test periods are outlined to span a certain time frame, the experimental results in **Table 5.3** are presented as a range in numbers to provide qualitative observations and do not necessarily represent steady-state operation. The time frames for the test periods are mostly meant to bound general operating states in order to provide average reactant inlet feed compositions to be used for the modelling portion of this work. The modelling was used to provide quantitative insight into the results that would be theoretically expected if the reactor were operating at steady-state under those conditions.

5.4.1. Experimental Results

All four test periods took place over one run. Butanol-Graphite (BG1) test period 1 spanned from time 0:03 to 0:10 (h:mm) after reactor thermal steady state was achieved. Butanol-graphite test period 2 (BG2) spanned from time 0:09 to 0:19. For Butanol-graphite test period 3 (BG3), which spanned from 0:19 to 0:23, the oxygen flow was

reduced to around 50 kg/h and the water moderator to the burner was reduced to 38 kg/h for a total of 55.3 kg/h water. The CO content increased throughout this period due to the sudden drop in water and O_2 flow rates. This caused flow instabilities resulting in increased CO emissions. After butanol-graphite test period 3 the oxygen flow rate was reduced to achieve as close to stoichiometric combustion as possible. Throughout this period, oxygen contents in the gas as low as 0.25 mol% dry were achieved. Unfortunately, the CO analyzer had periods where it was over range (above 2600 ppm) and, therefore, it was not possible to collect any CO data. At 0:47, the butanol flow was reduced to approximately 4 kg/h and the O_2 flow was increased to about 55 kg/h. Butanol-graphite test period 4 (BG4) then spanned from time 0:50 to 0:56. Throughout this period the O_2 flow was increased in order to ensure operator comfort. The average flows over the time period were used for the simulation in order to model this low n-butanol test condition. After BG4 the butanol flow to the burner was stopped, the burner water moderator was decreased to about 6 kg/h and the slurry flow rate was slowly increased to counter the effects of increased slurry viscosity caused by reduced water and n-butanol flows which were previously helping to dilute the slurry to the burner. Graphite test period 1 (G1) spanned from time 0:57 to 1:03 with the slurry flow rate increasing from 30 to 34 kg/h over that time frame and the dry molar O_2 content reaching a point where it exceeded the range of the O_2 analyzer (approx. 24 mol%). The O_2 content in the flue gas for this time period was thus determined by assuming that CO_2 was the balance of the dry gas with a check based on a mass balance of the flows entering the reactor. After Graphite test period 1 the water moderator flow was increased to 20 kg/h and the O_2 flow was reduced to 45 kg/h. Graphite test period 2 (G2) took place at these conditions from time 1:09 to 1:11. Throughout that period the CO_2 analyzers began to fluctuate and due to the short time frame never reached a stable reading. The CO_2 content was determined based on the O_2 content with validation based on the simulations. The graphite test period data was difficult to analyze because there were issues with temporary burner plugging due to settling of particles in the slurry line. The upper reactor temperature fluctuations indicate that the flame was most unstable for graphite only combustion. Overall, unassisted combustion of slurried graphite was achieved for a period of 20 minutes. These results indicate that pressurized oxy-fuel combustion in a

direct contact steam generation firing mode of low volatile fuels such as petroleum coke is feasible, but feeding issues with the slurry will need to be addressed. The data trends for the reactant flows and product compositions are presented in **Figure 5.4** and the data for the process pressures and temperatures are presented in **Figure 5.5**. The test results are summarized in **Table 5.3**.

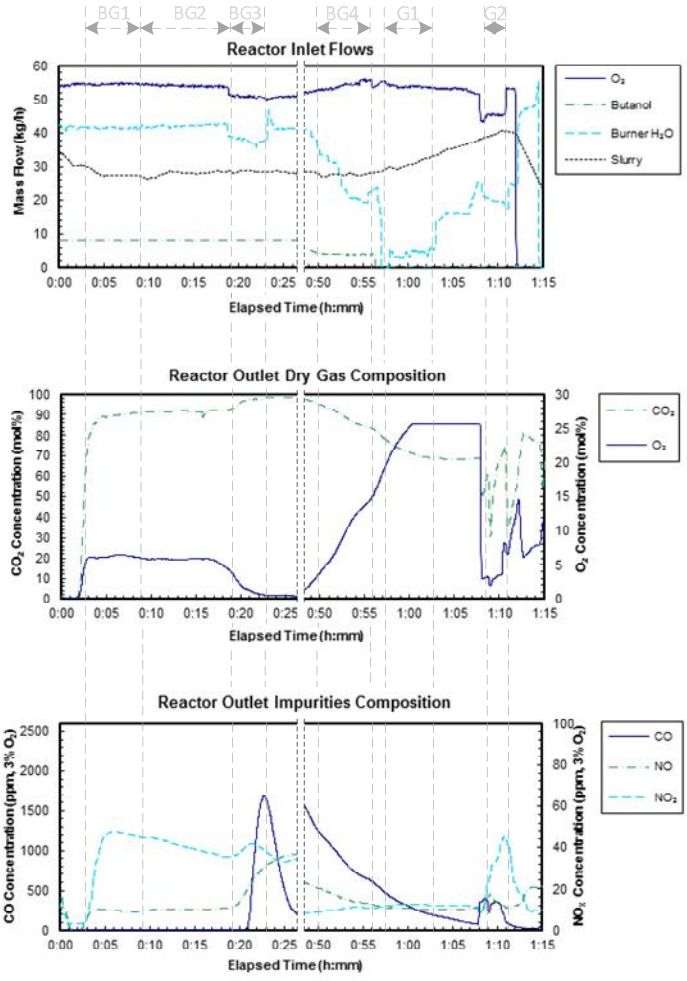

Figure 5.4 – Reactant flows and product gas compositions

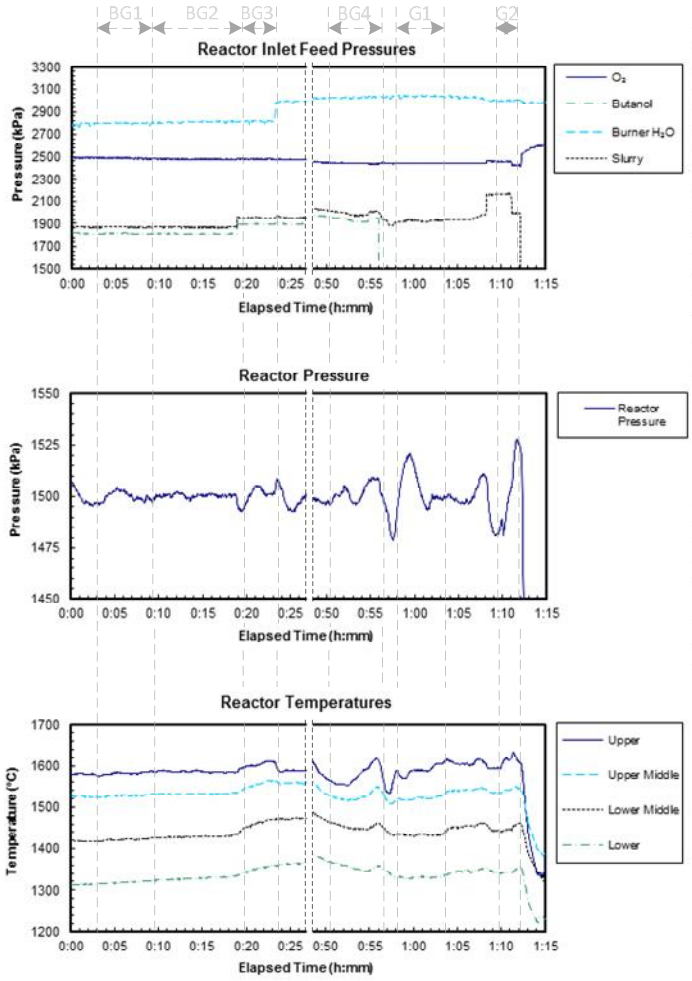

Figure 5.5 – Process pressures and temperatures

Table 5.3 – Test result summary

Description	BG1	BG2	BG3	BG4	G1	G2
Time Period (h:mm - h:mm)	0:03-0:09	0:09-0:19	0:19-0:23	0:50-0:56	0:57-1:03	1:09-1:11
Combustor gauge pressure (kPa)	1499.9	1499.4	1502.0	1501.6	1501.4	-
Standard deviation of pressure (kPa)	2.2	1.9	2.1	4.2	11.5	-
Combustor upper temperature (°C)	1527	1588	1555	1568	1602	1605
Standard deviation of upper temperature(°C)	2.7	3.0	4.6	-	17.6	-
Combustor outlet Temperature (°C)	1333	1388	1370	1350	1331	1341
Combustor heat loss (kW)	53.3	52.2	53.7	53.3	62.2	62.6
Combustor heat loss (%)	30.3	29.2	30.1	37.8	49.3	38.1
Quench water flow (kg/h)	262.8	267.5	262.8	291.5	289.7	287.5
Quench outlet temperature (°C)	161.3	160.3	158.9	145.5	128.2	132.5
Dry gas composition						
O_2 (mol% dry)	5.9	6.0	0.4	4.0-15.5	20.7-27.6[a]	2.5-7.9
CO_2 (mol% dry)	93.7	93.5	99.3	95.8-84.3	79.1-72.2	92.0-97.4[a]
CO (ppm dry, 3% O_2)	13	12	12-1644	650-1225	205-465	100-335
NO (ppm dry, 3% O_2)	11	10	37	11	11	12
NO_2 (ppm dry, 3% O_2)	41	38	34	13	12	13
NO_X (ppm dry, 3% O_2)	52	48	71	24	23	36
NO_2/NO	3.92	3.69	0.93	1.13	1.14	1.14
SO_2 (ppm dry, 3% O_2)	<10	<10	<10	<10	<10	<10

a – determined by difference with a check from the mass balance

Over the butanol-graphite test periods, the CO emissions ranged from as low as 12 ppm to about 1750 ppm on a dry gas basis corrected to 3% O_2, which corresponds to a maximum of 240 ppm at the saturation point. Although CO fluctuated significantly, it seemed to generally increase when the graphite content of the fuel mixture was increased and/or when the O_2 flow to the burner was decreased below a threshold that was close to the stoichiometric point. It is important to note that the periods where the CO analyzer reading was over range are not included in the analysis because they are considered operating anomalies too close to the stoichiometric point. The periods of relatively low CO emissions (such as BG1 and BG2) indicate that good conversion of carbon is achievable, especially considering the low O_2 content in the wet gas (around 1.6 mol% in the combustor for BG1 and BG2). Very little fluctuation in the combustor upper temperature indicates that the flame was stable for BG1-BG3, with flame stability decreasing for BG4 and worst for G1 and G2. There was no measurable carbon containing residues found in the liquid and gas bag filters, indicating that no unburned carbon made it through the system and that high conversion was achieved.

Other impurities such as NO_x were very low, averaging about 49 ppm on a dry gas basis corrected to 3% O_2. Formation of NO_x was attributed to thermal NO_x created by the impurities in the O_2 supply. Furthermore, the NO_x at the saturation point in a product gas would be on the ppb scale as a result of dilution with water, well below any reasonable detectable limit. It was noticed that the NO_2/NO ratio at these conditions was quite high and ranged from 0.5 to 3.92 as a result of the increased partial pressure of O_2 driving NO to NO_2 [13].

5.4.2. Modeling Results

The modeling results are presented in **Table 5.4**. The CO, NO, NO_2 and SO_2 compositions were based on the analyzer readings.

Table 5.4 – Modeling results summary

Description	BG1	BG2	BG3	BG4	G1
Flame temperature (°C)	1959	1989	1994	2134	2393
Combustion products composition dry					
O_2 (mol% dry)	5.9	6.0	0.4	22.9[a,b]	27.1[a]
CO_2 (mol% dry)	93.8	93.7	99.4	76.9	72.8
N_2 (ppm dry, 3% O_2)	464	461	462	429	900
Ar (ppm dry, 3% O_2)	1856	1845	1847	1717	1804
Combustion products composition wet					
H_2O (mol% wet)	72.9	72.5	73.0	61.3	46.6
O_2 (mol% wet)	1.60	1.66	0.11	8.84	14.5
CO_2 (mol% wet)	25.4	25.8	26.8	29.7	38.8
N_2 (ppm wet, 3% O_2)	125	127	124	166	410
Ar (ppm wet, 3% O_2)	502	507	498	664	822
CO (ppm wet, 3% O_2)	3	3	-	-	-
NO (ppm wet, 3% O_2)	2.7	2.6	9.8	3.7	5.1
NO_2 (ppm wet, 3% O_2)	10.7	10.1	9.1	4.1	5.8
SO_2 (ppm wet, 3% O_2)	<10	<10	<10	<10	<10
Water to saturation	94.4	99.1	97.5	70.3	52.55
Saturation temperature	194.4	199.4	194.4	190.9	186.5
Saturated gas composition					
H_2O (mol% wet)	86.5	86.6	86.8	80.8	73.2
O_2 (mol% wet)	0.80	0.81	0.06	4.40	7.3
CO_2 (mol% wet)	12.7	12.5	13.1	14.8	19.5
N_2 (ppm wet, 3% O_2)	62	73	61	83	190
Ar (ppm wet, 3% O_2)	250	293	243	332	380
CO (ppm wet, 3% O_2)	2	2	-	-	-
NO (ppm wet, 3% O_2)	1	1	5	2	2
NO_2 (ppm wet, 3% O_2)	5	5	4	2	3
SO_2 (ppm wet, 3% O_2)	<10	<10	<10	<10	<10
Balance of quench (kg/h)	168.4	168.4	165.3	221.2	237.1

a – based on the average flows over the test period, b – does not correlate to analyzers due to response lag to step change in n-butanol flow.

It was not possible to provide an accurate comparison of graphite combustion under different firing scenarios because there was not enough reliable data produced. The models assumed the average reactant flows observed in G1 with results supported through qualitative observations based on the trends in **Figure 5.4** and **Figure 5.5**.

5.5. Discussion

After evaluating the experimental and modelling results from Parts 1 and 2 of this study, several trends in the data were observed. **Figure 5.6** compares the fuel hydrogen to carbon ratio with the theoretical maximum attainable H_2O concentration in the product gas. It can be observed that H_2O content in the flue gas increases with an increasing ratio of hydrogen to carbon in the fuel. This is to be expected because the saturation point of the gas is affected by the partial pressure of the balance non-condensable combustion products (mainly CO_2). Therefore a fuel that produces more water as a combustion product compared to CO_2 will produce a product gas with a higher purity steam because the partial pressure of CO_2 will be lower. The experimental data supports this conclusion. The graphite tests show that the steam purity achieved was around 80.5 mol% on average, with the butanol-graphite tests (BG1-BG3) it was around 86.5 mol% and with BG4 it was around 81 mol%. The butanol tests gave a steam purity of 90 mol% [7]. Therefore, the highest steam production favours fuels with high H/C ratios such as natural gas.

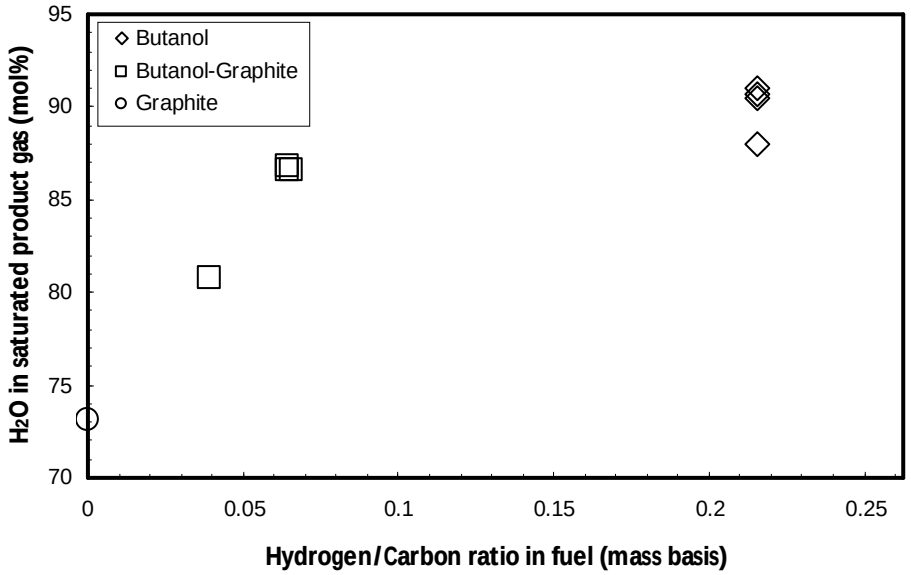

Figure 5.6 – Maximum attainable steam concentration (effect of fuel H/C ratio)

When this effect was investigated using AspenTech HYSYS® it was found that the fuel hydrogen to carbon ratio and excess O_2 play a significant role on the outlet saturation point because they determine the composition of the balance gas after the additional water has been added. The higher the hydrogen to carbon ratio the greater the amount of H_2O compared to CO_2 that will be produced by the fuel, which will lead to a higher H_2O content in the saturated flue gas. Also, the higher the O_2 concentration in the product gas the lower the H_2O content in the saturated flue gas because of the effect that O_2 has on the balance gas. These trends are illustrated in **Figure 5.7**. As a result of these factors, care must be taken when selecting the fuel for a DCSG process because the fuel will have an effect on the product gas. Excess O_2 should also be minimized.

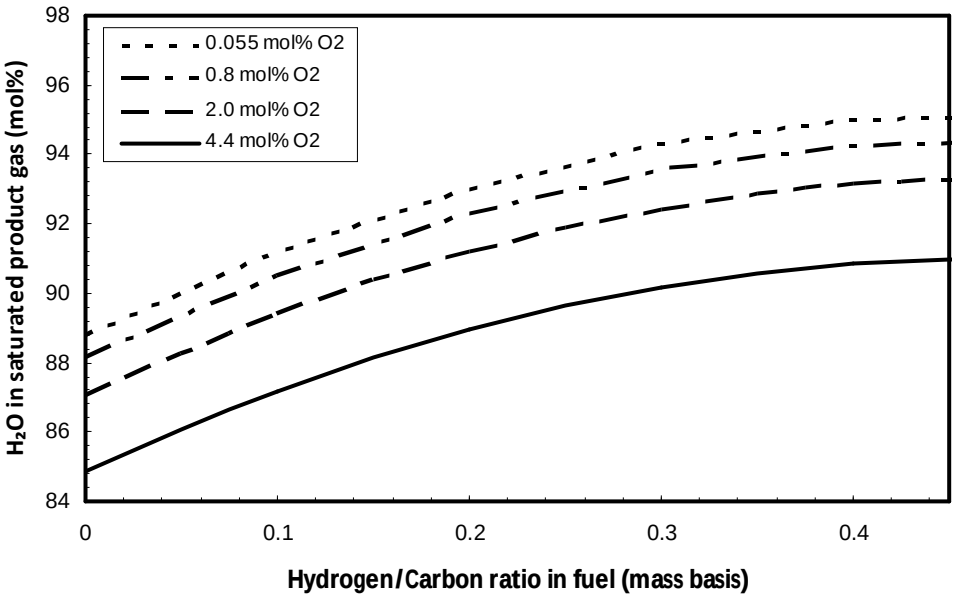

Figure 5.7 – Maximum attainable steam concentration (effect of fuel H/C ratio) with various O_2 concentrations in the product gas

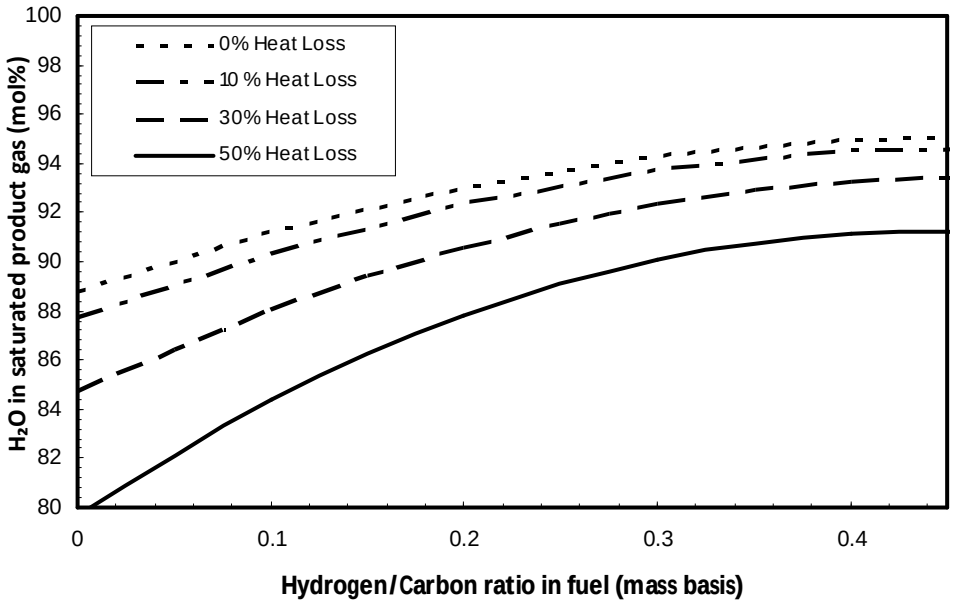

Figure 5.8 – Maximum attainable steam concentration (effect of fuel H/C ratio) with various heat losses to the system

Any heat losses to the system will affect the outlet conditions. Mainly, any heat lost from the system is heat that is unused to evaporate H_2O which will reduce the maximum attainable H_2O content in the saturated flue gas. This trend is illustrated in **Figure 5.8**.

Another interesting trend in **Figure 5.8** is the combined effect of the fuel H/C ratio and heat loss. The diverging curves with decreasing H/C ratio indicate that: the lower the H/C ratio of the fuel the greater the effect of heat loss. Fuels with lower H/C ratios require more addition of water to reach the saturation point than fuels with higher H/C ratios because less of the H_2O is produced by the fuel. Therefore, a greater amount of water that relies on available heat to be converted to steam is used for the lower H/C ratio fuels making these fuels more sensitive to heat loss.

Figure 5.9 presents the standard deviation of the upper reactor temperature and reactor pressure versus fuel volatile content. These data provide insight into flame stability because they represent the flow and heat fluctuations caused by the burner and the flame. The standard deviation decreases with increasing volatile content, indicating that the

flame was less stable with increasing graphite. Although the stability decreased, combustion was still maintained with this difficult to combust fuel, indicating that combustion with other low volatile fuels such as petroleum coke is possible in these conditions.

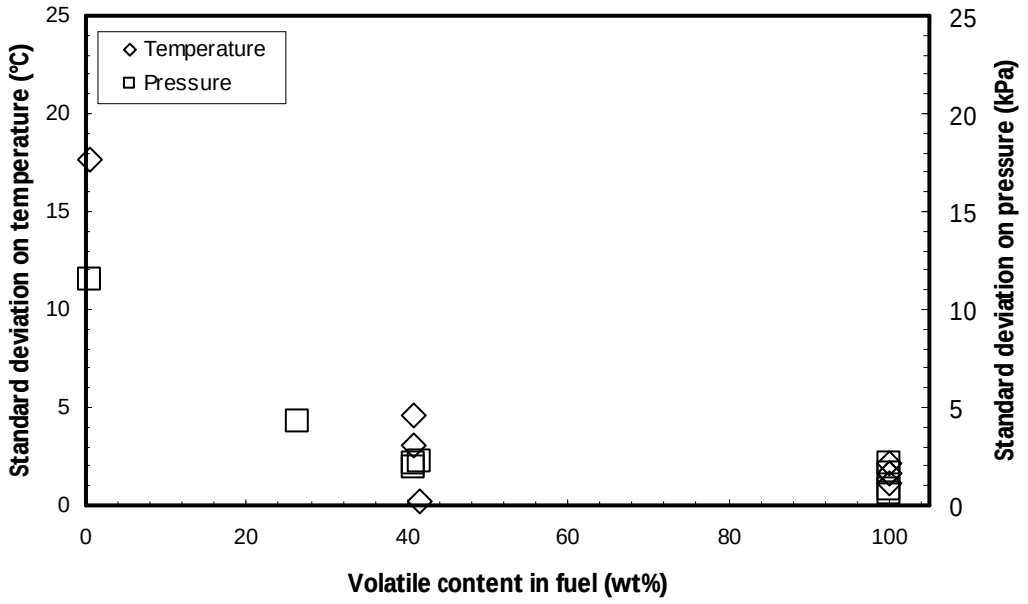

Figure 5.9 – Standard deviation of upper reactor temperature and reactor pressure as a function of volatile content as a method to determine flame stability

5.6. Conclusions

1. Sustainable flames were achieved with the graphite slurry mixtures.
2. The maximum attainable H_2O content increased with increasing hydrogen to carbon ratio in the fuel, as expected. These findings suggest that a fuel such as natural gas will produce a higher steam concentration in the product gas than petroleum coke would produce.
3. Low CO emissions were achieved indicating high combustion efficiency.
4. Standard deviation in temperature and pressure were below 1% for the graphite runs indicating considerable flame stability.
5. Flame stability generally decreased with decreasing volatile content.

6. NO_2/NO ratio was higher than ambient combustion conditions because of increased oxidation of NO due to higher partial pressure of O_2.
7. No measurable carbonaceous material was found in the liquid and gas bag filters, indicating that high conversion was achieved.
8. Pressurized oxy-fuel combustion in a direct contact steam generation firing mode of low volatile fuels such as petroleum coke is feasible.

5.7. Acknowledgements

The authors would like to acknowledge the financial support received for this project through the Panel on Energy R&D (PERD), as well as technical assistance by Jeff Slater and Ryan Burchat with the pilot-scale facility.

5.8. References

[1] Analysis Brief: Canada [Internet]. Washington (DC): U.S. Energy Information Administration – [cited 2013 Feb 27]. Available from: http://www.eia.gov/countries/cab.cfm?fips=CA.

[2] Alberta Government. *In-situ* process steam assisted gravity drainage. 2013 Feb. 1, p. 3. Canadian Association of Petroleum Producers. Crude oil: forecast, markets & pipelines. 2012 June. 7 p.

[4] Bohm M, Goold S, Laux S, Neu B, Sharma A, Aasen K. Application of oxy-fuel CO_2 capture for in-situ bitumen extraction from Canada's oil sands. Energy Proc. 2011; 4: 958-965.

[5] Clements B, inventor; Her Majesty the Queen in Right of Canada as Represented by the Minister of Natural Resources, assignee. High pressure direct contact oxy-fired steam generator. Unites States patent US 20110232545A1. 2011 Aug 29.

[6] McKellar JM, Bergeson JA, MacLean HL. Replacing natural gas in Alberta's oil sands: trade-offs associated with alternative fossil fuels. Energy Fuel. 2010; 24(3): 1687-1695.

[7] Cairns P, Hughes R, Clements BR, Herage T, Zheng L, Macchi A, *et al.* High pressure oxy-firing (HiPrOx) of fuel with water for the purpose of direct contact steam generation – part 1: butanol. Fuel. Forthcoming 2013.

[8] Makino A, Fujizaki H, Araki N. Combustion rate of burning graphite in a stagnation flow of water vapour. Comb Flame. 1998; 113: 258-263.

[9] Culbertson B, Brezinsky K. High-pressure shock tube studies on graphite oxidation reactions with carbon dioxide and water. Proc Comb Inst. 2011; 33: 1837-1842.

[10] Lang T, Hurt R.H. Char combustion reactivities for a suite of diverse solid fuels and char-forming organic model compounds. Proc Comb Inst. 2002; 29: 423-431.

[11] Yang HC, Eun HC, Lee DG, Jung CH, Lee KW. Analysis of combustion kinetics of powdered nuclear graphite by using a non-isothermal, thermogravimetric Method. J Nuclr Sci Tech. 2006; 43 (11): 1436-1439.

[12] Yoon SJ, Choi YC, Lee SH, Lee JG. Thermogravimetric study of coal and petroleum coke for gasification. Kor J Chem Eng. 2007; 24(3): 512-517.

[13] Mallet C, Aho M, Hamalainen J, Rouan JP, Richard JR. Formation of NO, NO_2, and N_2O from Gardanne lignite and its char under pressurized conditions. Energy Fuel. 1997; 11: 792-800.

Chapter 6. Conclusions and Recommendations

6.1. Summary of findings and thesis conclusions

In **Chapter 2** a HiPrOx/DCSG system was presented that can replace conventional steam generators in the SAGD process. It was found that when the DCSG was integrated into SAGD and compared against the base case: produced oily water treatment was reduced by ~54%, produced water treatment was completely eliminated, the water-to-oil ratio was decreased by up to ~7%, make-up water requirements per barrel of oil were reduced by 37.5% – 100%, energy intensity was decreased by ~3.5% to ~7.5%, and CO_2 emissions were reduced by ~80% (assuming CO_2 emissions from utility companies are not captured) compared to the status quo.

These findings resulted from the high thermal efficiency of the steam generators (95% – 98%), the increased production of steam resulting from the combustion of hydrogen in the fuel, by assuming it was possible to use low quality and hydrocarbon containing water for steam generation and, by assuming the CO_2 would be sequestered in the reservoir. It was shown that the fraction of injected CO_2 that is sequestered down well did not significantly impact the energy intensity results. Furthermore, the energy associated with water treatment was not significant compared to fuel consumption, therefore if additional treatment is required for the DCSG case than was assumed, it will not significantly impact the energy intensity.

These results indicate that on a conceptual basis, the HiPrOx/DCSG system is feasible from an energy and CCS perspective. Based on these results, it was decided to investigate the feasibility of the technology from a combustion perspective. Bench scale testing was chosen as a first step in this respect, which led to the second study.

Bench scale testing using a PTGA was detailed in **Chapter 3**. The objective was to determine whether the high moisture environments encountered in the DCSG would reduce solid fuel combustion efficiency. This was performed by combusting a Canadian lignite coal char in various $O_2/CO_2/H_2O$ environments at different pressures. It was

found that at atmospheric pressure the higher thermal conductivity and heat capacity of H_2O led to higher burnout temperatures in Regime I conditions with heterogeneous ignition. With increased pressure, the net effect of a higher H_2O gas mixture similar to that for DCSG seemed to have the same reactivity as a pressurized O_2/N_2 environment and worked to counteract the inhibiting effect caused by the presence of CO_2. These results helped show the potential feasibility of this technology at the bench scale because they indicated that burnout times will decrease with increasing pressure, and a high presence of steam will not greatly affect combustion efficiency and burnout when compared to O_2/N_2 mixtures at high pressure.

However, when further investigation into the literature regarding effects of steam addition in ambient oxy-fuel environments at the pilot-scale was performed it was discovered that factors such as radiation and the suppression of radical concentrations resulting from the presence of H_2O and CO_2 during homogeneous ignition may potentially have a greater effect than heat capacity and thermal conductivity. Furthermore, the PTGA data were not a proper representation of the high temperatures, heterogeneous ignition, and char structures that would be found in pilot-scale applications. Thus, it was decided that pilot-scale studies would be required to truly evaluate the feasibility of this technology.

To start, the highly volatile and simple to inject n-butanol fuel was selected as initial proof-of-concept because it would be easy to ignite and combust and would give indications into the combustion behaviour of natural gas, without the added requirements of installing compressed gas delivery equipment. The pilot-scale testing at 1500 kPag using n-butanol fuel with municipal water moderator was presented in **Chapter 4**. The significant findings were that high product gas O_2 concentrations were not required, high concentrations of H_2O in the product gas were theoretically attainable, the CO emissions were low, and fluctuations in the upper reactor temperature and reactor pressure were low.

Low O_2 concentrations in the product gas were important because they will help reduce corrosion issues in downstream piping, decrease non-condensable gas concentration into the well, and reduce energy and cost requirements associated with oxygen generation. High concentrations of H_2O in the product gas were important to maintain the latent heat in the product gas at levels similar to those for pure steam from OTSGs, and low CO emissions and fluctuations were important because they indicate high combustion efficiencies and stable flames. In summary, the results from the n-butanol pilot-scale testing indicated that combustion with a highly volatile fuel such as natural gas would be technically feasible because highly efficient and stable combustion, coupled with low O_2 requirements were achievable in this high H_2O environment.

Following proof-of-concept with a volatile fuel, it was necessary to prove the feasibility of the technology using a low volatile solid fuel. This was achieved by combusting graphite and n-butanol/graphite mixtures at the pilot-scale. The testing with these fuels was presented in **Chapter 5**.

Graphite/butanol mixtures were selected because certain combinations could represent the range of proximate analyses of waste fuels and to serve as a proof of concept that fuels with very little volatile matter and relatively inert chars would combust. Furthermore, graphite and n-butanol do not contain any sulphur which prevents added complications due to the condensation of acidic sulphuric species on the interior of the pressure vessel during start-up and cool down, for which it was not guarded against at the time. The pressure vessel was recently coated with Inconel 625 to help withstand sulphuric acid corrosion.

The findings associated with this study were that a sustainable graphite slurry flame could be achieved, the maximum attainable H_2O content increased with increasing hydrogen-to-carbon ratio in the fuel, flame stability generally decreased with decreasing volatile content, standard deviation caused by pressure and temperature fluctuations were below 1% of mean, and that no measurable material was found in the liquid and gas bag filters.

The results from this testing indicated that combustion with a low volatile fuel such as petroleum coke is feasible in high moisture environments because a sustained and relatively stable flame was produced and combustion efficiency was close to 100% as indicated by the lack of unburned carbon found in the back end.

In conclusion, when these four studies are considered, HiPrOx/DCSG is technically feasible from an energy perspective, from a combustion standpoint at the bench scale, and from a combustion efficiency and theoretically achievable product gas standpoint at the pilot-scale.

6.2. Recommendations for future work

Throughout this document, several knowledge gaps were identified that must be addressed from a process and operating standpoint. These include: corrosion issues associated with the product flue gas, the effect of CO_2 on bitumen production, the nature of the mineral melt formed by the deposition of the TDS and TSS in the combustor, and scaling issues associated with mineral deposits from the TDS and TSS in the produced water.

A possible method of reducing corrosion issues would be to operate under fuel rich combustion conditions. This will act to reduce the oxygen concentration in the product gas, which will reduce the amount of oxidation to sulphuric and nitric species. Another alternative would be to inject a sorbent downstream of the steam generator that would act to neutralize any acidic species formed downstream. The alkalinity of the well and produced water itself may cause this phenomena to occur naturally. Therefore, it is recommended that pilot-scale combustion testing in a fuel rich environment in which actual SAGD produced water is injected be performed to first determine the nature of the product gas and the species formed. Following this study, it would be recommended that long operating time (on the scale of days) bench-scale tests be performed using an autoclave with a synthetic gas similar to that found at the pilot-scale with various materials and sorbents to determine the net corrosion rates. From the bench-scale testing

it will be possible to determine materials and sorbents (if necessary) to be used at the field-scale.

As mentioned earlier, laboratory and field test data regarding the effect of CO_2 on bitumen production are very limited. Furthermore, studies that investigate these effects through reservoir simulations seem to provide conflicting results. It is recommended that field-scale testing in which CO_2 is co-injected with steam be performed. During this testing, it is recommended that bitumen production, well temperature, and well corrosion be monitored over a long time period with varying CO_2 fractions in the injected gas.

The nature of the mineral melt formed by the deposition of the TDS and TSS in the combustor is important because the combustor is designed to operate similar to a slagging gasifier. Therefore, the operating conditions should be designed such that the mineral melt is in a molten state that will freely flow down the walls of the combustor to avoid plugging of the combustor outlet. Furthermore, the interactions between the mineral melt and the combustor hot-face material is important to ensure material compatibilities that will allow for long-term and reliable operation. It is therefore recommended that pilot-scale testing be performed and the mineral melt deposits be collected and analyzed. Once a mineral melt composition is obtained, it will be possible to perform bench-scale viscosity measurements and cup tests that will provide insight into desired hot face temperatures and liner materials, respectively.

Last, it is important to understand the effect that the evaporation of SAGD produced waters will have on scaling and fouling in the steam generator. It is recommended that pilot-scale testing in which SAGD produced water is injected into the process be performed where scaling is monitored. It is also recommended that steam generator bottoms be collected and analyzed in order to determine their composition and to calculate solubility data for the TDS in the solution. The solubility data will provide insight into the operating conditions (temperature and vapour phase fraction) in the steam generator required to keep the TDS in solution. This will help reduce scaling and fouling issues and provide reliable operating conditions that will be required at the field and commercial scales.

In the future, CanmetENERGY will be performing pilot-scale testing at 1500 kPag with natural gas as fuel, SAGD produced oily-water injected at the burner, and SAGD produced water injected in the steam generator. These tests should provide valuable insight into the above mentioned phenomena and provide data that can be used as a basis for bench-scale testing in the future.